Marine Biofouling of Surfaces:
Morphology, and Nanomechanics of Barnacle Cyprid Adhesion Proteins by AFM

Members of the committee:

Chairman	Prof. dr. C. Hoede	University of Twente
Secretary	Prof. dr. C. Hoede	University of Twente
Promotor	Prof. dr. G. J. Vancso	University of Twente
Members	Prof. dr. ir. J. Huskens	University of Twente
	Prof. dr. ing. M. Wessling	University of Twente
	Prof. dr. D. Grijpma	University of Twente
	Prof. dr. V. Subramaniam	University of Twente
	Prof. dr. A. S. Clare	University of Newcastle
	Dr. G. Bar	Dow Olefinverbund GmbH

Marine Biofouling of Surfaces: Morphology, and Nanomechanics of Barnacle Cyprid Adhesion Proteins by AFM

I. Y. Phang
Ph. D. Thesis
University of Twente, MESA$^+$ Institute for Nanotechnology
Enschede, The Netherlands

Cover design by In Yee Phang

This research was financially supported by the Dutch Polymer Institute (DPI), PO Box 902, 5600AX Eindhoven, The Netherlands, Project nr. #510.

ISBN: 978-90-365-2717-0

MARINE BIOFOULING OF SURFACES:

MORPHOLOGY, AND NANOMECHANICS OF BARNACLE CYPRID ADHESION PROTEINS BY AFM

PROEFSCHRIFT

ter verkrijging van
de graad van doctor aan de Universiteit Twente,
op gezag van de rector magnificus,
prof. dr. W.H.M. Zijm,
volgens besluit van het College voor Promoties
in het openbaar te verdedigen
op vrijdag 24 oktober 2008 om 16.45 uur

door

In Yee Phang
geboren op 1 september 1976
te Ipoh, Malaysia

Dit proefschrift is goedgekeurd door:

Promotor: **Prof. dr. G. J. Vancso**

This thesis is dedicated to my family and Xing Yi

Table of contents

Chapter 1

General introduction

1.1 General introduction

Marine biofouling is a costly and long-standing problem for the maritime industry.[1] Current solutions to prevent biofouling, mainly in the form of fouling resistant marine coatings, are biocidal in nature. Hence, an effective and environmentally benign solution is in high demand to tackle the fouling problems.[2, 3] Barnacles, green algae, diatoms, and mussels are particularly notorious for their attachment to and/or damage of man-made structures.[4] The growth of fouling assemblages on ship hulls causes increased drag, reduces its maneuverability, increases fuel consumption and greenhouse gas emissions, which contributed to significant economic and environmental costs.[5] Barnacle is a particular problematic biofouler due to its large size and gregarious nature. Hence, in this Thesis we shall focus on fouling caused by barnacles.

A generalized barnacle life-history involves six planktotrophic (i.e. feeding) nauplius stages, a non-feeding cypris stage and the adult.[6, 7] The cyprid is the settlement stage, whose sole purpose is to locate and attach to a suitable surface for adult growth. Historically, adult barnacles have been the primary focus of (barnacle related) antifouling research, probably due to their obviously troublesome presence on ship hulls and the fact that they are large and easy to manipulate in experiments. Combating a problem such as biofouling only once it has become established, however, seems counter-intuitive. A more preferable strategy is the prevention of larval settlement, or promotion of detachment of larval forms at an early stage.[8] We have chosen this strategy in our collaborative efforts involving biologists (University of Newcastle, UK and Tropical Marine Science Institute, Singapore), our group working in materials science, and our industrial collaborators (DOW Chemical Co.).

Although biologists have demonstrated, by chemical staining, that the temporary adhesive is deposited as ‘footprints’ on some surfaces during the cyprid larva exploration[9] and that it acts a settlement cue for subsequently exploring cyprids, its morphology and mechanical properties have never been investigated.[10, 11] Any data regarding the nanomechanical properties of this secretion would provide a useful insight into how such natural adhesives function and, more importantly, how to prevent their function. Hence, to

study the larva settlement behavior and the bioadhesive properties on a surface, a nanoscale characterization technique is needed.[12]

Over the last decade, nanoscale testing and characterization techniques have slowly proliferated from the field of materials science, where they were once viewed by many in other disciplines as arcane and unapproachable, and are now easily accessible to those in the broader scientific arena. In the present context, atomic force microscopy (AFM)[13] based force spectroscopy[14] has allowed the 'scaling down' of traditional mechanical materials testing by several orders of magnitude. Where fibers of material were once required to be on at least the centimeter scale for testing, nanofibers consisting of thin bundles of molecules, or even single proteins, can now be manipulated mechanically, allowing detailed investigation of nanoscopic samples, and single macromolecules.[15, 16] One of the main advantages of AFM in this area of science is its ability to first locate objects to be "interrogated" on the nanoscale, and then measure nano-scale properties of natural bioadhesive materials and adhesive interfaces in native conditions, i.e. hydrated in a saline solution.[17] The information that this mode of study provides, regarding the structure and function of adhesive proteins *in situ* will, undoubtedly, encourage more informed surface design leading to novel methods of interfering with the bioadhesive/substratum interface. Furthermore, the ability of AFM to map specific surface interactions would allow us to shed light on the specific composition of cyprid footprints.[18]

1.2 Concept/scope of this Thesis

This Thesis describes the study of barnacle cyprid larvae adhesion system by atomic force microscopy (AFM), which is a powerful nano-scale characterization technique. The aim is to obtain better fundamental understanding of marine biofouling, especially regarding the formation, structure and properties of bioadhesive-interfaces, across the length scales, down to the molecular level, under native environment.

This Thesis consists of three major parts. First we focused on the visualization of the morphology of footprints, which is studied by AFM imaging. The second aim is to study the nanomechanical properties of the footprint proteins by the AFM based force-spectroscopy and chemical force microscopy, using chemically functionalized tips. The last focus is on the behavior of the barnacle cyprid larva adhesives in different environment. This allows an in-depth understanding of adhesives properties subjected to different environment parameters.

Chapter 2 provides a literature review regarding marine biofouling. This Chapter describes the impact of marine fouling, the fouling process and gives a short overview of the

fouling organisms. In particular, the life cycle of barnacle and its adhesion processes are extensively reviewed. A short introduction to the history of antifouling coatings, current antifouling solutions and other solutions in development are introduced. Antifouling coating assessment methods are also discussed. The last section of this Chapter is dedicated to the principle of the atomic force microscopy and its applications as nanoscale testing and characterization technique.

Chapter 3 presents the observation on the microscopic morphology of footprints deposited by cyprid larva of *Semibalanus balanoide*. The goal is observe *in situ* the bioadhesives left behind by cyprid larva during surface exploration, in native conditions. Glass surfaces with different chemical functionalities are used for the comparison of footprint morphology.

Chapter 4 studies the footprint deposited by cyprid larva of *Balanus amphitrite* by AFM imaging and force spectroscopy. Force spectroscopy allows *in situ* mechanical stretching of bundles of footprint proteins, or single chains of the corresponding protein, in a native form. In this way, the nanomechanical properties of the footprint adhesives, in the presence of single and/or bundles of protein(s) can be measured. In particular, the footprint protein segment reformation and energy dissipation are measured by applying the stretching at different relaxation time scale. The force-extension behavior of the footprint proteins is simulated with a classical polymer model to gain more insight into the molecular behavior of the footprint proteins.

In Chapter 5, a chemical force microscopy approach utilizing AFM tips with controlled surface chemistry is used to study the specific footprint protein-surface interactions. The footprints are allowed to be deposited on surfaces functionalized with silanes on glass, featuring amino-end groups at the exposed surface. Commercial Si_3N_4 and chemically-functionalized AFM tips are used to probe the (bioadhesives) interfacial, specifically the interface of footprint protein and AFM tip. Force-extension curves obtained from footprints deposited are analyzed.

In Chapter 6, the settlement inducing behaviour of cyprid footprints is examined and compared by three different experiments, i.e. (a) AFM, (b) settlement assays and (c) field tests. The aim of the study is to combine the structural and macroscopic settlement information obtained from these three experiments, and to correlate the influence of settlement inducing protein complex deposited on surfaces to the barnacle cyprid larva conspecies settlement behaviour as derived in the previous Chapters. In addition, the results

from laboratory observations to panel immersion test where actual marine biofouling occurs is also compared.

The study of the effect of the enzyme-serine protease, Alcalase®, on the adhesives of barnacle cyprids is studied in Chapter 7. The efficacy of this commercially available serine endopeptidase, Alcalase® as an antifoulant and its mode of action on barnacle cypris larvae are investigated. AFM is used to monitor the *in situ* enzymatic degradation of footprints adhesives of barnacle cyprid adhesives during the exposure to Alcalase®.

In Chapter 8, the curing process of the permanent cement, which is used by cyprid larvae to attach permanently under water once it found the favor location, is extensively examined with force spectroscopy. The nanomechanical properties of permanent cement of cyprid larva are monitored *in situ* over the course of its curing process. The curing of the permanent cement can be manifested in the distribution of the pull-off force and molecular stretch length over time. The correlation between maximum pull-off force and molecular stretch length obtained from the force curves provides a monitoring platform for the 'curing' of the adhesive.

1.3 References

1. Yebra, D. M.; Kiil, S.; Dam-Johansen, K. *Prog. Org. Coat.* **2004,** *50*, 75-104.
2. Clare, A. S. *J. Mar. Biotechnol.* **1998,** *6*, 3-6.
3. Fusetani, N. *Nat. Prod. Rep.* **2004,** *21*, 94-104.
4. Smith, A. M.; Callow, J. A., *Biological adhesives.* 1st ed.; Springer: Berlin, 2006.
5. Townsin, R. L. *Biofouling* **2003,** *19*, 9-15.
6. Anderson, D. T., *Barnacles: structure, function, development and evolution.* Chapman & Hall: London, 1994; p 357.
7. Rainbow, P. S. *Field Stud.* **1984,** *6*, 1-51.
8. Rittschof, D.; Branscomb, E. S.; Costlow, J. D. *J. Exp. Mar. Biol. Ecol.* **1984,** *82*, 131-146.
9. Matsumura, K.; Nagano, M.; Kato-Yoshinaga, Y.; Yamazaki, M.; Clare, A. S.; Fusetani, N. *Proc. R. Soc. Lond. B* **1998,** *265*, 1825-1830.
10. Walker, G.; Yule, A. B. *J. Mar. Biol. Ass. U. K.* **1984,** *64*, 679-686.
11. Clare, A. S.; Matsumura, K. *Biofouling* **2000,** *15*, 57-71.
12. Engel, A.; Muller, D. J. *Nat. Struct. Biol.* **2000,** *7*, 715-718.
13. Binnig, G.; Quate, C. F.; Gerber, C. *Phys. Rev. Lett.* **1986,** *56*, 930-933.
14. Gerber, C.; Lang, H. P. *Nat. Nanotechnol.* **2006,** *1*, 3-5.
15. Janshoff, A.; Neitzert, M.; Oberdorfer, Y.; Fuchs, H. *Angew. Chem. Int. Ed.* **2000,** *39*, 3213-3237.
16. Bustamante, C.; Macosko, J. C.; Wuite, G. J. L. *Nat. Rev. Mol. Cell Biol.* **2000,** *1*, 130-136.
17. Drake, B.; Prater, C. B.; Weisenhorn, A. L.; Gould, S. A. C.; Albrecht, T. R.; Quate, C. F.; Cannell, D. S.; Hansma, H. G.; Hansma, P. K. *Science* **1989,** *243*, 1586-1589.
18. Hinterdorfer, P.; Dufrene, Y. F. *Nat. Methods* **2006,** *3*, 347-355.

Chapter 2

An introduction to marine biofouling and antifouling assessment*

2.1 An introduction to marine biofouling

Marine biofouling is the undesirable building up of microorganisms, plants, and animals on manmade surfaces immersed in sea water. It has been a major problem in several industries, in particular in the shipping industry where fouling causes severe negative effects.[1] The biological colony on the ship hull results in higher frictional resistance and substantially reduces speed and maneuverability. This results in higher fuel consumption and more frequent need of dry docking services causing enormous economic loss. Several environmental issues such as an increase of green house gas emission due to higher fuel consumption; production of large quantities of organic waste during the cleaning and repainting process, and introduction of organisms into new environments must also be considered. Figure 2.1 shows an example of a heavily fouled ship and the cleaning processing by dry docking.[1] It is estimated that the fouling problem costs the US Navy $150 million dollars per year for excess fuel consumption and cleaning costs.[2, 3] Moreover, recent estimation showed direct and indirect annual savings from reduction of fouling on the world fleet is estimated to about US $30 billion worldwide.[3, 4]

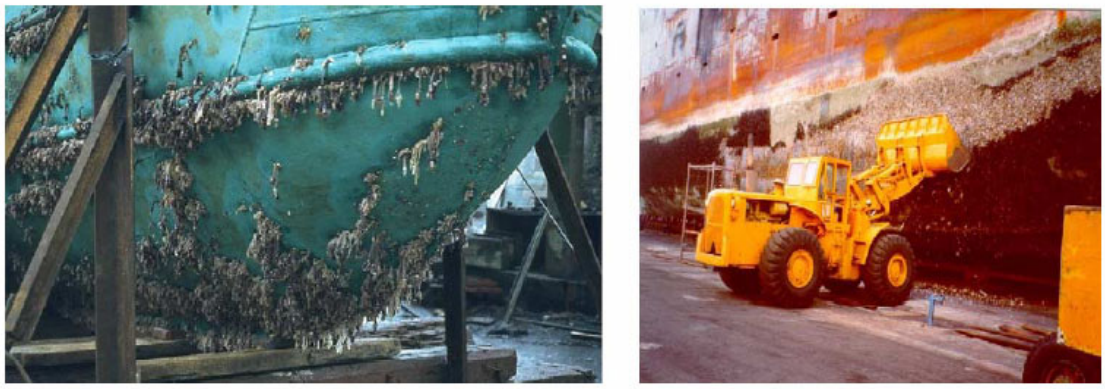

Figure 2.1. Example of heavily fouled hulls and the removal of fouling layer from the ship at dry dock.[1]

---

*A general review has been published as: I. Y. Phang, N. Aldred, A. S. Clare, G. J. Vancso. *Nano**S*** **2007,** ***01*****,** 34-39.

The fouling problem is not only restricted to vessels traveling across the globe. It is also commonly found in offshore structures, oilrigs and water-cooling pipes in power plants.[5-8] Fouling obscures sensors used in monitoring the coastal environment, corrodes the surfaces of harbor installations and blocks (membrane) filtration processes with obvious detrimental consequences.[9] The heavily fouled surfaces increase the wave loading and reduce the stability of offshore platforms. Fouling of sea water intake structures in vessels or cooling water systems of power plant reduces the effective diameter of the pipe and therefore reduces the cooling capacity.

2.2 The process of fouling

Fouling occurs in two main forms, microfouling and macrofouling, both lead to corrosion of surfaces.[10, 11] Microfouling that includes slime (bacterial and diatoms) and other microscopic algae usually occurs first, and is followed by macrofouling, e.g. by barnacles, mussels and hydroids. The fouling process has been generally categorized into four stages: i.e., formation of organic film, primary colony, secondary colony and tertiary colony. The first stage involves rapid accumulation of organic molecules, such as polysaccharides, proteins, proteoglycans, and possibly inorganic compounds on surfaces in contact with seawater, forming a so-called conditioning film (Table 2.1). Physical forces such as electrostatics interactions and van der Waals forces between surface and adsorbates govern the initial formation of conditioning film. Secondly, bacteria and single cell diatoms settle on the conditioning film, forming a primary colony. A microbial biofilm (microfouling) is formed as bacterial, diatom, protozoa and rotifiers adhere physically on the conditioning film. The presence of bioadhesives and proteins on the surface and the roughness created by the primary colony help to trap more particles and organisms, and create an environment suitable for the formation of irregular microbial colonies. A transition from conditioning film to a more complex secondary colonial community starts to form on the surface, when settlements of algal spores, barnacle cyprid, marine fungi and protozoa happen.[12] The growth of microfouling colony provides better protection from the predators, and environmental changes for easier capture of necessary nutrients. The final stage involves settlement and growth of larger marine macroorganisms, which arrive later and settle as macrofoulers. These macrofouling communities consist of organism that secrete hard calcium carbonate tubes, shells or skeleton (e.g. barnacles, mussels, tubeworms, bryozoans and corals), and soft organisms (e.g. algae, hydroids, sponges).

Table 2.1. Temporal structure of fouling settlements.[1]

	Microfouling			Macrofouling
Time	1 min	1-24 h	1 week	2-3 weeks
Substrate	Organic film	Primary colonizers	Secondary colonizers	Tertiary colonizers
	Adhesion of organic particles (e.g. protein)	Bacteria Diatoms	Spores of macroalgae Protozoa	Larvae of macrofoulers

It is known that the conditioning biofilm plays an important role in influencing the tenacity of the attachment organisms because it serves as food for young superior organisms and changes the free energy of the surface. In addition, it is widely accepted that the presence of different molecules and organisms on the film influences the settlement of subsequent organisms.[13] In order to circumvent the fouling problem, an effective and promising strategy should be based on the development of antifouling techniques that interfere with the initial settlement of superior organisms such as barnacle, mussel, at the early stage. Hence to achieve an efficient antifouling solution, more research should be focused on the fundamental studies of the bioadhesion in the early stage (larva) of species development and the interactions between different organisms.[14]

2.3 Fouling organisms

All marine biofoulers use special underwater “glues” to attach themselves temporarily or permanently to surfaces. The interactions between the corresponding adhesive materials and the substrate involve two main mechanisms, i.e. wetting of the substrate by the adhesives and curing of the adhesives on the surface. However, the physiochemical nature of these underwater adhesives remained largely unknown.[15-17] The production of extracellular polymeric substances (EPS) by microorganisms is unequivocally accepted as a key mechanism facilitating the irreversible attachment of microorganisms in aqueous environment. It is now generally acknowledged that microbial EPS is a complex mixture of macromolecules such as proteins, polysaccharides, lipids, and nucleic acids.[18] Their composition and properties are affected by the microbial species and its physiological status and a wide range of environmental factors.[18] In this section, the adhesion proteins of several fouling organisms and the physiochemical nature of their adhesives are discussed. These

fouling organisms include diatom, alga, mussels and adult barnacles, as shown in Figure 2.2. [19-23]

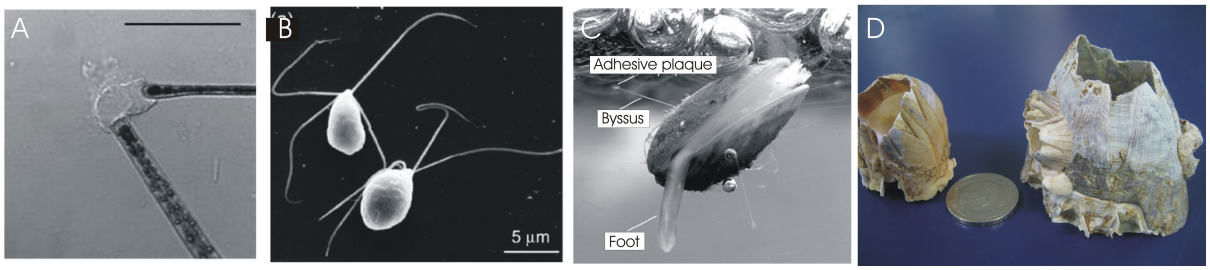

Figure 2.2. Different fouling organisms commonly found on ship hull, (A) diatom,[24] (B) alga,[11] (C) mussel[25] and (D) barnacle.

2.3.1 Diatom

Diatom is a significant component of marine biofilms formed on all wetted and illuminated surfaces. They are unicellular microalgae encased in siliceous cell wall, called the frustule. Diatoms exist in nature as benthic (organism that attach to a sediment surface) and/or planktonic (free-floating) forms. Some diatoms adhere to the substratum by releasing bioadhesive through a distinct slit in the frustule called the raphe. The attached cells divide, rapidly giving rise to colonies that eventually coalesce to form a compact biofilm, with maximum achievable thickness of 500 µm (Figure 2.2A).[18, 24, 26-30]

The adhesion of benthic diatoms is associated with the secretion of mucilaginous materials or extracellular polymeric substances (EPS) which are complex and multi-component materials. Early studies revealed the carbohydrates dominating in diatom EPS. These studies suggested that the carbohydrates comprise of complex, anionic polysaccharides with heterogeneous monosaccharide composition, sulfate ester, and/or uronic acids. Neutral monosaccharides that have been identified include hexoses, pentoses, 6-deoxyhexoses, and o-methylated sugars. The structures, properties, and compositions of diatom EPS vary according to the function. The composition and properties of the adhesives also vary between diatom species.[23, 24, 27-31]

2.3.2 Alga

The green alga *Ulva* is known as the slippery grass-like plant that covers rocks in the intertidal zone. *Enteromorpha* colonises new surfaces through the production of vast quantities of microscopic motile spores (Figure 2.2B). Swimming spores attach rapidly once they have ‘detected’ a suitable surface for settlement, resulting in firm attachment to the

substratum. This is followed by an irreversible adhesion that involved withdrawal of flagella and the secretion of a powerful adhesive.[11, 32-34]

2.3.3 Mussel

Mussels (*Mytilus, Dreissena* and *Perna*) cause a serious and persistent fouling problem concerning particular aquaculture nets, off-shore rigs and industrial coolant outflows (Figure 2.2C).[6, 35, 36] Mussels produce threads to attach themselves to solid surfaces in the intertidal zone. Individual adhesive proteins from mussels are produced by the foot organ of the animal, where it forms a strong underwater attachment. The underwater adhesion is formed by reactive and oxidized form of 3,4-dihydroxyphenylalanine (DOPA) to provide the water-resistance characteristic.[37-39] DOPA is formed by the hydroxylation of tyrosine residues by a polyphenoloxidase (tyrosinase). It has been shown that DOPA can complex with metal ions and oxides (Fe^{3+}, Mn^{3+}) and thus explaining its ability to adhere to rocks and glass.[40-42] The catecholic content of mussel adhesive proteins has been linked by hydrogen-bonding and strong metal-ligand chelating.[16, 22, 40, 41, 43-46]

2.3.4 Barnacle

Barnacles are of particular concern because of their large size that causes vast increase in hydrodynamic drag on vessels; significant increase in fuel costs and the necessity for costly cleaning procedures (Figure 2.2D).[47] Prior to the attachment on surface, the cyprids larvae of barnacles explore surfaces by using a pair of attachment organs ‘antennules’ (see next section for more details). In this exploratory phase, the cyprids are capable of temporarily attaching onto and detaching from surfaces. To complete the transition to adult life, the cyprid form of barnacle larvae must permanently attach to a hard substrate.[48-53]

The adult barnacle cement fixing the barnacles permanently to substrates is substantially different from mussel adhesives. They comprise of three groups of proteins that contain high levels of the amino acids serine, threonine, glycine, and alanine.[25, 54] The adult barnacle cement is layered between the calcareous base and foreign substrate, which can be >5 μm in thickness, depending on the surface energy of the substrate.[55, 56] The cement is highly proteinaceous with more than 90% of its content is multiproteins complexes proteins.[15, 19, 21, 54] In addition, the cement composed of more than 10 different cement proteins (CPs), of which four have not yet been identified. Five of six identified CPs (Cp-100k, Cp-52k, CP-68k, CP20k, and CP-19k) are novel in respect of their primary structure, and the six CPs (CP-16k) is kind of enzyme.[19, 21]

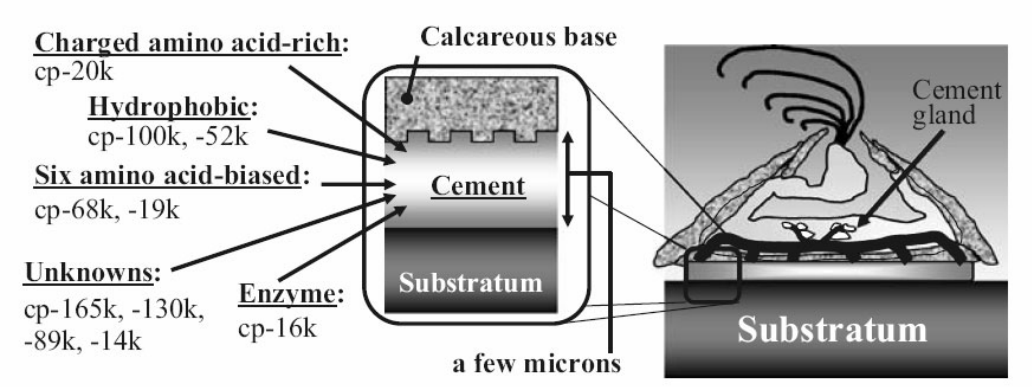

Figure 2.3. Cross-section of the acorn barnacle. The cement is biosynthesized in the cement gland and is transported via a duct to the narrow gap between the animal's own calcareous base and the foreign substratum. The thickness of the cement layer is generally only a few microns. The cement, which is a multiprotein complex, joins the two different materials in water.[21]

The instantaneous functions of barnacle cement would include the displacement of water bound to the surface, and promote spreading of adult cement and coupling the secreted cement to the surface after the extrusion of cement (Figure 2.3). Several cement proteins, i.e. CP-19k, CP-20k and CP-68k are candidates for these functions. CP-16k is probably a lysozyme, which is responsible for removing the biofilm and protecting the cement from microbial degradation, may also help on the spreading and adsorption to the surface.[19] Almost simultaneously or immediately after successful coupling between the substratum and its own calcerous base, cement proteins (CP-52k and CP-100k) self-assemble together to join the two materials through intermolecular hydrophobic interaction or by another mechanism.[21] Following this self-assembly process, curing may occur to make the holdfast stiff and tough, whereby further intermolecular cross-linking may be involved in the process.

2.3.4.1 Life cycle of barnacle

In this Thesis, we focus on the barnacle biofouling and hence a short introduction to the biology of barnacles is discussed here. Barnacles exhibit a metamorphic life-cycle consisting of several stages. Figure 2.4 shows the life history of barnacle. A generalized barnacle life-history includes 6 planktotrophic "nauplius" stages, a non-feeding "cyprid" stage and an adult stage. After fertilization, the eggs are reared on the mantle cavity until the release as free swimming planktonic nauplius larvae. During the moult from the sixth stage nauplius to the cyprid, the structure of the body is reorganized to a bi-valved carapace. The antennules of the cyprid are much altered in structure and function from those of the nauplius

stage (Figure 2.5). It is the cyprid that is of most interest to anti-biofouling studies, as this is the stage that involves the exploration of submerged surfaces in search of appropriate settlement sites. The cyprid depends on its ability to attach to solid surface for survival. The reason for this is simple: the roughest waters may challenge the animal's tenacity but, succeeding in this, the cyprid profits directly from the abundance of dissolved nutrients and rapid rate of gas exchange. Failing in attachment on surface, the cyprid is to be dislodged and crushed by the waves.[44]

During exploration, the cyprid scrutinizes the substrata by using a paired antennules to walk in a bi-pedal fashion. The antennules of the cyprid become adapted as walking appendages and are equipped with unicells secreting temporary glycoproteinaceous adhesive. The third segment of the antennule has become adapted both as an adhesive disc and as a sensory probe with the sensory fourth segment arising laterally. A combination of electrostatic adhesion and a glycoproteinaceous secretion, originating from unicellular glands within the antennules, are thought to be the mechanisms allowing cyprids to temporarily attach to surfaces under water.[57] It has been observed that cyrid test substrate surfaces by placing the disc and then attempting to withdraw it. When the substrate is favorable the disc is less easily detached and the force of adhesion may play a role in the recognition on a suitable settlement site.[49]

Once a settlement site has been selected, permanent cyprid cement is released from each of a pair of cement glands in the body of the larva. [58-61] The glands consist of two cell types which produce protein and protein with phenols and polyphenol oxidase respectively.[62] The secretions mix after exudation and the presence of phenols and polyphenol oxidase indicate that *quinine tanning* (cross-linking of proteins) resulted in permanent setting of the cement. The cyprid adhesive cures rapidly with maximum strength obtained within 3 hours. Cyprid permanent cement may only be exuded once and serves to maintain the attachment of the metamorphose barnacle until the adult cement system has developed sufficiently to produce new cement, about 40 days in *Balanus amphitrite* (Figure 2.6).[60, 63]

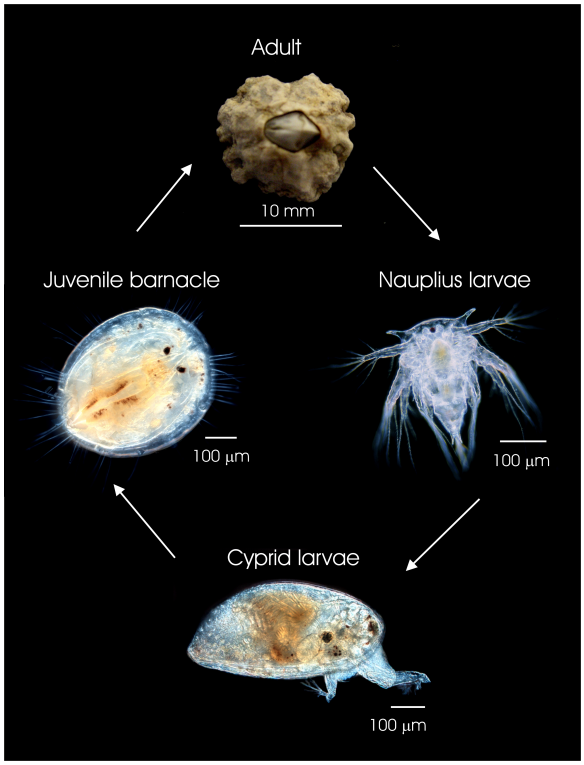

Figure 2.4. The life cycle of a barnacle[64]

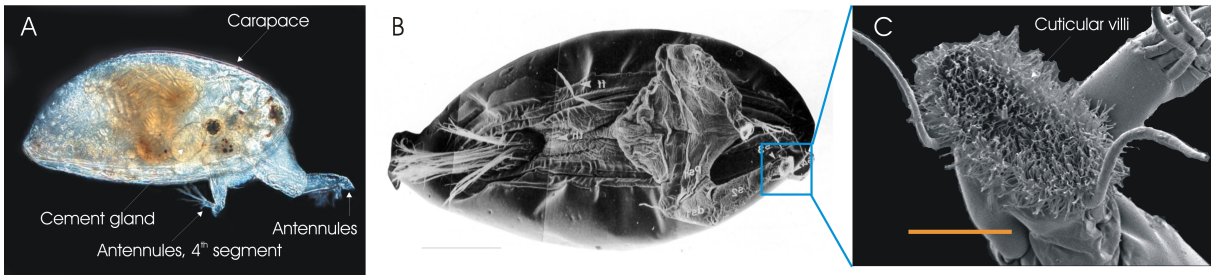

Figure 2.5. (A) The optical micrograph of a barnacle cyprid, (B) SEM montage taken from Glenner et al.[65] and (C) the ultrastructure of the antennular attachment disc from *B. amphitrite*. Scale bars: B = 100 µm and C = 10 µm.

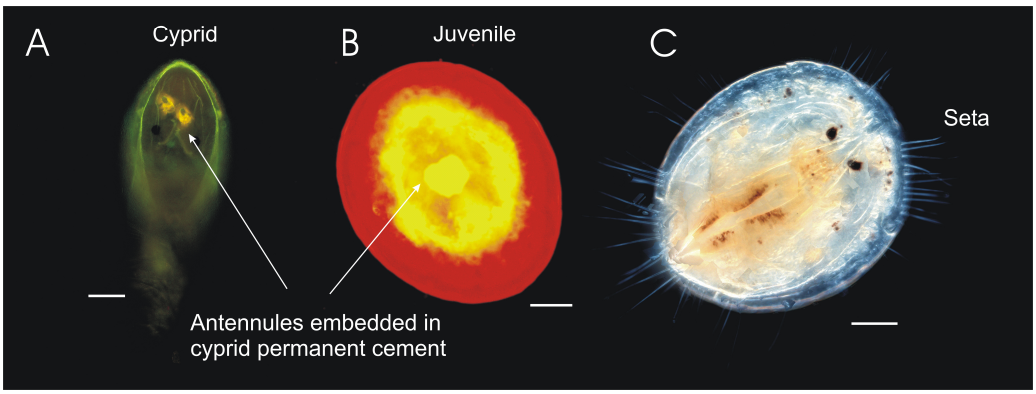

Figure 2.6. Fluoresceinamine label cyprid permanent cement (A) cyprid and (B) juvenile barnacle. (C) Optical micrograph of juvenile barnacle. (All scale bars are100 µm)

2.3.4.2 Cyprid larva culture and collection

B. amphitrite cyprids were cultured as described by Hellio *et al.* for this study.[66] Briefly, adult *B. amphitrite*, collected from North Carolina (USA) and Japan, were maintained in ~26 °C aquaria at Newcastle University in natural sea water (Figure 2.7). The water was changed once per day; prior to the barnacles being fed with freshly hatched *Artemia* sp. nauplii (*Artemia* International, USA). Barnacle nauplii were released by adults after aerial exposure of ~14 hours. During exposure, adults were kept moist using damp laboratory roll. On re-immersion, nauplii released by the barnacles were attracted towards a fibre-optic 'cold' light source where they were collected and placed immediately into 10 μm filtered seawater containing *Skeletonema costatum*. Ten thousand nauplii were cultured at 1 larva ml^{-1} in a single 10-litre bucket where the seawater was constantly aerated and 750 ml *S. costatum* solution was added every day. Nauplii were incubated at 28 °C and usually metamorphosed into cyprids in 5 days under these conditions. Following metamorphosis, cyprids were collected by filtration and stored at 6 °C until use. *S. balanoides* cyprids were collected by plankton tow from the wild population at Cullercoats, NE UK (55.1N 1.26W) and were also stored at 6 °C prior to use.[64] cyprid larvae were stored in a 50 ml sterile culture tube and post it to Twente in a cold box. Cyprid used for the experiment were generally from day 3 onwards and most of the time the experiment finished with cyprid of day 6. Culturing and collection was performed by Dr. Nick Aldred in University of Newcastle.

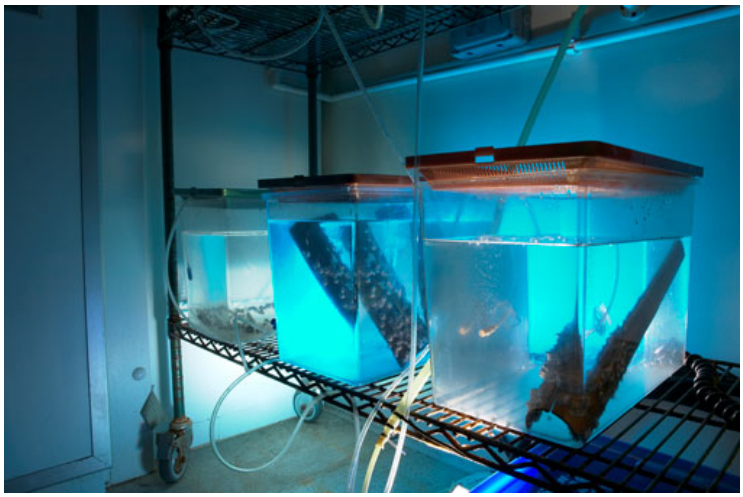

Figure 2.7. *B. amphitrite* culture at Newcastle University (blue light was not used during culture).[64]

2.3.4.3 Barnacle gregarious settlement and settlement inducing protein complex (SIPC)

Nature appears to have developed strategies to encourage gregarious and associated settlements, i.e. group settlement behavior. Barnacle gregarious settlement is induced by specific surface or waterborne chemical cues from the exploring cyprid or adult barnacle (conspecifics). Whereas associated settlement is the response of larvae to chemical cues from food, hosts, symbionts, and specific substances prior to permanent settlement.

The chemical basis of gregarious settlement of barnacles has been studied for the past five decades.[13, 48, 67-69] Studies have shown that cyprid larva of barnacles is able to distinguish between adults of their own and other species. The extracts of barnacles applied to slate surfaces promoted the settlement of larger numbers of cyprids than the untreated controls. A surface associated factor "arthropodin",[13, 48] extracted from adults shells of *Balanus balanoides*, was shown to be able to induce barnacle gregarious settlement. Arthropodin extract from conspecies showed stronger stimulus for settlement of cyprid larva than arthropodin from other species. The arthropodin was not unique to each species but belongs to a class of glycoprotein.[70, 71] Larman et al.[70] presented a physicochemical characterization of the settlement factor of *S. balanoides*. The settlement factor in the adult extract was identified as a polymorphic system of a closely related protein derived from subunits of molecular mass between 5000 to 6000 and 18000 daltons. The settlement inducer of *B. amphitrite* has been purified and termed the settlement inducing protein complex (SIPC).[72] The SIPC is a glycoprotein of high molecular mass, consisting of three major subunits of 76, 88 and 98 kDa, all with lentil lectin (Lens culinaris agglutinin, LCA)-binding sugar chains.[72-74] Recently, Dreanno showed that SIPC is a glycoprotein complex, i.e. α_2-macroglobulin-like protein, present in or comprise entirely of barnacle cyprid footprint materials.[75-78]

2.3.4.4 Barnacle adhesion processes

There are at least four distinct adhesion mechanisms occurring in the entire life history of barnacle, i.e. temporary adhesive during cyprid exploration, cyprid permanent cement for settled cyprid larva, "pinhead" seta adhesion (see Figure 2.6C) at juvenile barnacle and finally adult barnacle cement at adult stage. During the pre-settlement exploratory phase, cypris larvae "walk" on its two antennules (see Figure 2.5C) which adhere temporarily on surface by antennules consisting of a dense cloak of minute cuticular villi (Figure 2.5C for *Balanus amphitrite* and Figure 2.8B for *Semibalanus balaniode*) with typical dimensions of 0.2 μm x 2 μm. A thin layer of glycoproteinaceous secretion is secreted via the cuticular hairs (Figure 2.8A). It subsequently provides a firm adhesion that allows the cyprid

to temporarily attach to surfaces underwater. Once settled, a relatively large volume of larval permanent cement is discharged immediately through pores in the attachment disc from the major cement glands (See Figure 2.5A) on either side of the body. This large blob of permanent cement embeds both antennules to prevent further translation. Approximately a week after metamorphosis, the basal area of the "pinhead" adheres to the substratum by a mechanism that is not yet understood. As the adult barnacle develops, the secondary cement glands are formed, adult cement is spread between the base and the substratum. Adult barnacle cement is largely proteinaceous, which probably cross links on curing. It also contains a high proportion of amino acids with hydroxyl groups, characteristics of many tacky materials.[15, 19, 54, 69, 79, 80]

2.3.4.5 Barnacle cyprid larva footprints

As mentioned in the previous section, cyprid larvae utilize footprint secretions to facilitate temporary attachment to the surface. Walker et al. showed that the antennular discs were covered with footprint materials in glutaraldehyde treated cyprid (Figure 2.8).[57] However, there was no trace of secretion found when individual cyprid were monitored under optical microscope and scanning electron microscope (SEM). [81] Any evidence of the presence of a footprint secretion would suggest that thin film adhesive was used to trap the disc to the substratum and to facilitate a stronger adhesion with surface. Nevertheless, indirect footprint visualization can be achieved *ex situ* by staining the cyprid explored area with coomassie blue Bio-Rad protein dye reagent (CBB).[57] The size of the blue color stained area by CBB was in close agreement with the antennular size of the *Semibalanus balanoide*. Clare et al. adopted similar staining procedures to visualize the footprints of *Balanus amphitrite.* The footprint sizes were about 34 μm, which is in good agreement with the antennular disc diameter (d = 30 μm) of *B. amphitrite*.[53, 82] Another more specific staining method was developed by Matsumura et al., which ultilized anti-76 kDa antiserum to target toward *B. amphitrite* footprints (Figure 2.9).[74]

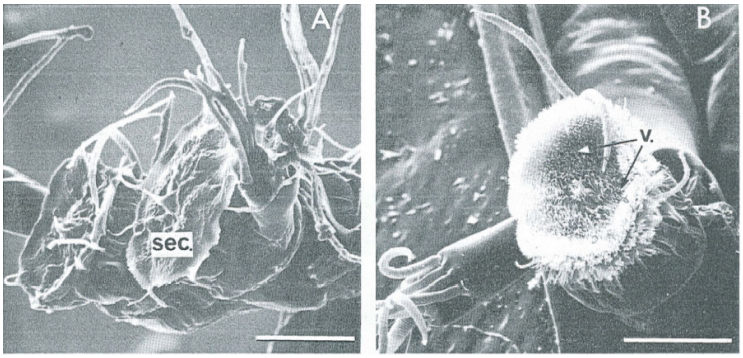

Figure 2.8. (A) Scanning electron micrograph of the secretion on the antennular discs. Scale bar is 20 μm. (B) Scanning electron micrograph of the antennular disc of larva. The secretion has been lost, hence exposing the cuticular villi.[57] Scale bar = 20 μm.

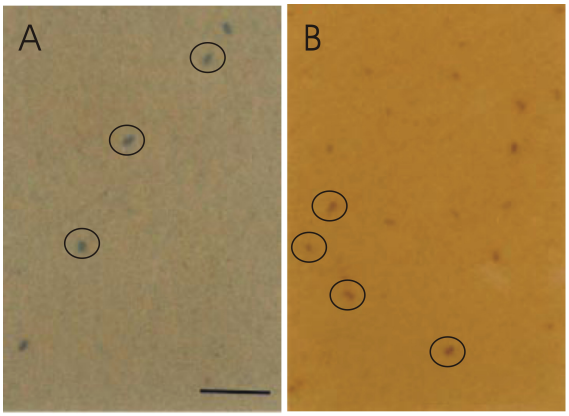

Figure 2.9. Footprints (marked as circle) stained with (A) CBB and (B) anti-76-kDa antiserum on nitrocellulose membrane. Scale bar = 200 μm.[74]

2.3.4.6 Barnacle cyprid larva adhesion strength

The adhesion strength between the cyprid larvae of *S. Balanoide* were measured by Yule at al..[49-52] The authors attached the cyprid to a nickel-chromium wire by acrylate glue, in which the cyprid remained robust and alive. The cyprids were then allowed to walk on the surface. Once the cyprids started exploration on the surface, the surface was gently lowered and the detachment force was measured using a microbalance. The detachment force was determined as a function of season of settlement.[49] Their studies showed that the average adhesion force of cyprid footprint to the surface was comparatively higher (0.2 – 0.4 MPa) during the main settlement period (mid April to early May) as compared to non-settlement period, i.e. lower than 0.1 MPa. Their finding showed that cyprid employ an adhesion equivalent to 2 - 3 atmosphere pressure for the temporary attachment on the surface during exploration, which excludes the suction mechanism used during temporary attachment.

2.4 History and development of antifouling systems

The problem of marine biofouling has been recognized and tackled for more than 2000 years. Antifouling activities have been dated back to the Greek and Roman times when copper sheathing was used to prevent fouling. This sheathing technique later became widely used in vessels around the world. The first record on the use of copper as an antifoulant is a lethal recipe with the combination of arsenic; copper and gunpowder. It is a British patent filed by William Beale in 1625.[1, 10] Around 18th century, copper sheathing was the most efficient resistance to biofouling in wooden ship and was used in the British Navy. England even forbid the export of copper and it was labeled as "war material" in the 1780s. The antifouling mechanism of copper sheathing became known only in the 19th century when Sir Humphry Davy studied the cathodic protection of ship hull and found the dissolution of copper in seawater which prevented biofouling.[83, 84]

In 1841, Mallet patented an antifouling paint with slightly water soluble poisonous materials. However this paint lacked the control of the abrasion and solubility rate in seawater. A century later, in 1958, Montermoso and co-workers[1] suggested the possibilities of using tributyltin (organotin) acrylate ester as an antifouling coating. In their protocol, organotins were initially used as co-toxicants in copper paints. (Table 2.2).[1] In 1970s, the introduction of self polishing copolymers (SPCs) containing copper, tin and other metallic compounds was widely accepted as a effective and cheap "silver bullet" for combating fouling.[85] Highly poisonous metal containing paints, i.e. tributyl tin SPC (TBT-SPC paints) covers approximately 70% of the present world fleet. It is the most successful approach nowadays to prevent biofouling on ships and has led to huge economic benefits.[86] The direct and indirect annual savings due to the reduction of fouling on world fleet is estimated to about US $3 billion worldwide and an annual fuel saving of 7 million tones.[3]

Table 2.2. Historical development of antifouling systems in chronological order.[1]

Year		
2000 years ago	Early Phoenicians and Carthaginians	Copper sheathing on ship's bottoms
5th century B.C.		Arsenic and sulphur mixed with oil
3rd century B.C.	Greeks	Tar, wax and even lead sheathing
10 A.D.	Vikings	Seal tar
13th to 15th century		Pitch, pitch and tallow
1618	Danish King Christian IV	First underwater use of copper
1625	William Beale	First British patent of copper as an antifoulant
1758	HMS *Alarm*	First authenticated use of copper sheating
1841	Mallet	Patented a slightly soluble coating s of poisonous materials
1860	James McInness	Hot-plastic paint, used copper sulphate as antifoulant in a metallic soap composition
1863	Jame Tarr and Augustus Wonson	US patent for A/F paint using copper oxide in tar with naphtha or benzene
1906	US Navy	Tested hot-plastic and othe A/F paints at Norfolk Navy Yard
mid 1950s	Van de Kerks et al.	A/F possibilities of high toxicity TBT-containing compounds
Early 1960s		Excellent A/F properties of the TBT moiety were discovered and commercialized
1974	Milne and Hails	Patented TBT-self polishing paints (TBT-SPC)
1987	International Coatings	Foul release coating, ,Intersleek was applied to company yacht *Artemis*
1990		Tin-free antifoulants

2.4.1 Tributyltin self polishing copolymer paints (TBT-SPC)

Montermoso and co-workers first suggested the possibility of using TBT acrylate esters as antifouling coatings in 1958.[1] Later, TBT self-polishing copolymer technology patented by Milne and Hails[87] in 1974, revolutionized the antifouling paints and achieved worldwide acceptance quickly by the shipping industries. These tributyl tin self-polishing antifouling paints are based on an acrylic polymer (usually hydrophobic polymer such as methyl methacrylate) with TBT groups bonded onto the polymer backbone by an ester linkage (Figure 2.10). At the beginning, ZnO was used as a biocide together with insoluble pigments. The poor antifouling activity of zinc ions was compensated for by high removal rates. The shift to cuprous oxide (Cu_2O) made it possible to reduce the removal rate and attain a better efficiency against algae fouling. [1, 88, 89]

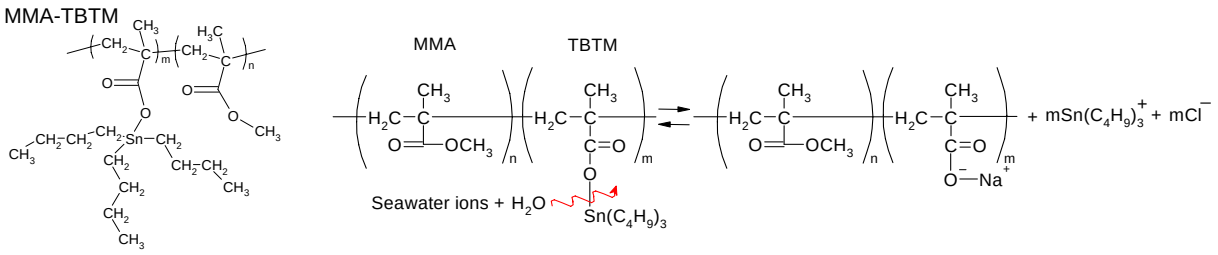

Figure 2.10. Chemical formula of a repeating unit of a copolymer of tributyltin methacrylate (TBTM) and methyl methacrylate (MMA). Controlled release mechanism of TBT copolymer by hydrolysis.[90]

After immersion, the soluble pigment particles in contact with sea water begin to dissolve and leach into seawater. The copolymer of TBT methacrylate and methyl methacrylate in the paint are hydrophobic, which prevents sea water from penetrating into the paint film. Thus, sea water can only fill the voids created after the dissolution of the soluble pigment particles. The carboxyl-TBT linkage is hydrolytically unstable under slightly alkaline conditions. This is usually the case in marine waters, and results in a slow, controlled hydrolysis that cleaves the TBT moiety form the copolymer. This hydrolysis reaction takes place, to varying extent throughout the leached layer (Figure 2.10).[90]

With time, the seawater slowly dissolves more pigment particles and extends the reacting zone (the leached layer). Once a sufficient number of TBT moieties have been released from the paint film surface, the partially reacted brittle polymer backbone can be easily eroded by the moving sea water and exposes a less reacted paint surface (self-polishing effect). This antifouling coating is easy to apply and could provide protection against

biofouling for several years. The roughness of end coating is not exceeding 100 μm in average hull roughness which ensures low levels of the hydrodynamic drag. The dissolution of biocides (copper) provide wide range of protection particularly effective against animal fouling, whereas the TBT, which is released through hydrolysis, is effective against copper-resistant slime and weed fouling.[91]

However the success of TBT-SPC was not long-lasting. Marine biologists have assembled the evidence of the negative effects of TBT on coastal marine life. The main reason for the adverse effects may be due to the direct dumping of organic waste containing tin during dry docking.[92-95] The toxic compounds accumulated in the marine environment was found to be severely harmful to the non-targeted organisms.[96] It has been shown that extremely low concentrations of tributyltin moiety (TBT) can cause defective shell growth in the oyster and imposex. As a result, a worldwide ban on the use of TBT was implemented effectively from 1 January 2003, and the presence of such paints on the surface of the vessel from 1 January 2008. The ban of TBT has prompted an increase in research into funding sustainable antifouling alternatives. The paint industry has been urged to develop TBT-free products that yield the same economic benefits and cause less harmful effects on the environment. Currently, new environmentally friendly approaches are based on other biocidals (coppers) or non-toxic solutions such as natural antifoulants in the coatings or the design of surfaces with microstructures to mimic nature to prevent the settlement of marine organisms.[97, 98]

2.4.2 Development of tin-free antifouling systems

After an International Convention held on 5 October 2001 in London, parties are required to ban the application of TBT-based antifouling (A/F) paints from 1 January 2003, and the presence of such paints on the surface of the vessel from 1 January 2008. Therefore, news designs of antifouling coatings are urgently needed. The following section introduces several different alternative designs that might be suitable for the future requirements.[1, 93, 94] The future challenges include developing a polymer system, which may acts as a controlled release vehicle for suitable antifouling biocides but having no side effects to non-target organisms and no accumulation potential in the environment.[91] Other approaches to engineering designer surfaces with controlled chemical composition, surface pattern, and surface mechanical properties (passive protection) have also been considered.

Though TBT-containing paints are facing bans, the TBT-SPC paint system with its unique features provides a basis for the development of new, non-toxin SPC paints to be used

as delivery systems for environmentally non-hazardous biocides. However, developing a product with similar characteristics as TBT-based paints is not an easy assignment. To achieve a controllable biocide release system in the acrylic polymer backbone, factors should take into accounts such as steric and electronic interaction with the complex chemical neighborhood (co-binder, additives, pigments and etc.).[99]

2.4.3 Biocidal antifoulings

Biocidal antifoulings depend for their effectiveness on both the biocide itself and on the technology used to control the biocide release, or leaching rate. Copper is one of the main biocide used in TBT free antifoulings, together with rapidly degrading boosting biocides which do not accumulate in the marine environment.[100, 101] The release of the biocides is typically controlled using high Rosin product, which slowly dissolves in sea water over time. This product is referred to as controlled depletion polymer (CDP). The deliver of biocide could be achieved by using self-polishing polymer or combination of CDP and SPC technologies.

As chemical companies developed these new resins, they upgraded and improved soluble matrix antifoulings, i.e. the main polymer binder must be soluble in water, providing increased film integrity and toughness. Continuing improvement has resulted in Controlled Depletion Polymer (CDP) antifoulings available today. Most marine paint companies market their own versions of CDP antifoulings, and use a wide variety of nomenclatures to describe them. Typical of these are “Eroding”, “Ablative”, “Polishing”, “Hydration”, “Ion Exchange”, ”Hydrolysable Activated” and “Self-Polishing”. The common feature in all of these products is the high proportion (> 50 %) of Rosin, or Rosin derivatives, in the binder component. The main biocide used in CDP antifoulings is copper oxide, together with boosting biocides. Over the past decades, the following tin-free antifouling paint systems have been introduced commercially to replace the TBT-SPC:[102-107]

A) Copper-acrylates (Nippon Paint: Ecoloflex SPC I, International Paint: Intersmooth Ecoloflex)[102]

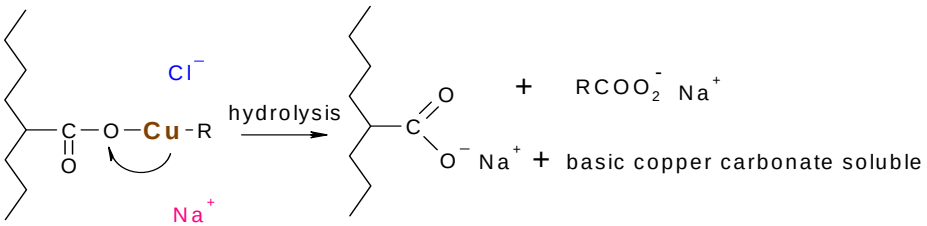

It is questionable whether this highly polar system works kinetically in the same way as the TBT-SPC system. In this system, the release of copper compounds is insufficient to provide biocidal efficacy; thus, booster biocides and high loadings of copper compounds are necessary.

(B) Ionexchange copolymers (Kansai Paint: Exion)[107]

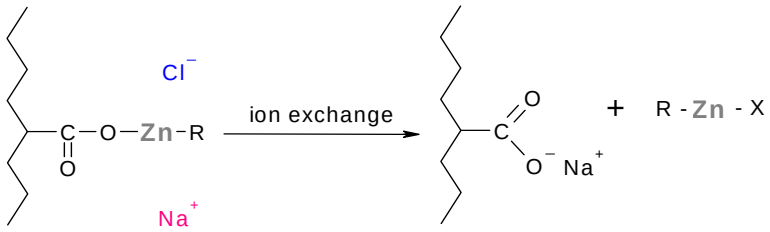

It is postulated that the ion exchange mechanism is a one step mechanism and works differently than the TBT-SPC mechanism. Further biocide loading is necessary if the paint is to maintain its efficacy.

(C) Silane functionalized methacrylates (Chugoku Marine Paint: Sea Grand Prix)[104]

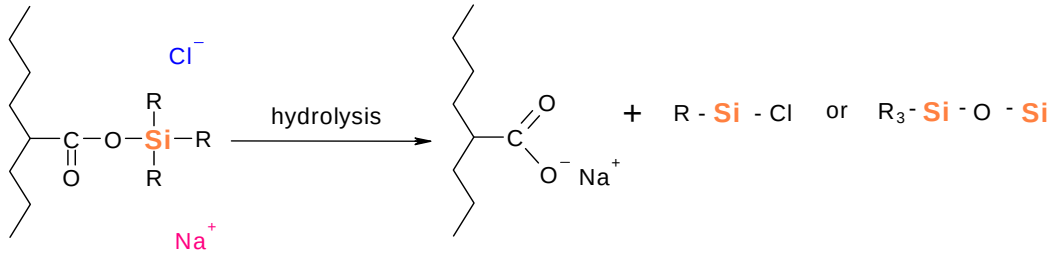

This class, in which the tin atom is substituted by silicone, is chemically quite similar to the TBT system. However, the alkyl substituents must be carefully selected and the entire system must be combined with internal or external plasticizers to create the desired hydrolysis rate. Since the Si-C bond is stronger than the Sn-C bond, it is expected that the released alkylsilanes might be persistent in the environment. If these systems are introduced on a large scale, it must be proven that there are no effects to the marine ecosystem. Also these paints are effective only with combinations of copper compounds and booster biocides.

2.4.4 Fouling release coatings (FRC)

Another alternative to biocides-based paints under development is the foul release paint which is the only non-toxic method of fouling control. This is a form of nonstick coating, based on silicone, which provides a very smooth, slippery surface, often called fouling release coatings.[87, 105, 106, 108] Over the past twenty years, the fouling release technology has progressed from a novel concept, to feasible solutions for a range of marine applications. The design of coating materials are largely based on low-modulus, lubricious silicone polymers (e.g. polydimethylsiloxane) [87, 109, 110] or fluoropolymers. It is important to distinguish the modes of fouling control between the FRC and the toxic antifouling paints. The FRC relies on the easy release of accumulated foulings from the coating under hydrodynamic shear, i.e., when the vessels are moving. The fouling release property of the coatings can be further improved by the incorporation of low molecular weight silicone elastomers.

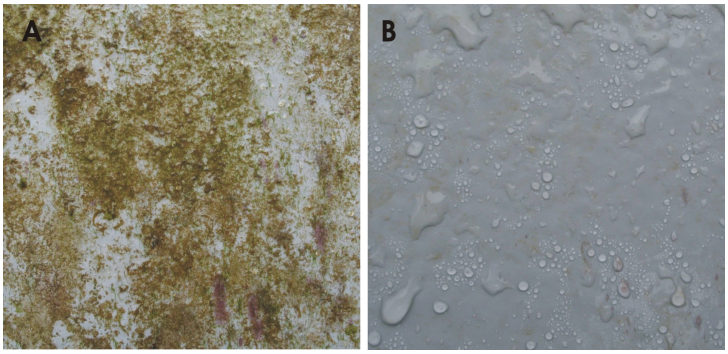

Figure 2.11. Fouling release panel (Intersleek 425) (A) after exposed in field test for 3 weeks and (B) after cleaning with water jet. (Courtesy by Dr. Serena Teo, Tropical Marine Science Institute, National University of Singapore, Singapore.)

Fouling release coatings are non-toxic, hence the coating will most probably still fouled, on vessels that are mostly moored. However, the fouling organisms are only weakly attached, and much of the fouling will be 'released' in response to hydrodynamic forces when the vessel moves in the water. For vessels that operate regularly at high speed, the hydrodynamic shear forces will keep the hull in a foul-free condition. Macroalgae and some hard foulers such as barnacles can be detached relatively easily from such surfaces. But diatom slimes,[24] oysters and tubeworms become attached tenaciously on surfaces. Hence they cannot be easily removed at high speed. To keep the surface in pristine condition, the coating may also require some cleaning (see Figure 2.11). Silicone elastomers are also expensive and prone to tearing, so are only employed at the present time for specific applications, such as on

high speed vessels (around 30 knots) (where release of biofouling is effective) and in locations where toxic paints are prohibited.

To circumvent the diatom fouling on FRC surface, Ober et al. have prepared comb-like block-copolymers with amphiphilic side-chains of ethylene oxide and fluorinated methacrylate.[111-113] This unique block-copolymer structure allows environment dependent surface reconstruction by simple flipping of the side chains. The thin layer of ethoxylated fluoroalkyl side chains allows a uniform change throughout the surface, without complex topographic changes. Surfaces of the comblike block copolymers with ethoxylated fluoroalkyl side chains are unique because they show a high removal of both green alga *Ulva* and diatom *Navicula* .

2.4.5 Enzyme based antifouling coating

The low surface energy fouling release surface is not the “silver bullet” for the marine biofouling solution.[112] Currently, fouling release coatings only occupy a small portion of the marine coating market (~ 5%) owing to its relatively high cost and low durability. The boat owners often opt for a cheaper and biocidal alternative. The mode of action of FRCs also restricts their applicability to the relatively fast-moving vessels.

Enzymes are environmental friendly due to its rapid biodegradibility. Enzymatic antifouling is used to interfere directly with the adhering fouling organisms by degrading the adhesives and reducing the ability of the fouling organisms attachments. Commercial enzymatic products have been shown to be harmless to the environment, they are the potential candidates to replace biocides as AF additive. However, to obtain an effective and general enzyme-based industrial coatings based on single or a few enzymes is still far fetched.[114, 115] Thus, more efforts are needed to develop a universally applicable antifouling solution for vessels of all kinds that against a broad range of fouling organism. The most widely held view is that the preferred future antifouling system includes a bioactive ingredient, with moderate non-target toxic effect, incorporated in a marine paint to deter colonization rather than killing the established foulers.[97, 98, 116, 117]

2.4.6 Surface topology control

In marine environment, the evolution of fouling prevention involves different strategies and different antifouling mechanisms.[118] In particular, the physical defenses of natural organisms such as surface roughness and different surface topology have inspired a different perspective in coatings design. In this section, we will focus on the effect of surface topology that hinders the fouling process. In nature, several marine organisms, plant and

animals have shown specific surface structures that prevent or inhibit fouling. These organisms include mussels,[119-121] sea star,[122] shark[123-125], etc.. These types of natural antifouling surfaces have been subject of growing interest over the past decades. Surface roughness and micro-topological features of artificial surfaces and their influence on cell,[126-128] larva settlement[129-131] and accumulation[132-137] have been under intensive investigation.

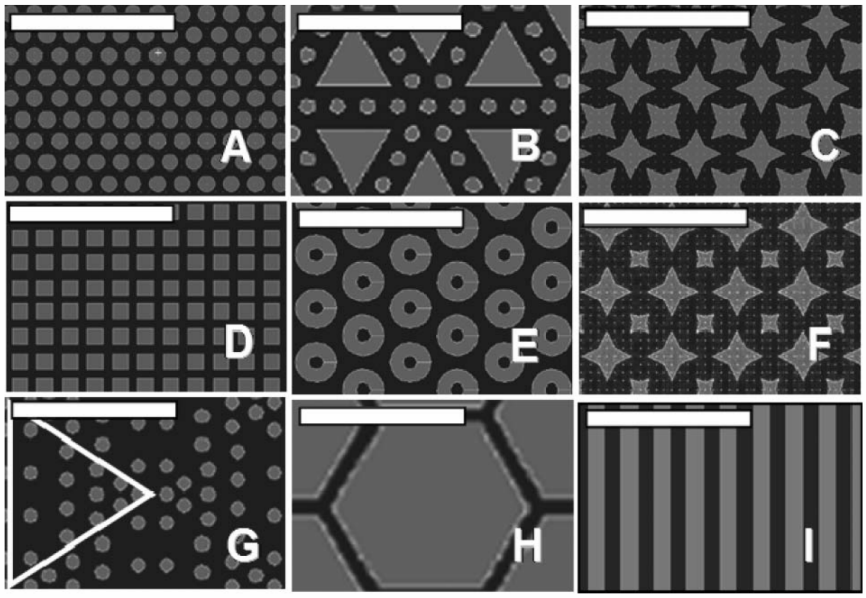

Figure 2.12. AutoCad sketches of proposed topographies of Sharklet™. (A) 2 μm diameter, 2 μm spaced pillars; (B) triangles and 2 μm pillars; (C) 4 μm wide, 2 μm spaced stars; (D) 2 μm wide, 1 μm spaced square pillars; (E) Rings with 2 μm inner diameter and 6 μm outer diameter, spaced 2 μm apart; (F) 4 and 2 μm wide stars; (G) 2 μm diameter pillars spaced 1, 2 and 4 μm apart in a gradient array (repeat unit designated by triangle); (H) Hexagons with 12 μm long sides and spaced 2 μm apart; (I) 2 μm wide, 2 μm spaced channels. Scale bars = 20 μm.[136]

Current strategies exploit the surface topology based on the consideration of the length scale of settling body of each target fouling organisms.[135] Micro- and nano-scale topology could be tailored across the length scales to tackle from bacterial (< 1 μm), green algae (5-7 μm) and up to barnacle cypris larvae (~ 500 μm for *Balanus amphitrite*).[135] For example, Callow et al.[136] created artificial topology inspired by the skin of shark (Sharklet™) with different arrangements combining of pillars and ridges as shown in Figure 2.12. These artificial topological surfaces were replicated with low surface energy coating, i.e. polydimethylsilane (PDMS) elastomer. The settlement of zoospore was reduced by 85% on

the finer (i.e. 2 μm) and more complex topology. This result demonstrated that engineering micro-topology could inhibit the settlement of spores of a marine alga via biomimetic surface design inspired by nature.[132-136]

2.5 Antifouling coating assessment methods

Tests are performed on the antifouling paints/coatings to evaluate the design and to improve the paints/coatings formulations. These tests can be applied to the entire group of formulations such that inferior coatings with poor physical qualities and poor fouling release properties can be eliminated. These tests include accelerated laboratory tests which can be performed quickly on a large number of samples, settlement assays which evaluate the antifouling performance towards certain species, and field tests or service tests that evaluate the coating performance on ship hulls.

2.5.1 Atomic force microscopy (AFM)

Over the last decade, nanoscale testing and characterization techniques have slowly proliferated from the field of materials science,[138] where they were once viewed by many in other disciplines as arcane and unapproachable, and are now easily accessible to those in the broader scientific arena. In the present context, atomic force microscopy (AFM) based force spectroscopy has allowed the 'scaling down' of traditional mechanical materials testing by several orders of magnitude.[139-148] Where fibers of material were once required to be on at least the cm scale for testing, nanofibres, or single proteins, can now be manipulated mechanically, allowing detailed investigation of nanoscopic samples.[24, 27, 29, 30]

For the purposes of the biofouling research, however, one of the main advantages of AFM is its ability to measure nano-scale properties of natural bioadhesive materials and adhesive interfaces in native conditions; i.e. hydrated in a saline solution. The information that this mode of study provides, regarding the structure and function of adhesive proteins *in situ* will, undoubtedly, encourage more informed surface design leading to novel methods of interfering with the bioadhesive/substratum interface.

AFM utilises a sharp probe for imaging (with a tip radius typically on the order of 10-50 nm), whose position is controlled by electronic feedback, to measure surface morphology. The tip is attached to the edge of a microcantilever beam, which serves as a force-sensing spring. The position and deflection of the cantilever-tip assembly is monitored by an optical position sensing unit, where a low-noise laser light is shined to, and reflected from the back of the gold coated silicone nitride cantilever. The relative position between tip and sample

surface is controlled via a piezoelectric positioning system whereby, most often, the sample is moved and scanned with respect to a stationary tip (there are also instruments available which utilize scanned tips and stationary sample.). The tip deflection (i.e. force between tip and sample, vs, tip-sample distance and tip position) is measured by reflection of the laser beam onto a quadruple photodiode detector (Figure 2.13A). Here, movement of the laser signal is detected as voltage potential and subsequently calibrated into distance/force units for analysis. Topological images of surfaces are obtained from the variation of force vs. tip position (x,y,z) with respect to the sample surface.

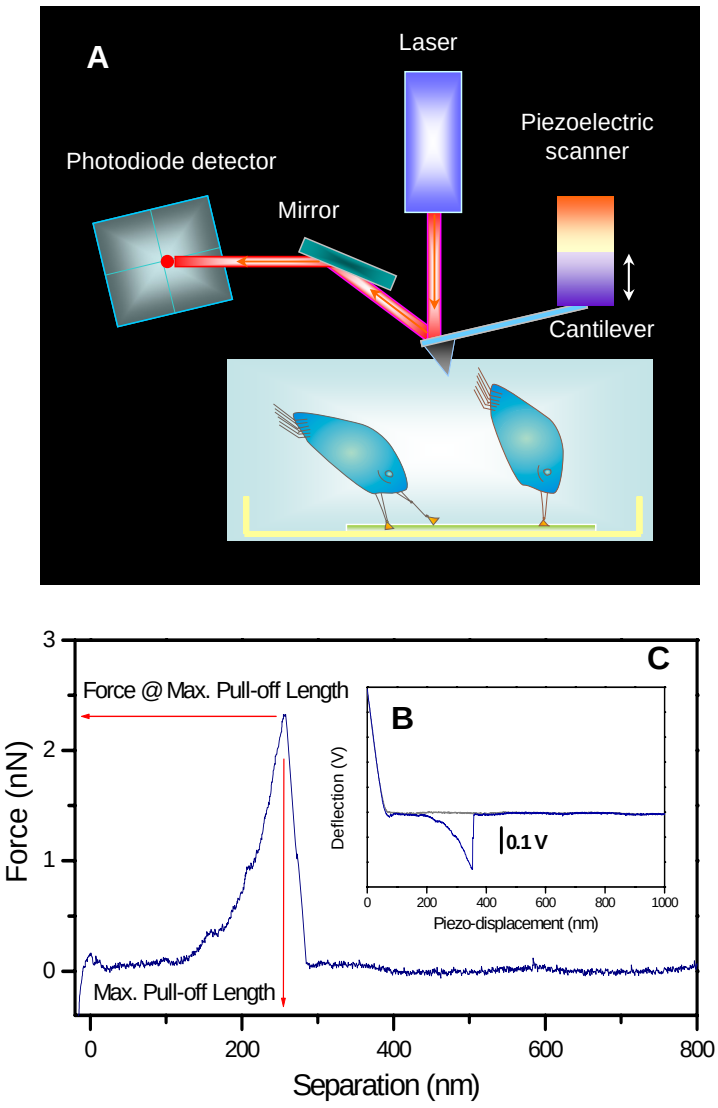

Figure 2.13. Schematic (A) shows the principle of atomic force microscopy, (B) a typical raw signal obtained from a force-spectroscopy experiment and (C) a typical force-separation curve – calculated from the raw data.

Unlike electron microscopy, for example, AFM provides three-dimensional information of the surface topology as well as allowing determination of material properties from affinity of the tip to the substrate. Such force measurements can be performed as the tip approaches, contacts and retracts from the surface. Within a short time in contact with the tip, polymer chains or molecules such as proteins may adsorb to the tip surface and their mechanical properties can be measured in tension as the tip is retracted. Adsorbed molecules are stretched and elongated under this retraction force. The photodiode signal (Figure 2.13B, recorded raw signal) is converted to cantilever deflection by correction for sensitivity (in volts per meter) as determined from the slope of the indentation part of the curve. Force is then determined by multiplying cantilever deflection by the spring constant of the tip. Scanner displacement is converted to separation between the tip and sample by selecting contact points in the approach force curve and retraction force curves.[149] Figure 2.13C is typical force-extension curve containing information related to force experienced during pull-off and molecular pull-off length.

Nanoindentation and probe-based techniques such as AFM have been successfully applied to the study of biological samples and are now sensitive enough as to allow measurement of localized nanomechanical properties in, for example, plant cell-walls.[150-152] Since the AFM instrument was first reported two decades ago, it has demonstrated its flexibility as an analytical tool and is now highly pervasive, being used in fields as diverse as material science and biology,[153, 154] including even chemically sensitive imaging of polymer surfaces, via mapping of local variations in adhesion forces on the nanoscale.[155] AFM has truly opened the door to the "nanoworld"[156] with geologists using the technique to investigate bacteria-mineral interactions[157, 158] and botanists studying the nanostructure and adhesive properties of diatoms.[27, 28, 31] Probe-based techniques confer significant advantages to the experimenter, such as the ability to control surface modification by selective deposition of organic molecules, or even performance of 'nano-surgery' to gain insights into the internal structure of collagen fibers.[159-161]

2.5.2 Settlement assay

Several laboratory cultured cyprid larvae of fouling species, for example alga, barnacle and diatom, are generally used in settlement assay to study their preferences for designed coating surfaces. The settlement assay can be used as a small-scale evaluation of the antifouling coating surface performance prior to field test. The settlement assay of barnacle is usually performed with the cyprid larvae of barnacle *B. amphitrite*.[162] *B. amphitrite* has

become widely used in laboratory testing because its ability to release larvae all-year round and also its tendency to settle in static water assay. Coating can be prepared on the glass slide and a drop of solution contained hundred of cyprid are allowed to incubate for overnight. The numbers of cyprid larvae settlements on the surfaces are compared with control surface. Another type of assay is the choice assay where target species are allowed to choose between different coatings overnight in the dark.

2.5.3 Panel test (field test)

The panel test of the resistance of coating to fouling is perhaps the most traditional antifouling assessment. Yet, it is still widely used and viewed as the most important and valuable test, provided it is performed under proper and well controlled conditions. For example, Figure 2.14 shows the raft of field test conducted by Tropical Marine Science Institute (TMSI) in Singapore in part discussed in this Thesis. It evaluates the formulation of antifouling coatings in two ways: the ability of the coating to prevent fouling, and the physical performance of the coating when exposed to natural conditions in the sea. To ensure accuracy, the water temperature, pH, salinity, oxygen level should be constantly monitored. Field tests can be carried out at different locations worldwide but the test results can be varied according to local fouling community and fouling conditions. In addition, the fouling condition is very dependence on the physical environments during the field test, such as salinity, temperature, current flow that will affect the test outcome significantly. Hence, the test result will be different if they are carried out at different times of the year.

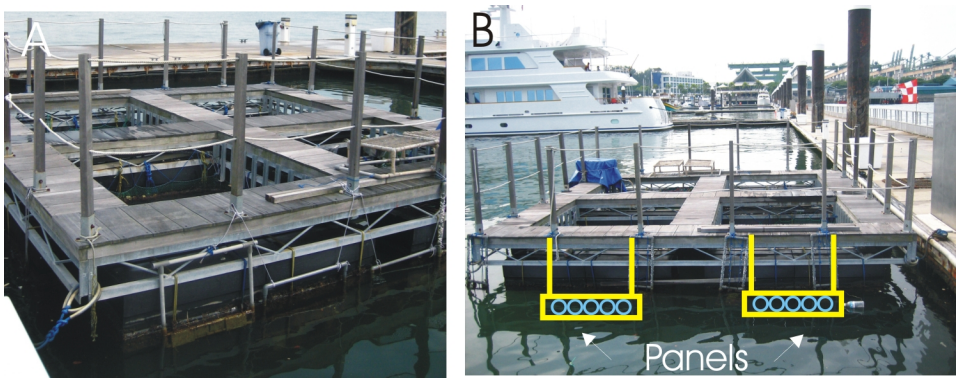

Figure 2.14. Raft placed in Royal Singapore Yacht Club (RSYC), Singapore (A) and test panels were located at 0.5 m to 1 m under the seawater level and facing the wave (B).

2.5.4 Service test

The selection of the coating with best formulation always depends upon the performance of the respective coatings/paints on the type of applied vessel and under the conditions of service. Such service tests are the most expensive and time-consuming of all. Therefore, all unsatisfactory formulations must be eliminated before service tests are attempted. Two coatings/paints can be compared on the same vessel by applying them to the opposing sections of the hull of the ship. This system provides large area coating assessments, hence eliminating the positional effects. In order to obtain statistically reliable results, several vessels must be used at each assessment, providing an antifouling quality check such as fouling species and fouling condition on the respective paint under different conditions of service and exposure.[10]

2.6 Summary

A brief accounts on marine biofouling process, fouling organisms, antifouling coating history, type of antifouling coatings and antifouling coating assessment method were presented in this chapter. To improve the design of antifouling surface, the understanding and knowledge should be advanced in all dimensions concurrently. Currently, antifouling coating industries rely on the empirical trial and error methods to improve the antifouling coating or paints system. The new approach to solve the problem of marine antifouling should involve meticulous effort that coordinated between marine biologists, materials scientific and coating engineers. To circumvent the problem of fouling organisms attached on the surface, the antifouling surfaces should target on the earlier stage, i.e. hindered settlement of larva, rather than killing the fouling organisms. However, the larva and surface interactions were confined to a small interface which is usually tens of micrometers in its native environment. This interface was difficult to assess by conventional microscopy such as optical microscopy or scanning electron microscopy. In the following chapters, a nanoscale characterization technique – AFM was applied to study the nanoscale interface between the cyprid larva and surfaces in the native environment. The knowledge acquired from AFM study was with enormous success which enables us to bridge the understanding gap between microscopic events and macroscopic world.

2.7 References

1. Yebra, D. M.; Kiil, S.; Dam-Johansen, K. *Prog. Org. Coat.* **2004,** *50,* 75-104.
2. Kill, S.; Dam-Johansen, K.; Weinell, C. E.; Pedersen, M. S. *Prog. Org. Coat.* **2002,** *45,* 423-434.

3. Townsin, R. L. *Biofouling* **2003,** *19*, 9-15.
4. http://www.ambio.bham.ac.uk/about/what%20is%20biofouling.htm.
5. Wolfson, A.; Vanblaricom, G.; Davis, N.; Lewbel, G. S. *Mar. Ecol. Prog. Ser.* **1979,** *1*, 81-89.
6. Whomersley, P.; Picken, G. B. *J. Mar. Biol. Ass. U.K.* **2003,** *83*, 897-901.
7. Qian, P. Y.; Rittschof, D.; Sreedhar, B.; Chia, F. S. *Mar. Ecol. Prog. Ser.* **1999,** *191*, 141-151.
8. Stoodley, P.; Lewandowski, Z.; Boyle, J. D.; Lappin-Scott, H. M. *Biotechnol. Bioeng.* **1999,** *65*, 83-92.
9. In *Biofouling prevention technologies for coastal sensors/sensor platforms*, ACT 2003 workshop, Solomons, Maryland, 2003; Solomons, Maryland, 2003.
10. *Marine fouling and its prevention.* US Naval Institute: Annapolis, 1952.
11. Callow, M. E.; Callow, J. A. *Biologist* **2002**, 1-5.
12. Lindner, E., The attachement of macrofouling invertebrates. In *Marine Biodeterioration: and interdisciplinary study*, Costlow, J. D.; Tipper, R. C., Eds. US Naval Institute: Annapolis, 1984; pp 183-201.
13. Crisp, D. J.; Meadows, P. S. *Proc. R. Soc. Lond. Ser. B.* **1962,** *156*, 500-520.
14. Steinberg, P. D.; De Nys, R.; Kjelleberg, S. *J. Chem. Ecol.* **2002,** *28*, 1935-1951.
15. Kamino, K.; Odo, S.; Maruyama, T. *Biol. Bull.* **1996,** *190*, 403-409.
16. Waite, J. H. *Interg. Comp. Biol.* **2002,** *42*, 1172-1180.
17. Montsant, A.; Jabbari, K.; Maheswari, U.; Bowler, C. *Plant Physiol.* **2005,** *137*, 500-513.
18. Hoagland, K. D.; Rosowski, J. R.; Gretz, M. R.; Roemer, S. C. *J. Phycol.* **1993,** *29*, 537-566.
19. Kamino, K. *Barnacle Underwater Attachment*, Springer: New York, 2006.
20. Haag, A. P., Mechanical properties of bacterial exopolymeric adhesives and their commercial development. In *Biologival Adhesives*, Smith, A.; Callow, J. A., Eds. Springer: Heidelberg, 2006; pp 1-19.
21. Kamino, K. *Mar. Biotech.* **2008,** *10*, 111-121.
22. Silverman, H. G.; Roberto, F. F. *Mar. Biotech.* **2007,** *9*, 661-681.
23. Chiovitti, A.; Dugdale, T. M.; Wetherbee, R., Diatom adhesives: molecular and mechanical properties. In *Biologival Adhesives*, Smith, A.; Callow, J. A., Eds. Springer: Heidelberg, 2006; pp 79-103.
24. Dugdale, T. M.; Dagastine, R.; Chiovitti, A.; Mulvaney, P.; Wetherbee, R. *Biophys. J.* **2005,** *89*, 4252-4260.
25. Wiegemann, M. *Aquat. Sci.* **2005,** *67*, 166-176.
26. Arce, F. T.; Avci, R.; Beech, I. B.; Cooksey, K. E.; Wigglesworth-Cooksey, B. *Biophys. J.* **2004,** *87*, 4284-4297.
27. Higgins, M. J.; Molino, P.; Mulvaney, P.; Wetherbee, R. *J. Phycol.* **2003,** *39*, 1181-1193.
28. Higgins, M. J.; Sader, J. E.; Mulvaney, P.; Wetherbee, R. *J. Phycol.* **2003,** *39*, 722-734.
29. Dugdale, T. M.; Dagastine, R.; Chiovitti, A.; Wetherbee, R. *Biophys. J.* **2006,** *90*, 2987-2993.
30. Dugdale, T. M.; Willis, A.; Wetherbee, R. *Biophys. J.* **2006,** *90*, L58-L60.
31. Higgins, M. J.; Crawford, S. A.; Mulvaney, P.; Wetherbee, R. *Protist* **2002,** *153*, 25-38.
32. Finlay, J. A.; Callow, M. E.; Schultz, M. P.; Swain, G. W.; Callow, J. A. *Biofouling* **2002,** *18*, 251-256.
33. Callow, J. A.; Callow, M. E., The *Ulva* spore adhesive system. In *Biologival Adhesives*, Smith, A.; Callow, J. A., Eds. Springer: Heidelberg, 2006; pp 63-78.
34. Callow, J. A.; Crawford, S. A.; Higgins, M. J.; Mulvaney, P.; Wetherbee, R. *Planta* **2000,** *211*, 641-647.
35. Aldred, N.; Ista, L. K.; Callow, M. E.; Callow, J. A.; Lopez, G. P.; Clare, A. S. *J. R. Soc. Interface* **2006,** *3*, 37-43.
36. Aldred, N.; Wills, T.; Williams, D. N.; Clare, A. S. *J. R. Soc. Interface* **2007,** *4*, 1159-1167.
37. Waite, J. H. *J. Biol. Chem.* **1983,** *258*, 2911-2915.
38. Yu, M. E.; Hwang, J. Y.; Deming, T. J. *J. Am. Chem. Soc.* **1999,** *121*, 5825-5826.
39. Dalsin, J. L.; Hu, B. H.; Lee, B. P.; Messersmith, P. B. *J. Am. Chem. Soc.* **2003,** *125*, 4253-4258.
40. Monahan, J.; Wilker, J. J. *Langmuir* **2004,** *20*, 3724-3729.
41. Sever, M. J.; Weisser, J. T.; Monahan, J.; Srinivasan, S.; Wilker, J. J. *Angew. Chem. Int. Ed.* **2004,** *43*, 448-450.
42. Monahan, J.; Wilker, J. J. *Chem. Commun.* **2003**, 1672-1673.

43. Lee, H.; Scherer, N. F.; Messersmith, P. B. *Proc. Natl. Acad. Sci. U. S. A.* **2006,** *103*, 12999-13003.
44. Waite, J. H. *Int. J. Adh. Adh.* **1987,** *7*, 9-14.
45. Waite, J. H. *Int. J. Biol. Macromol.* **1990,** *12*, 139-144.
46. Waite, J. H.; Qin, X. X.; Coyne, K. J. *Mat. Biol.* **1998,** *17*, 93-106.
47. Brady, R. F.; Singer, I. L. *Biofouling* **2000,** *15*, 73-81.
48. Crisp, D. J.; Meadows, P. S. *Proc. R. Soc. Lond. Ser. B.* **1963,** *158*, 364-387.
49. Yule, A. B.; Crisp, D. J. *J. Mar. Biol. Ass. U.K.* **1983,** *63*, 261-271.
50. Yule, A. B.; Walker, G. *J. Mar. Biol. Ass. U.K.* **1984,** *64*, 147-156.
51. Yule, A. B.; Walker, G. *J. Mar. Biol. Ass. U.K.* **1984,** *64*, 429-439.
52. Yule, A. B.; Walker, G. *J. Mar. Biol. Ass. U.K.* **1985,** *65*, 707-712.
53. Clare, A. S.; Freet, R. K.; McClary, M. *J. Mar. Biol. Ass. U.K.* **1994,** *74*, 243-250.
54. Kamino, K.; Inoue, K.; Maruyama, T.; Takamatsu, N.; Harayama, S.; Shizuri, Y. *J. Biol. Chem.* **2000,** *275*, 27360-27365.
55. Saroyan, J. R.; Lindner, E.; Dooley, C. A. *Biol. Bull.* **1970,** *139*, 333-&.
56. Wiegemann, M.; Watermann, B. *J. Adhes. Sci. Tech.* **2003,** *17*, 1957-1977.
57. Walker, G.; Yule, A. B. *J. Mar. Biol. Ass. U.K.* **1984,** *64*, 679-686.
58. Nott, J. A.; Foster, B. A. *Phil. Trans. R. Soc. Lond. Ser. B.* **1969,** *256*, 115-134.
59. Crisp, D. J., Settlement responses in marine organisms. In *Adaptation to environment. Essays on the physiology of marine animals.*, Newell, R. C., Ed. Butterworths: London, 1976.
60. Rainbow, P. S. *Field Stud.* **1984,** *6*, 1-51.
61. Anderson, D. T., *Barnacles: structure, function, development and evolution*. Chapman & Hall: London, 1994; p 357.
62. Walker, G. *Mar. Biol.* **1971,** *9*, 205-212.
63. Berglin, M.; Larsson, A.; Jonsson, P. R.; Gatenholm, P. *J. Adhes. Sci. Tech.* **2001,** *15*, 1485-1502.
64. Aldred, N. The adhesion and adhesives of barnacle cyprids (Balanus amphitrite; Semibalanus balanoides) and mussels (Mytilus edulis). University of Newcastle, 2007.
65. Glenner, H.; Hoeg, J. T. *J. Crust. Biol.* **1995,** *15*, 523-536.
66. Hellio, C.; Marechal, J. P.; Veron, B.; Bremer, G.; Clare, A. S.; Le Gal, Y. *Mar. Biotech.* **2004,** *6*, 67-82.
67. Knight-Jones, E. W. *J. Exp. Biol.* **1953,** *30*, 584-598.
68. Knightjones, E. W. *Nature* **1955,** *175*, 266-266.
69. Crisp, D. J.; Walker, G.; Young, G. A.; Yule, A. B. *J. Coll. Interf. Sci.* **1985,** *104*, 40-50.
70. Larman, V. N.; Gabbott, P. A.; East, J. *Comp. Biochem. Phys. B* **1982,** *72*, 329-338.
71. Larman, V. N. *Comp. Biochem. Phys. B* **1984,** *77*, 73-81.
72. Matsumura, K.; Nagano, M.; Fusetani, N. *J. Exp. Zool.* **1998,** *281*, 12-20.
73. Matsumura, K.; Mori, S.; Nagano, M.; Fusetani, N. *J. Exp. Zool.* **1998,** *280*, 213-219.
74. Matsumura, K.; Nagano, M.; Kato-Yoshinaga, Y.; Yamazaki, M.; Clare, A. S.; Fusetani, N. *Proc. R. Soc. Lond. Ser. B.* **1998,** *265*, 1825-1830.
75. Dreanno, C.; Kirby, R. R.; Clare, A. S. *Biol. Lett.* **2006,** *2*, 423-425.
76. Dreanno, C.; Matsumura, K.; Dohmae, N.; Takio, K.; Hirota, H.; Kirby, R. R.; Clare, A. S. *Proc. Natl. Acad. Sci. U. S. A.* **2006,** *103*, 14396-14401.
77. Dreanno, C.; Kirby, R. R.; Clare, A. S. *Proc. R. Soc. Lond. Ser. B.* **2006,** *273*, 2721-2728.
78. Clare, A. S.; Matsumura, K. *Biofouling* **2000,** *15*, 57-71.
79. Togi, A.; Kamino, K.; Adachi, K.; Shizuri, Y. *Tetrahedron* **1998,** *54*, 15581-15588.
80. Nakano, M.; Shen, J. R.; Kamino, K. *Biomacromolecules* **2007**.
81. Nott, J. A. *Mar. Biol.* **1969,** *2*, 248-&.
82. Clare, A. S.; Nott, J. A. *J. Mar. Biol. Ass. U.K.* **1994,** *74*, 967-970.
83. Davy, H. *Phil. Trans. R. Soc. Lond. Ser. B.* **1824,** *114*, 151-158.
84. Davy, H. *Phil. Trans. R. Soc. Lond. Ser. B.* **1825,** *115*, 328-346.
85. Phang, I. Y.; Aldred, N.; Clare, A. S.; Vancso, G. J. *Nano**S*** **2007,** *01*, 35-39.
86. Milne, A.; Hails, G. 1971.
87. Anderson, C.; Atlar, M.; Callow, M.; candries, M.; Milne, A.; Townsin, R. L. *J. Mar. Des. Oper.* **2003,** *B4*, 11-23.
88. Gitlitz, M. H. *J. Coat. Tech.* **1981,** *53*, 46-52.

89. Milne, A.; Hails, G. 1977.
90. Anderson, C. D.; Dalley, R. *Oceans* **1986,** *18*, 1108-1113.
91. Kiil, S.; Weinell, C. E.; Pedersen, M. S.; Dam-Johansen, K. *Ind. Engin. Chem. Res.* **2001,** *40*, 3906-3920.
92. Champ, M. A. *Mar. Poll. Bull.* **1999,** *38*, 239-246.
93. http://www.imo.org/Conventions/mainframe.asp?topic_id=529.
94. Champ, M. A. *Mar. Poll. Bull.* **2003,** *46*, 935-940.
95. Champ, M. A. *Sci.Total Environ.* **2000,** *258*, 21-71.
96. Evans, S. M.; Birchenough, A. C.; Brancato, M. S. *Mar. Poll. Bull.* **2000,** *40*, 204-211.
97. de Nys, R.; Steinberg, P. D. *Curr. Opin. Biotechnol.* **2002,** *13*, 244-248.
98. Fusetani, N. *Nat. Prod. Rep.* **2004,** *21*, 94-104.
99. Vallee-Rehel, K.; Langlois, V.; Guerin, P. *J. Environ. Polym. Degrad.* **1998,** *6*, 175-186.
100. McGinniss, V. D. *Prog. Org. Coat.* **1996,** *27*, 153-161.
101. Anderson, C. D.
102. http://www.npacorp.com/products/marine.html.
103. http://www.b8.s005v.squarestart.ne.jp/news_e/2003/wn1215.html.
104. http://www.cmp.co.jp/en/product/marine_main_product.html.
105. http://www.international-marine.com/.
106. http://www.sigmacoatings.com/marine/.
107. http://www.kpamerica.com/root/operation.html.
108. Meyer, A. E.; Baier, R. E.; Forsberg, R. E. In *Degradation of nontoxic fouling-release coatings as a result of abrasion and long term exposure*, Proceedings of the Fifth International Zebra Mussel and Other Aquatic Nuisance Organisms, Toronto, 1995; Toronto, 1995.
109. Adkins, J. D.; Mera, A. E.; RoeShort, M. A.; Pawlikowski, G. T.; Brady, R. F. *Prog. Org. Coat.* **1996,** *29*, 1-5.
110. Brady, R. F. *Prog. Org. Coat.* **1999,** *35*, 31-35.
111. Krishnan, S.; Ayothi, R.; Hexemer, A.; Finlay, J. A.; Sohn, K. E.; Perry, R.; Ober, C. K.; Kramer, E. J.; Callow, M. E.; Callow, J. A.; Fischer, D. A. *Langmuir* **2006,** *22*, 5075-5086.
112. Finlay, J. A.; Krishnan, S.; Callow, M. E.; Callow, J. A.; Dong, R.; Asgill, N.; Wong, K.; Kramer, E. J.; Ober, C. K. *Langmuir* **2008,** *24*, 503-510.
113. Krishnan, S.; Wang, N.; Ober, C. K.; Finlay, J. A.; Callow, M. E.; Callow, J. A.; Hexemer, A.; Sohn, K. E.; Kramer, E. J.; Fischer, D. A. *Biomacromolecules* **2006,** *7*, 1449-1462.
114. Turner, K.; Serantoni, M.; Boyce, A.; Walsh, G. *Proc. Biochem.* **2005,** *40*, 3377-3382.
115. Olsen, S. M.; Pedersen, L. T.; Laursen, M. H.; Kiil, S.; Dam-Johansen, K. *Biofouling* **2007,** *23*, 369-383.
116. Omae, I. *Chem. Rev.* **2003,** *103*, 3431-3448.
117. Rittschof, D.; Hooper, I. R.; Branscomb, E. S.; Costlow, J. D. *J. Chem. Ecol.* **1985,** *11*, 551-563.
118. Wahl, M. *Mar. Ecol. Prog. Ser.* **1989,** *58*, 175-189.
119. Wahl, M.; Kroger, K.; Lenz, M. *Biofouling* **1998,** *12*, 205-226.
120. Scardino, A.; De Nys, R.; Ison, O.; O'Connor, W.; Steinberg, P. *Biofouling* **2003,** *19*, 221-230.
121. Scardino, A. J.; de Nys, R. *Biofouling* **2004,** *20*, 249-257.
122. Guenther, J.; Walker-Smith, G.; Waren, A.; De Nys, R. *Biofouling* **2007,** *23*, 413-418.
123. Ball, P. *Nature* **1999,** *400*, 507-507.
124. Wainwright, S. A.; Vosburgh, F.; Hebrank, J. H. *Science* **1978,** *202*, 747-749.
125. Hutchinson, H. *Mech. Eng.* **2008,** *130*, 42-44.
126. Singhvi, R.; Kumar, A.; Lopez, G. P.; Stephanopoulos, G. N.; Wang, D. I. C.; Whitesides, G. M.; Ingber, D. E. *Science* **1994,** *264*, 696-698.
127. Chen, C. S.; Mrksich, M.; Huang, S.; Whitesides, G. M.; Ingber, D. E. *Science* **1997,** *276*, 1425-1428.
128. Weibel, D. B.; DiLuzio, W. R.; Whitesides, G. M. *Nat. Rev. Microbiol.* **2007,** *5*, 209-218.
129. Berntsson, K. M.; Andreasson, H.; Jonsson, P. R.; Larsson, L.; Ring, K.; Petronis, S.; Gatenholm, P. *Biofouling* **2000,** *16*, 245-261.
130. Petronis, S.; Berntsson, K.; Gold, J.; Gatenholm, P. *J. Biomater. Sci.-Polym. Ed.* **2000,** *11*, 1051-1072.

131. Berntsson, K. M.; Jonsson, P. R.; Lejhall, M.; Gatenholm, P. *J. Exp. Mar. Biol. Ecol.* **2000,** *251*, 59-83.
132. Callow, M. E.; Jennings, A. R.; Brennan, A. B.; Seegert, C. E.; Gibson, A.; Wilson, L.; Feinberg, A.; Baney, R.; Callow, J. A. *Biofouling* **2002,** *18*, 237-245.
133. Hoipkemeier-Wilson, L.; Schumacher, J.; Carman, M.; Gibson, A.; Feinberg, A.; Callow, M.; Finlay, J.; Callow, J.; Brennan, A. *Biofouling* **2004,** *20*, 53-63.
134. Schumacher, J. F.; Carman, M. L.; Estes, T. G.; Feinberg, A. W.; Wilson, L. H.; Callow, M. E.; Callow, J. A.; Finlay, J. A.; Brennan, A. B. *Biofouling* **2007,** *23*, 55-62.
135. Schumacher, J. F.; Aldred, N.; Callow, M. E.; Finlay, J. A.; Callow, J. A.; Clare, A. S.; Brennan, A. B. *Biofouling* **2007,** *23*, 307-317.
136. Carman, M. L.; Estes, T. G.; Feinberg, A. W.; Schumacher, J. F.; Wilkerson, W.; Wilson, L. H.; Callow, M. E.; Callow, J. A.; Brennan, A. B. *Biofouling* **2006,** *22*, 11-21.
137. Schumacher, J. F.; Long, C. J.; Callow, M. E.; Finlay, J. A.; Callow, J. A.; Brennan, A. B. *Langmuir* **2008**.
138. Hangen, U. D.; Downs, S.; Hoogenboon, R.; Kranenburg, H.; Schubert, U. S. *NanoS* **2006,** *01*, 18-22.
139. Mitsui, K.; Hara, M.; Ikai, A. *FEBS Lett.* **1996,** *385*, 29-33.
140. Bustamante, C.; Rivetti, C.; Keller, D. J. *Cur. Opin. Struct. Biol.* **1997,** *7*, 709-716.
141. Rief, M.; Gautel, M.; Oesterhelt, F.; Fernandez, J. M.; Gaub, H. E. *Science* **1997,** *276*, 1109-1112.
142. Rief, M.; Oesterhelt, F.; Heymann, B.; Gaub, H. E. *Science* **1997,** *275*, 1295-1297.
143. Oberhauser, A. F.; Marszalek, P. E.; Erickson, H. P.; Fernandez, J. M. *Nature* **1998,** *393*, 181-185.
144. Bustamante, C.; Macosko, J. C.; Wuite, G. J. L. *Nat. Rev. Mol. Cell Biol.* **2000,** *1*, 130-136.
145. Marszalek, P. E.; Li, H. B.; Fernandez, J. M. *Nat. Biotechnol.* **2001,** *19*, 258-262.
146. Li, H. B.; Linke, W. A.; Oberhauser, A. F.; Carrion-Vazquez, M.; Kerkviliet, J. G.; Lu, H.; Marszalek, P. E.; Fernandez, J. M. *Nature* **2002,** *418*, 998-1002.
147. Lee, G.; Abdi, K.; Jiang, Y.; Michaely, P.; Bennett, V.; Marszalek, P. E. *Nature* **2006,** *440*, 246-249.
148. Giannotti, G. I.; Vancso, G. J. *ChemPhysChem* **2007,** *8*, 2290-2307.
149. Janshoff, A.; Neitzert, M.; Oberdorfer, Y.; Fuchs, H. *Angew. Chem. Int. Ed.* **2000,** *39*, 3213-3237.
150. Cross, S. E.; Jin, Y. S.; Rao, J.; Gimzewski, J. K. *Nat. Nanotechnol.* **2007,** *2*, 780-783.
151. Pelling, A. E.; Sehati, S.; Gralla, E. B.; Valentine, J. S.; Gimzewski, J. K. *Science* **2004,** *305*, 1147-1150.
152. Walker, G. C.; Sun, Y. J.; Guo, S. L.; Finlay, J. A.; Callow, M. E.; Callow, J. A. *J. Adhes.* **2005,** *81*, 1101-1118.
153. Horber, J. K. H.; Miles, M. J. *Science* **2003,** *302*, 1002-1005.
154. Magonov, S. N.; Reneker, D. H. *Annu. Rev. Mater. Sci.* **1997,** *27*, 175-222.
155. Vancso, G. J.; Hillborg, H.; Schonherr, H., Chemical composition of polymer surfaces imaged by atomic force microscopy and complementary approaches. In *Polymer Analysis, Polymer Theory*, 2005; Vol. 182, pp 55-129.
156. Gerber, C.; Lang, H. P. *Nat. Nanotechnol.* **2006,** *1*, 3-5.
157. Lower, S. K.; Hochella, M. F.; Beveridge, T. J. *Science* **2001,** *292*, 1360-1363.
158. Kempe, A.; Schopf, J. W.; Altermann, W.; Kudryavtsev, A. B.; Heckl, W. M. *Proc. Natl. Acad. Sci. U. S. A.* **2002,** *99*, 9117-9120.
159. Jaschke, M.; Butt, H. J. *Langmuir* **1995,** *11*, 1061-1064.
160. Wen, C. K.; Goh, M. C. *Nano Lett.* **2004,** *4*, 129-132.
161. Severin, M.; Barner, J.; Kalachev, A. A.; Rabe, J. P. *Nano Lett.* **2004,** *4*, 577-579.
162. Rittschof, D.; Branscomb, E. S.; Costlow, J. D. *J. Exp. Mar. Biol. Ecol.* **1984,** *82*, 131-146.

Chapter 3

Towards a nanomechanical basis for temporary adhesion in barnacle cyprids (*Semibalanus balanoides*)*

Cypris larvae of barnacles are able to use a rapidly reversible adhesion mechanism for exploring immersed surfaces and selecting a location for permanent attachment, metamorphosis and growth into an adult. Barnacles are thus of considerable interest for the development of biomimetic adhesives and also to the marine coatings industry that strives to develop the means by which barnacle settlement, and associated economic costs, can be reduced. How barnacle cyprids temporarily attach to immersed surfaces is, however, poorly understood. In this Chapter, we investigate cyprid temporary adhesion and provide the first published data concerning a natural adhesion system that combines 'dry' and 'wet' mechanisms in an aqueous medium. Present data were acquired using atomic force microscopy (AFM). 'Footprints' of a glycoproteinaceous secretion, deposited by exploring cyprids (*Semibalanus balanoides*), were probed in artificial seawater on silane-modified glass surfaces. AFM imaging of footprints revealed the fibrillar nature of the adhesive, suggesting that these deposits are composed of single proteins or bundles of proteinaceous nanofibrils with height varying between 7 nm and 150 nm. Estimation of dry and wet adhesion forces allowed calculation of a total tenacity value that closely approximated force data obtained empirically in earlier studies. Results suggest that previously proposed mechanisms of cyprid adhesion do not explain the great tenacity with which these organisms stick and that cyprids likely require a combination of both 'wet' and 'dry' adhesion mechanisms for temporary attachment.

---

*Parts of this Chapter have been published as: I. Y. Phang, N. Aldred, A. S. Clare, G. J. Vancso. *J. R. Soc. Interface* **2008,** *5,* 397-401.

3.1 Introduction

Biofouling, resulting from the settlement of propagules (pelagic larvae or spores) from marine invertebrates, has received much interest of late,[1] particularly with regard to larval settlement on surfaces with differing chemical and physical characteristics. The reasons behind the preferences of settling propagules are, however, still largely unknown. More importantly, there remains a considerable dearth of information on the composition of the adhesives themselves and, in many cases, the fundamental mechanisms by which adhesion occurs have yet to be identified. These deficiencies are particularly apparent in the case of barnacles. Barnacles are the most important marine fouling organisms due to their large size, hard, calcareous body form[2] and generally gregarious nature.[3] They settle readily on man-made structures, increasing hydrodynamic drag and damaging protective coatings.[4] In fact, the prevention and remediation of marine fouling is a multi-billion dollar (US$) industry and improved knowledge regarding marine bioadhesives would undoubtedly aid the development of more effective fouling-resistant coatings.[5]

The bioadhesion mechanisms of many sessile marine organisms such as algae, mussels and echinoderms involve initial surface exploration and reversible attachment followed by secretion of a permanent adhesive for final, irreversible, settlement.[6-8] Barnacles are no different.[9] The barnacle cypris larva (Figure 3.1A - B [*Balanus amphitrite*]), has two discreet adhesion systems; one temporary and one permanent (both unrelated to the well-studied adult cement system). Prior to permanent attachment, cyprids explore surfaces using a form of bi-pedal ‘walking’. It has been suggested, although never proven experimentally, that cyprid temporary adhesion is facilitated by a glycoproteinaceous secretion derived from modified hypodermal glands within the antennules.[10, 11] This secretion is expressed externally onto the antennular attachment disc (Figure 3.1C) and, during surface exploration, ‘footprints’ are deposited by cyprids serving as a settlement cue for subsequently exploring larvae.[12-15] In fact, the cyprid’s mode of attachment seems to share more in common with ‘wet/dry-adhesive’ systems from terrestrial organisms such as flies that use a principally ‘dry’ system, enhanced by delivery of an oily secretion into the interface.[16] This is a common mode of improving adhesion by organisms that use unbranched setae for attachment. The thousands of cuticular villi (Figure 3.1C) present on the cyprid attachment disc are not branched like those of spiders, beetles and geckos and, as a result, it is hypothesized that cyprids require a liquid adhesive for additional tenacity.[17-21] Cyprids would not achieve anything like maximal theoretical tenacity for ‘dry’ adhesion since their cuticular villi are not orientated in an ordered way – as appears to be a common theme across all studied

organisms. This could be because, unlike insects, arachnids and lizards, cyprids are bi-pedal and, therefore, have no central point to draw towards.[21] Further, forces in the marine environment are much stronger and directionally unpredictable than on land, requiring a system that is sturdy in all directions. A system that manifests tenacity in all directions, however, raises interesting questions regarding detachment.

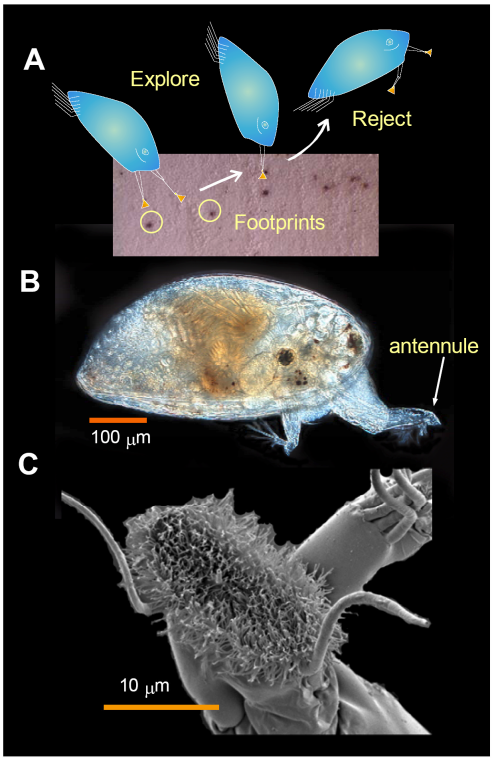

Figure 3.1. The ultrastructure and morphology of the cyprid temporary adhesive system. (A) Cyprid exploration with footprints made visible by immunostaining on nitrocellulose membrane (B) a light micrograph of a *Balanus amphitrite* cyprid (similar, but larger, cyprids of *S. balanoides* were used in experiments) and (C) the ultrastucture of the antennular attachment disk from *Balanus amphitrite*.

For two decades, researchers have attempted to isolate cyprid footprints in a form that would permit investigation by scanning electron microscopy (SEM), environmental SEM (ESEM) and other techniques, without any notable success.[10] Nitrocellulose membrane retains cyprid footprints due to its high protein binding capability (Figure 3.1C), but is not a suitable substratum for atomic force microscopy (AFM).[12, 18] Previously, AFM has been used to investigate adhesion of low motility organisms such as bacteria, diatoms and algae, however, barnacle adhesives are less conducive to AFM study being heterogeneous, dynamic and, in the case of the footprint material, difficult to locate on surfaces.[22-26] Despite these

technical difficulties, this Chapter present the first mechanistic study of cyprid temporary adhesion, drawing conclusions about the nature and function of the deposited footprint material as well as speculating on the contribution of the antennular structure itself to overall adhesion. Natively 'sticky' materials have been the focus of considerable study in recent years, and a mechanism that also worked in aqueous conditions would have a range of technical applications, from adhesive tape to microgrippers.[21, 27-29]

3.2 Results and discussion

3.2.1 Morphology of cyprid footprints

By using AFM, footprints of *S. balanoides* antennular secretion (Figure 3.2) were probed on glass surfaces with different wettabilities.[23, 30-33] Footprints deposited onto -CH_3 (θ_{adv} = 85°; θ_{rec} = 55°) (Figure 3.2A) or -NH_2 functionalized surfaces (θ_{adv} = 60°; θ_{rec} = 25°) (Figure 3.2B & Table 3.1) appeared to have different dimensions, with greater spreading on -CH_3 (mean area 2.2×10^3 μm^2) than -NH_2 (mean area 1.9×10^3 μm^2). This difference could be the result of a simple balance of thermodynamic forces, as described by the Young-Dupré equation and would, theoretically, be consistent with passive spreading of a non-polar adhesive in a three- phase aqueous system.[34]

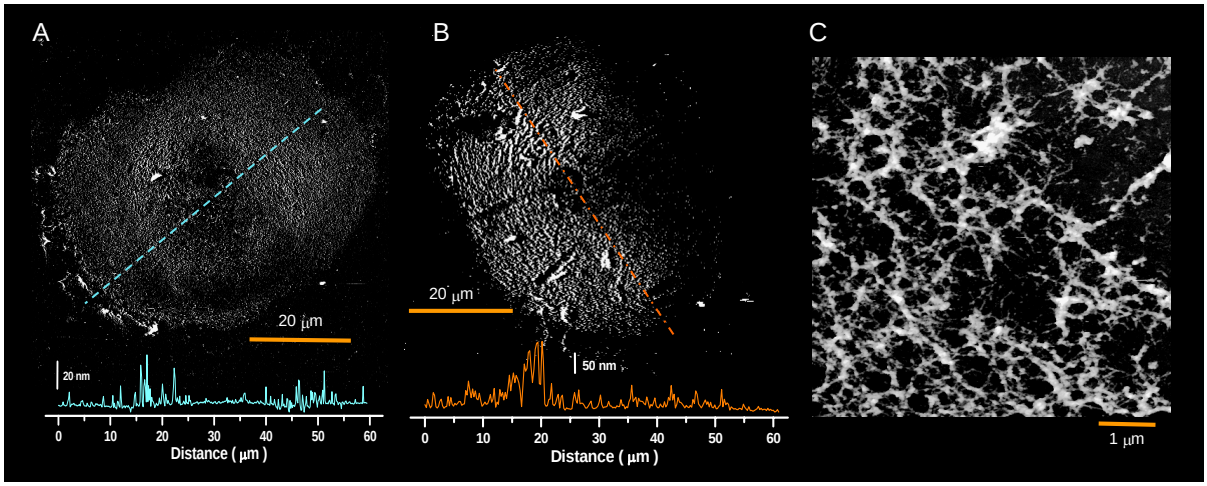

Figure 3.2. AFM micrograph (deflection mode image) of a cyprid (*S. balanoides*) footprint on silanized glass (A) terminated by CH_3 group and (B) terminated by NH_2 group. Cross-sectional plots from height along the dashed line are shown in different colors respectively. (C) High magnification AFM image (height) of the footprint material (z-scale from 0-100 nm).

Table 3.1. Information regarding cyprid footprints and their adhesive strength calculated from AFM measurements of the footprint material.

Glass surface functionalization	*Mean footprint area (μm^2)*	*RMS thickness (nm)*	*Volume (μm^3)*	*Estimated exploration steps*
NH_2 (θ_{Adv} = 60°)	1928 ± 259	18.9 ± 3.0	36.7 ± 10.7	535
CH_3 (θ_{Adv} = 85°)	2157 ± 201	5.3 ± 1.0	11.4 ± 1.1	1663

More obvious was the difference in volume of footprints deposited on the different surfaces. Route-mean-square thickness of the footprints, calculated from AFM results, was used to determine footprint volume giving a mean of 11.4 μm^3 for -CH_3 and 36.7 μm^3 for -NH_2 functional group. Again, the limited number of samples precluded statistical analysis, however this three-fold difference is considerable. Assuming finite production, Walker & Yule estimated that hypodermal glands responsible for adhesive synthesis could produce up to $1.9x10^4$ μm^3 of the material. Using the footprint volume data, a finite resource would limit the number of footprints to 530 ± 20 on -NH_2 terminated glass and 1600 ± 40 on -CH_3 terminated glass from a single *S. balanoides* cyprid, which corresponds to a distance traversed of between 35 cm and 110 cm, respectively, assuming an individual pace distance of 660 μm (pace distance estimated from observation of cyprid behaviour).[10]

High-resolution imaging revealed that the antennular secretion is fibrillar (Figure 3.2C) and that the appearance of footprints on the micrometer scale corresponds well to the surface texture of the antennular disc. The heights of nanofibrils varied between 7 nm and 150 nm as estimated by AFM height section (Figure 3.2B bottom). These measurements indicated that isolated protein chains, as well as bundles of protein aggregates, were deposited during exploration. Diagnostic 'fingerprint' signatures of self-assembled adhesive nanofibers have been observed by AFM-force spectroscopy in the mucilage of diatoms and have recently been shown to be amyloid fibrils in the terrestrial alga *Prasiola linearis*.[23-25, 35] In these organisms the adhesive proteins are able to self-assemble into web-like network structures in a co-operative effort to provide mechanical toughness that enhances the adhesive's ability to resist deformation under shear forces.[36]

In isolating footprints consistently on -NH_2 terminated glass, we discovered a surface that appeared to retain the footprint material well, and which is also conducive to study by AFM. It seemed clear that the antennular secretion (which is currently of unknown composition)[13] had a stronger affinity to -NH_2 terminated surfaces than to -CH_3, resulting in more material remaining on those surfaces after detachment and a preference of cyprids for -

NH_2 terminated surfaces (unpublished data). In addition, the interfacial energies between the footprint material and the glass surface, and also between the footprint material and the antennular disc, govern the frequency with which footprints remain on the test surfaces. The fact that more footprints were observed on -NH_2 terminated surfaces suggests higher adherence on this surface, since when the adhesive joint was broken, the adhesive remained on the surface more often than on -CH_3 terminated surfaces. In other words, on failure of the adhesive joint, whether water enters between the surface and glycoprotein interface or the glycoprotein and antennular disc interface depends on their respective surface tensions, and could explain the differences in footprint morphologies on different wettability surfaces, as well as the propensity for more footprints to be deposited on high wettability -NH_2 terminated surfaces. Importantly, since the footprints are also settlement inducing (containing or comprising settlement-inducing protein complex (SIPC)),[13] less footprint material deposited on -CH_3 terminated surfaces would correlate directly to potential reduction of con/allospecific settlement on those surfaces.

For many analytical techniques, it is necessary to first visualize a sample by staining in order to locate it. Staining was avoided here in order to garner more accurate information regarding the native material, although this came at a cost of low replication for this part of the study. The experiment can, in summary, be considered to have taken place *in vitro* and in native conditions.

3.2.2 Adhesion strength and drag estimation

A visco-adhesive mechanism, involving the antennular secretion as an adhesive, became the generally accepted theory regarding cyprid temporary adhesion, primarily through the exclusion of other possibilities.[37] Empirical estimates of adhesion were not made until the mid-1980's,[37-40] but demonstrated the strength of *S. balanoides* temporary adhesion to be in the order of 0.068-0.076 MPa on clean glass, precluding the earlier suggestion that attachment may be due to suction developed by the disc-encircling cuticular velum (Figure 3.1C).[41] If adhesion relies on the viscose resistance of a proteinaceous secretion, it seemed remarkable that cyprids could utilize such a tiny amount of adhesive (3.7×10^{-14} *l* on NH_2-terminated glass and 1.1×10^{-14} *l* on CH_3-terminated glass for each footprint) to secure themselves so tenaciously.

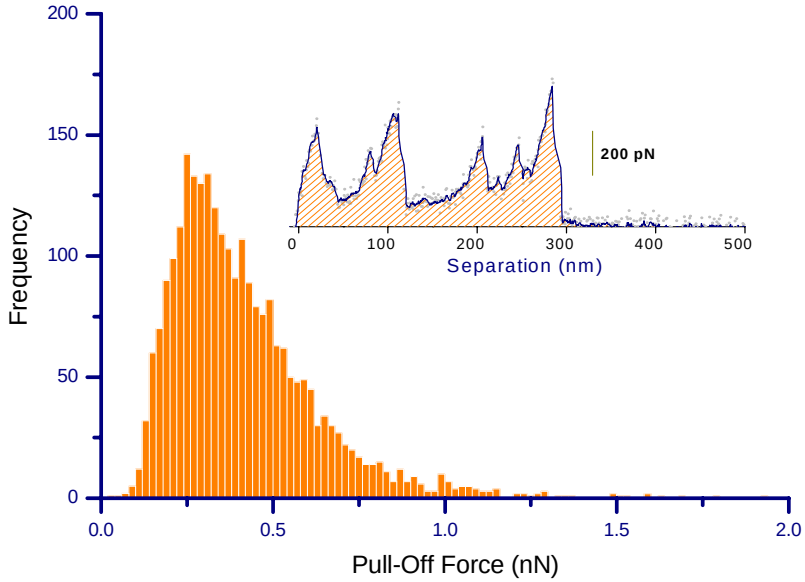

Figure 3.3. A frequency histogram representing the pull-off forces measured on different surfaces by force spectroscopy. Inset is a typical example of a force curve obtained throughout the experiments. The orange shaded area under the force-separation curve represents the energy dissipated by the system.

The hypothesis that attachment is facilitated only by visco-adhesive properties of the antennular secretion (wet adhesion) was tested. Pull-off forces were obtained by AFM for 3 different footprints (Figure 3.3) with a mean force of 0.41 ± 0.20 nN (n = 2500). This force was scaled from an AFM tip, with apex diameter 100 nm, to the area of two antennular discs, including an estimated 50 % porosity (Figure 3.4). From this estimation, it was clear that cyprids would only be able to achieve a tenacity of 0.026 MPa if the protein alone were responsible for adhesion; one-third of the empirical value (0.068 - 0.076 MPa on glass[39]). Tenacity to silicone nitrile AFM tips would differ from that on glass although, clearly, additional mechanisms must play a role in this adhesion process. The porous nature of the footprint's morphology, as shown in Figure 3.2C, correlated well with the dimensions of individual cuticular villi of the adhesive disc (diameter of individual cuticular villus, $\phi_{cuticular\ villus}$ ~ 200 nm). The porosity of the adhesive deposit might, it was hypothesized, result from individual setae contacting the surface in different orientations, suggesting the possibility that interactions between the villi and the surface could serve to enhance adhesion. Previously, the cuticular villi had been thought to serve only as a retention mechanism for the antennular secretion.[42]

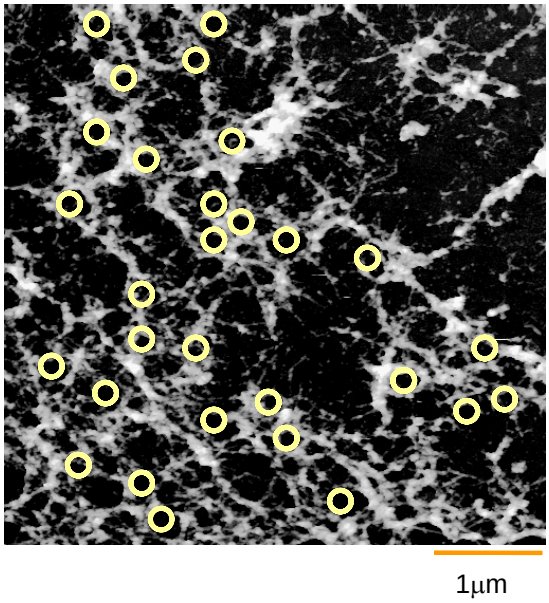

Figure 3.4. Enlarged image of footprint material showing the porous nature of the footprint's morphology that correlated well with the dimensions of individual cuticular villi of the adhesive disc ($\phi_{cuticular\ villus}$ ~ 200 nm).

Taking account of villus-surface interactions, putative van der Waals contributions to adhesion were then estimated from literature values (F_{vdW} = 2.40 ± 0.80 nN for *Gecko gecko* spatula pull-off force, measured on glass in water),[43] accounting for surface area, density and number of exposed cuticular villi on the attachment disc (Table 3.1). In combination with measured 'wet' adhesion forces, 'dry' adhesion resulted in a total tenacity value of 0.063 MPa. Electrostatic interactions from the cuticular villi alone contributed an estimated 0.037 MPa to total tenacity. In fact, these model values closely approximate (with only 7 - 20 % discrepancy) empirical values.[39] Evidence that cyprids, in fact, use a combination of both 'wet' and 'dry' adhesion mechanisms for their temporary attachment seemed convincing, yet the exact integration of 'wet' and 'dry' systems was still not understood. By varying the porosity parameter in the adhesion calculation, we modeled the full range of potential tenacity values, based on a spectrum of contributions from both adhesion components. The results are presented in Figure 3.5.

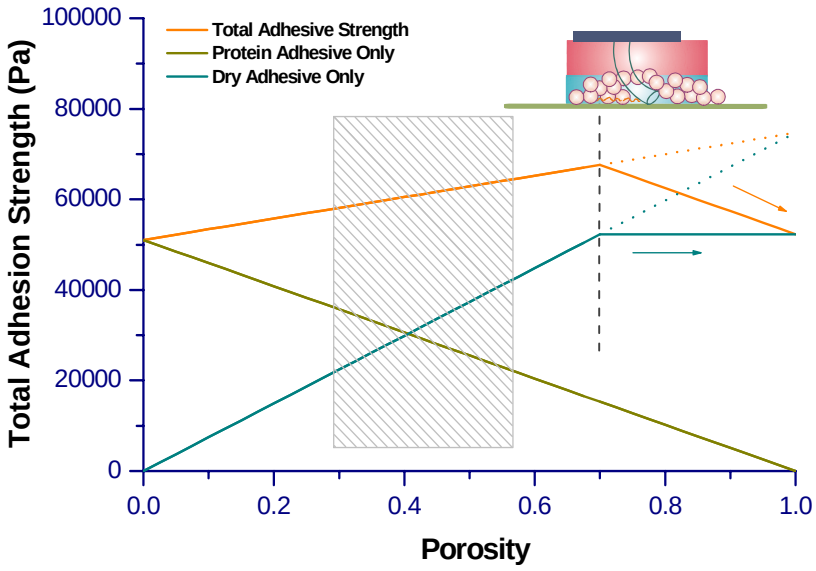

Figure 3.5. Total adhesion strength calculated from the scaled-up area of tip contact. Two separate adhesion mechanisms are involved, i.e. wet adhesion involving the proteinaceous secretion and dry adhesion between the cuticular villi and the surface. The shaded area is the optimal region for attachment, satisfying both mechanisms. Inset cartoon illustrates the interface between attachment disc and the surface.

From Figure 3.5, as the porosity of the deposited material increases, total tenacity increases slightly due to contributions from 'dry' adhesion alone. 'Wet' adhesion decreases with increasing porosity as would be expected. It is reasonable to assume that the cuticular villi would not be in 100% contact with the surface so, at some stage (higher porosity), the contribution from 'dry' adhesion will no longer increase in a linear fashion but will reach a plateau, resulting in reduction of total tenacity at higher porosity. This relationship could be the primary factor controlling evolutionary development of the cuticular villi – particularly with regard to their density. The shaded region in Figure 3.5 highlights the range of porosity that appears to be used by cyprids, based on AFM images of 3 footprints (e.g. Figure 3.4). The calculation, however, assumes that water is completely excluded from the interface and that the contact area is either occupied by cuticular villi or antennular secretion. This is probably not an unreasonable assumption;[18] especially considering the potentially superhydrophobic architecture of the adhesive disc.

Finally, by modeling the cyprid as an airfoil (approximating the organism's hydrodynamic body shape) and disregarding lift, boundary layer and turbulence effects, we calculated a generalized estimate of the potential drag resistance of a barnacle cyprid in

natural conditions, based on our tenacity estimates (Figure 3.6). Calculations suggested that the tenacity of a cyprid, as previously derived, would allow attachment to be maintained in a 'jet-flow'-like stream of up to 5 m/s (18 km/hr); tenacity approaching this magnitude would certainly be required during surface exploration by this temperate water, intertidal organism.[44] This is, of course, simply estimation, with hydrodynamics poorly understood at this micro-scale. On a smooth surface in flow, a cyprid would usually be protected within the surface boundary layer; however, this calculation is considered relevant to the high-force turbulent conditions of the intertidal, unlikely to manifest a stable boundary layer of any appreciable thickness.[44]

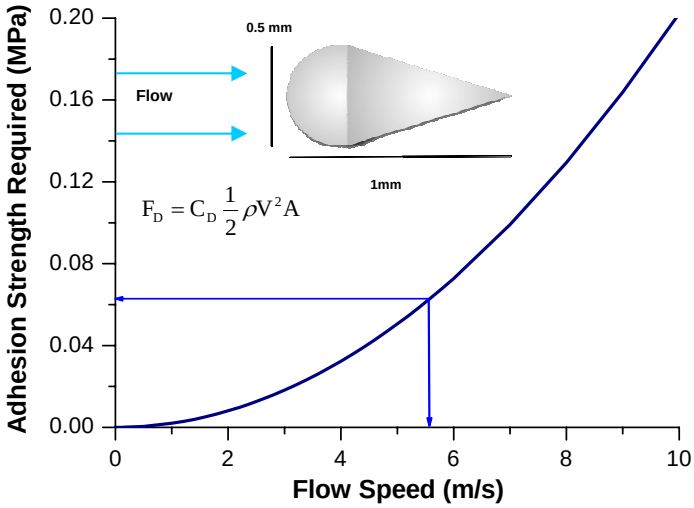

Figure 3.6. Estimation of the resistance of a cyprid to water flow. Inset is the air foil-shaped model of a cyprid with a drag coefficient (C_D) of 0.045. Tenacity estimation allows a cyprid to withstand flow speed of ~ 5 m/s.

As mentioned earlier, a large number of organisms across several phyla use viscous, protein-based adhesives for surface attachment. This system must, therefore, confer benefits over and above other potential methods of attachment. Smith,[45] suggested that 'wet' adhesion could only develop forces twenty times less (~ 1 MPa) than purely 'dry' systems[21] because the development of negative capillary pressures in an adhesive secretion under stress would invoke spontaneous fluid cavitation, interfering with adhesion. If true, this would seriously compromise the adhesion of barnacle cyprids. In reality, cavitation may well occur, but Singh *et al.*[46] recently proved experimentally that this process (on the micro scale at least) conversely serves to significantly enhance adhesion.

According to the sacrificial chain model proposed by smith et al.,[36, 47] the failure of a sacrificial bond, usually leading to unfolding of a protein domain or loop, prevents damage to the backbone of adhesive proteins, providing extreme toughness. This mechanism has been found to operate in many natural materials such as abalone shell, bone and diatom adhesive and is effective at dissipating large amounts of energy.[23, 36, 48] A sacrificial chain operates by preventing the propagation of microcracks that appear in adhesive deposits when a shear force is applied. This system could well operate in cyprid temporary adhesion. Nanomechanical information from this study suggests that the proteins comprising the cyprid antennular secretion are able to form nanofibers and provide modest adhesion, whilst aggregation and network formation increases total energy dissipation in order to resist deformation. However, adhesion by viscosity alone was not sufficient to explain observed adherence of exploring cyprids. By estimation of van der Waals interactions, we showed that overall adhesion must include a 'dry' adhesion aspect, similar to that of flies and geckos. The first time that such a phenomenon has been observed to occur in the aquatic environment. From this data we suggest a mechanism for cyprid temporary adhesion:

It is proposed that the natively hydrophobic nature of cyprid antennular discs, possibly aided by the properties of the antennular secretion, displaces water from the adhesion interface followed by glycoprotein secretion being delivered to the surface; sealing the adhesive joint from the aqueous medium. The resulting viscous capillary layer of protein, formed between the adhesive disc and the surface, contributes to high capillary forces and a lower dielectric constant in the joint, thus strengthening electrostatic forces between the cuticular villi and the surface.[18] Voluntary detachment could be facilitated by re-orientation of the villi, reducing the number of van der Waals interactions, breaking the capillary seal and allowing water into the interface.

3.3 Conclusions

Barnacle cyprids have evolved a method of attaching rapidly and reversibly to almost any immersed solid object, although exactly how they do so remains a mystery. The authors struggle to accept that the cuticular villi, with their diverse morphology between genera of barnacles, serve only as a retention mechanism for footprint material on the antennule[42] and if the villi can be shown to contribute to adhesion through surface interaction, cyprids would be the first organism documented to use such a mechanism under-water. Valuable insight into the mechanism of cyprid temporary adhesion has been presented here and it is hoped that future work will directly challenge this intriguing and complex system.

3.4 Experimental

Animals. *S. balanoides* cyprids were collected by plankton tow from the wild population at Cullercoats, UK (55.1 N 1.26 W) during April 2006 and were stored in 2 *l* glass containers, at 1 cyprid/ml, filled with artificial sea water (ASW; Tropic Marin™) at 6 ^{o}C prior to use. Feeding was not necessary as cyprids are lecithotrophic.

Surface preparation. Glass microscopy cover slips were sonicated in ethanol for 5 min and then immersed in piranha solution (a mixture of concentrated sulphuric acid and 33 % hydrogen peroxide in a 3:1 ratio) for 15 mins. The surfaces were rinsed with nanopure water and dried under N_2. Amino ($-NH_2$) and alkyl ($-CH_3$) terminated surfaces were obtained by gas-phase evaporation of 3-aminopropyl triethoxysilane (APTES) and dodecyltriethoxysilane (DTES) in a desiccator under vacuum. APTES and DTES were obtained from Sigma Aldrich. All chemicals were used as received, unless otherwise stated. Surfaces were incubated for several hours and then carefully rinsed with 99 % ethanol and nanopure water.

Immuno-staining of footprints. Footprints were Immunoblotted following the protocol of Matsumura *et al*.[12] Briefly, cyprids were washed and allowed to explore on 0.45 μm pore size nitrocellulose membrane. The membrane was then immersed in TBS, blocking buffer and incubated with a 1 % solution of the antibody to the 76 kDa subunit of barnacle settlement inducing protein complex (SIPC). Incubation with a secondary goat anti-mouse antibody (alkaline phosphatase conjugate) was followed by staining with a BCIP/NBT solution until footprints became obvious. The membrane was allowed to dry out before imaging to improve contrast.

AFM experiments. AFM measurements were carried out using a Dimension D3100 atomic force microscope equipped with NanoScope IVa controller and a hybrid scanner (H-153) with x-, y- z-feedbacks from Veeco (Veeco / Digital Instruments (DI), Santa Barbara, CA). Triangular-shaped silicon nitride cantilevers (Veeco/Digital Instruments (DI), Santa Barbara, CA) were used throughout the study and cantilever spring constants were calibrated using the thermal noise method.[49] The cantilever used for acquisition of the present results had a spring constant range from 0.062 to 0.100 Nm^{-1}. For experiments, cyprids were stored, prior to use, in 33 parts per thousand ASW and were then deposited onto prepared surfaces by micro-pipette. Surfaces were mounted in glass Petri-dishes prior to experimentation. Typically, cyprids would attach and begin exploration when stimulated by small water currents. Explored areas of the glass were marked on the base of the cover slip and cyprids were then removed from the Petri-dishes. Surfaces were flushed with large amount of filtered ASW to minimize contamination. Petri-dishes were then transferred to the AFM and the search for footprints was focused on the marked regions. Custom programmed software for LABVIEW™ was used for data analysis throughout to transform the raw data to force-separation curves according to method described by Janshoff *et al*.[50]

Estimation of cyprid drag resistance. A standard hydrodynamics expression was invoked to calculate the detachment forces that an attached cyprid could withstand in nature. The estimated drag coefficient (C_D) of a three-dimensional airfoil shape is 0.045, so the force per unit area (F_D) required for a cyprid with antennular disc area $2.0x10^{-9}$ m^2 to remain attached in flow was calculated using:[51]

$$F_D = \frac{1}{2} C_D \rho V^2 A$$

Where:

ρ = 1025 kgm^{-3} (density of seawater)

V^2 = velocity squared

A = πr^2 where r = 0.00025. Cross sectional area of *S. balanoides* = 1.9635 x 10^{-7} m^2

This delivered an approximate detachment force value, disregarding lift and boundary layer effects. How these physical parameters would affect an object as small as a barnacle cyprid (500 μm for *S. balanoides*) is impossible to predict with any degree of certainty.

3.5 Acknowledgements

Dr. Nikodem Tomczak is thanked for providing software for force-curve analysis and insightful discussions, Ms Xing Yi Ling for functionalized glass surfaces, Dr. Robert Mutton for his assistance with cyprid drag calculation and Dr. Holger Schönherr, Dr. Juang-Horng Chong and Dr. Tony Khor for critical reading.

3.6 References

1. Swain, G.; Herpe, S.; Ralston, E.; Tribou, M. *Biofouling* **2006,** *22*, 425-429.
2. Anderson, D. T., *Barnacles: structure, function, development and evolution*. Chapman & Hall: London, 1994; p 357.
3. Crisp, D. J.; Meadows, P. S. *Proc. R. Soc. Lond. Ser. B.* **1962,** *156*, 500-520.
4. Christie, A. O.; Dalley, R., Barnacle fouling and its prevention. In *Crustacean Issues 5: Barnacle Biology*, Southward, A. J., Ed. Balkema: Rotterdam, 1987; pp 419-433.
5. Yebra, D. M.; Kiil, S.; Dam-Johansen, K. *Prog. Org. Coat.* **2004,** *50*, 75-104.
6. Callow, M. E.; Callow, J. A. *Biofouling* **2000,** *15*, 49-56.
7. Waite, J. H.; Qin, X. X.; Coyne, K. J. *Matrix Biol.* **1998,** *17*, 93-106.
8. Haesaerts, D.; Jangoux, M.; Flammang, P. *Biol. Bull.* **2006,** *211*, 172-182.
9. Clare, A. S.; Matsumura, K. *Biofouling* **2000,** *15*, 57-71.
10. Walker, G.; Yule, A. B. *J. Mar. Biol. Ass. U. K.* **1984,** *64*, 679-686.
11. Nott, J. A.; Foster, B. A. *Philos. Trans. R. Soc. Lond. Ser. B.* **1969,** *256*, 115-134.
12. Matsumura, K.; Nagano, M.; Kato-Yoshinaga, Y.; Yamazaki, M.; Clare, A. S.; Fusetani, N. *Proc. R. Soc. Lond. Ser. B.* **1998,** *265*, 1825-1830.
13. Dreanno, C.; Kirby, R. R.; Clare, A. S. *Biol. Lett.* **2006,** *2*, 423-425.
14. Clare, A. S.; Nott, J. A. *J. Mar. Biol. Ass. U. K.* **1994,** *74*, 967-970.
15. Dreanno, C.; Matsumura, K.; Dohmae, N.; Takio, K.; Hirota, H.; Kirby, R. R.; Clare, A. S. *Proc. Natl. Acad. Sci. U. S. A.* **2006,** *103*, 14396-14401.
16. Niederegger, S.; Gorb, S.; Jiao, Y. K. *J. Comp. Physiol. A.* **2002,** *187*, 961-970.
17. Autumn, K., Properties, Principles, and Parameters of the Gecko Adhesive System. In *Biological Adhesives*, Smith, A. M.; Callow, J. A., Eds. Springer: Heidelberg, 2006; pp 225-256.
18. Aldred, N.; Clare, A. S., Mechanisms and principles underlying temporary adhesion, surface exploration and settlement site selection by barnacle cypris larvae: A short review. In *Functional surfaces in biology*, Springer: 2008.
19. Autumn, K.; Liang, Y. A.; Hsieh, S. T.; Zesch, W.; Chan, W. P.; Kenny, T. W.; Fearing, R.; Full, R. J. *Nature* **2000,** *405*, 681-685.
20. Arzt, E.; Gorb, S.; Spolenak, R. *Proc. Natl. Acad. Sci. U. S. A.* **2003,** *100*, 10603-10606.
21. Federle, W. *J. Exp. Biol.* **2006,** *209*, 2611-2621.
22. Razatos, A.; Ong, Y. L.; Sharma, M. M.; Georgiou, G. *Proc. Natl. Acad. Sci. U. S. A.* **1998,** *95*, 11059-11064.
23. Higgins, M. J.; Molino, P.; Mulvaney, P.; Wetherbee, R. *J. Phycol.* **2003,** *39*, 1181-1193.
24. Dugdale, T. M.; Dagastine, R.; Chiovitti, A.; Mulvaney, P.; Wetherbee, R. *Biophys. J.* **2005,** *89*, 4252-4260.
25. Dugdale, T. M.; Dagastine, R.; Chiovitti, A.; Wetherbee, R. *Biophys. J.* **2006,** *90*, 2987-2993.

26. Callow, J. A.; Crawford, S. A.; Higgins, M. J.; Mulvaney, P.; Wetherbee, R. *Planta* **2000,** *211*, 641-647.
27. Northen, M. T.; Turner, K. L. *Nanotechnology* **2005,** *16*, 1159-1166.
28. Yurdumakan, B.; Raravikar, N. R.; Ajayan, P. M.; Dhinojwala, A. *Chem. Commun.* **2005**, 3799-3801.
29. Hui, C. Y.; Glassmaker, N. J.; Tang, T.; Jagota, A. *J. R. Soc. Interface* **2004,** *1*, 35-48.
30. Horber, J. K. H.; Miles, M. J. *Science* **2003,** *302*, 1002-1005.
31. Engel, A.; Muller, D. J. *Nat. Struct. Biol.* **2000,** *7*, 715-718.
32. Sun, Y. J.; Guo, S. L.; Walker, G. C.; Kavanagh, C. J.; Swain, G. W. *Biofouling* **2004,** *20*, 279-289.
33. Phang, I. Y.; Aldred, N.; Clare, A. S.; Callow, J. A.; Vancso, G. J. *Biofouling* **2006,** *22*, 245-250.
34. Aldred, N.; Ista, L. K.; Callow, M. E.; Callow, J. A.; Lopez, G. P.; Clare, A. S. *J. R. Soc. Interface* **2006,** *3*, 37-43.
35. Mostaert, A. S.; Higgins, M. J.; Fukuma, T.; Rindi, F.; Jarvis, S. P. *J. Biol. Phys.* **2006,** *32*, 393-401.
36. Smith, B. L.; Schaffer, T. E.; Viani, M.; Thompson, J. B.; Frederick, N. A.; Kindt, J.; Belcher, A.; Stucky, G. D.; Morse, D. E.; Hansma, P. K. *Nature* **1999,** *399*, 761-763.
37. Yule, A. B.; Walker, G., Adhesion in barnacles. In *Crustacean Issues 5: Barnacle Biology*, Southward, A. J., Ed. A. A. Balkema: Rotterdam, 1987; pp 389-402.
38. Yule, A. B.; Crisp, D. J. *J. Mar. Biol. Ass. U. K.* **1983,** *63*, 261-271.
39. Yule, A. B.; Walker, G. *J. Mar. Biol. Ass. U. K.* **1984,** *64*, 429-439.
40. Yule, A. B.; Walker, G. *J. Mar. Biol. Ass. U. K.* **1985,** *65*, 707-712.
41. Lindner, E., The attachment of macrofouling invertebrates. In *Marine biodeterioration: An interdisciplinary study.*, Castlow, J. D.; Tipper, R. C., Eds. Naval Institute Press: Annapolis, 1984; pp 183-201.
42. Moyse, J.; Jensen, P. G.; Høeg, J. T.; Al-Yahya, H., Attachment organs in cypris larvae: using scanning electron microscopy. In *Crustacean Issues 10: New frontiers in barnacle evolution*, Schram, F., R.; Høeg, J. T., Eds. A.A. Balkema: Rotterdam, 1985; pp 153-178.
43. Huber, G.; Mantz, H.; Spolenak, R.; Mecke, K.; Jacobs, K.; Gorb, S. N.; Arzt, E. *Proc. Natl. Acad. Sci. U. S. A.* **2005,** *102*, 16293-16296.
44. Denny, M. W.; Gaines, S. D. *Limnol. Oceanogr.* **1990,** *35*, 1-15.
45. Smith, A. M. *J. Exp. Biol.* **1991,** *157*, 257-271.
46. Singh, S.; Houston, J.; van Swol, F.; Brinker, C. J. *Nature* **2006,** *442*, 526-526.
47. Rief, M.; Gautel, M.; Oesterhelt, F.; Fernandez, J. M.; Gaub, H. E. *Science* **1997,** *276*, 1109-1112.
48. Fantner, G. E.; Hassenkam, T.; Kindt, J. H.; Weaver, J. C.; Birkedal, H.; Pechenik, L.; Cutroni, J. A.; Cidade, G. A. G.; Stucky, G. D.; Morse, D. E.; Hansma, P. K. *Nat. Mater.* **2005,** *4*, 612-616.
49. Hutter, J. L.; Bechhoefer, J. *Rev. Sci. Instrum.* **1993,** *64*, 1868-1873.
50. Janshoff, A.; Neitzert, M.; Oberdorfer, Y.; Fuchs, H. *Angew. Chem. Int. Ed.* **2000,** *39*, 3213-3237.
51. http://www.grc.nasa.gov/WWW/K-12/airplane/shaped.html.

Chapter 4

Glycoprotein "footprints" of the barnacle cypris larva: Morphology and mechanical behavior at the nanoscale assessed by AFM*

Barnacles are among the most important biofoulers of man-made underwater structures having significant environmental and economic impact. Settlement-stage cypris larvae explore surfaces prior to settlement by reversible attachment effected by a 'temporary adhesive'. During this exploratory behavior the cyprid may deposit glycoproteinaceous 'footprints' of a putatively adhesive material. The deposition of footprint is dependent on the wettability of the surface. In this Chapter, footprints deposited by *Balanus amphitrite* cyprids were probed by atomic force microscopy (AFM) in artificial seawater on silane-modified glass surfaces. AFM imaging revealed the fibrillar nature of the secretion, suggesting that the deposits were composed of single proteinaceous nanofibrils, or bundles of fibrils. The force curves generated in pull-off force experiments consisted of sections of gradually increasing force, separated by sharp drops in the extension force, which gave a characteristic saw-tooth appearance. Following relaxation of fibrils stretched to high strains, force–distance curves in reverse stretching experiments could be described by the entropic elasticity model of a polymer chain. When subjected to relaxation exceeding 500 ms, extended footprint glycoproteins refolded and again showed saw-tooth unfolding peaks in subsequent force cycles. Observed rupture and hysteresis behavior was explained by the "sacrificial bond" model introduced by Hansma. Longer durations of relaxation (>5 s) allowed more sacrificial bond reformation and contributed to enhanced energy dissipation (higher toughness). The persistence length for the protein chains (L_P) was obtained by fitting a classical worm-like chain model to the force-extension curves. At high elongation, following repeated stretching up to increasing upper strain limits, a conspicuous step in the force curve was observed, resembling conformation transition observed during pulling of a polysaccharide. We attribute this to the presence of sugar units in the footprint glycoprotein.

*Parts of this Chapter have been submitted for publication.

4.1 Introduction

Biological organisms in seawater often attach themselves to solid surfaces for various reasons, e.g. to form colonies and improve their chances of survival.[1] Attachment is facilitated by an underwater glue - usually an adhesive protein[2] or, in the case of adult barnacles[3-7] and mussels,[8-11] a complex mixture of a number of different proteins or peptides. Two interfaces are involved, the substratum and the adhesive and the adhesive organ and its secretion. Beyond fundamental interest in the adhesion of fouling organisms, a strong driving force behind research into their bioadhesives has been to understand the adhesives in sufficient detail so as to aid the design of artificial water-tolerant adhesive formulations.[12, 13]

An additional incentive in the case of barnacles, however, is to use improved knowledge of their adhesives to design fouling-resistant surfaces for use on immersed structures.[14, 15] Preventing the attachment of various marine organisms, including e.g. barnacles, tubeworms and mussels poses a serious challenge for contemporary marine technology.[16] Biofouling of ship hull surfaces results in reduces maneuverability, enhances frictional resistance in seawater, which increases fuel consumption.[17] Fouling also obscures sensors , enhances corrosion and blocks filtration processes.[18] Thus, in addition to a motivation in biology and materials science to better understand the biological and chemical processes of marine foulant attachment, the economics of biofouling provide an immediate incentive to develop novel, effective antifouling technologies. Solutions offered so far that render surfaces biofouling-resistant (i.e. antifouling) have often relied on the release of a biocide.[16] Accumulation of high level of biocide may pose an unacceptable hazard to the environment through effects on non-target orgsanisms.[19, 20] With increasing environmental awareness and a drive for ‘green’ technologies, supported by environmental legislation, there is considerable interest in developing non-toxic antifouling surfaces. If progress is to be made in this area, a fuller understanding of the fouling process is necessary, which would eventually allow one to derive design criteria for coating materials selection and surface engineering.[21]

The barnacle *Balanus amphitrite* (*B. amphitrite* = *Amphibalanus amphitrite*)[22] has been chosen as a representative marine fouling species in this study. Barnacles cause a significant fouling problem due to their large size and hard calcareous shell. The life cycle of *B. amphitrite* comprises six planktonic nauplius stages, all bar the first of which are planktotrophic (feeding), a lecithotrophic (non-feeding) cyprid stage and the adult form. Settlement on solid surfaces occurs at the cyprid stage. To achieve the objective of designing

truly antifouling surface technologies, intervention must happen at the earliest stage of the attachment process to prevent barnacle colonisation.[23]

Cyprids (Figure 4.1A) are highly discriminating in their choice of settlement site[24] which they explore, prior to settlement, using a pair of specialized antennules (Figure 4.1B).[25] The antennules are terminated at the 3rd segment with adhesion organs (Figure 4.1C), reminiscent of the pulvilli of flies.[26] During surface exploration, the cyprid uses a rapidly reversible temporary adhesion mechanism to walk across surfaces in a 'bipedal' fashion.[27] It has been suggested that this temporary adhesion is facilitated, in part at least,[27, 28] by a proteinaceous secretion putatively derived from hypodermal glands in the 2nd antennular segment.[29-31] During surface exploration a small amount of this protein, hereafter referred to as 'footprint', is deposited by the cyprid. The morphology and size of deposited footprint is dependent on the wettability of the surface.[32] This secretion serves a secondary function as a settlement cue for subsequently exploring larvae (Figure 4.1D).[31-35] These footprints, their morphology, nanomechanical properties and deformability were studied using atomic force microscopy (AFM) both for imaging and for 'force spectroscopy' experiments. Our aim was to garner structural and mechanical information from footprint deposits that may elucidate their composition and inform us as to the interactions that occur at the interface between the adhesive organs of cypris larvae and immersed surfaces.

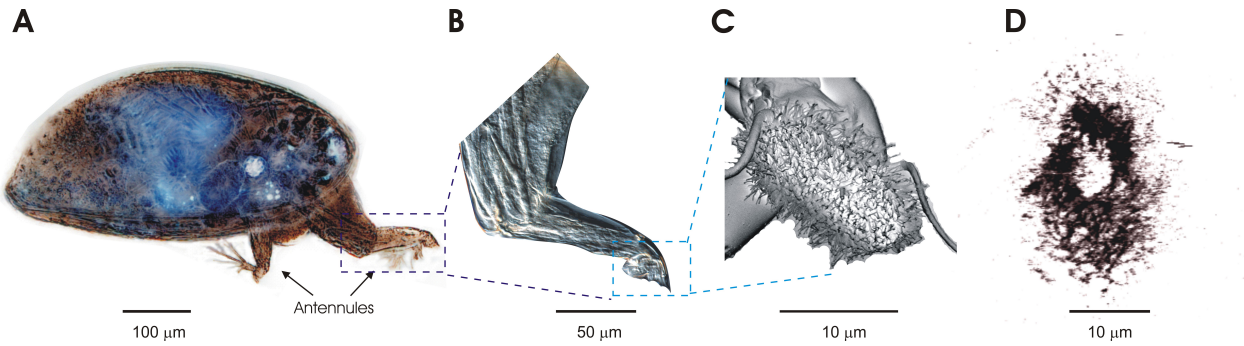

Figure 4.1. False color micrograph of a barnacle, *Balanus amphitrite*, cyprid (A), antennule of a cyprid (B), microstructure of the antennular attachment disc (C) and a deposited footprint (D).

AFM is well suited to imaging the surface morphology of soft matter across the nanometers to hundreds of micrometers length scale and was, therefore, ideally suited to this task.[36-39] In addition, AFM allows the micro- and nano-scale mechanical properties of synthetic and biological macromolecules to be examined *in situ*.[37-58] Previously, AFM has been used to investigate adhesion of low motility organisms such as bacteria,[59] diatoms[60-63]

and algae,[64] however barnacle adhesives, especially those of the cyprid, are less conducive to AFM study as they are heterogeneous and dynamic.[65, 66] AFM can also be used to stretch single macromolecule chains, or bundles of polymers, and measure force extension relationships by the so called AFM-based force spectroscopy (AFM-FS) technique.[67-73] The advantage of AFM-FS is that it allows the study of nanomechanical or mechano-chemical properties, such as the strength, elasticity and toughness of individual biomacromolecules, at the single chain level.[74-78] Useful information from these experiments is, at present, restricted to several purified proteins or engineered proteins. This limitation is related to the hierarchical structure of protein, which breaks up during extension in a highly complex manner. The complexity of natural materials is not restricted to the single molecule level[79] since larger molecules network through linked biomolecules into larger superstructures such as nanofibers.[80]

In most natural materials, especially natural bioadhesives, so called sacrificial bonds can prevent the breakdown of the main structure under an applied stress. Sacrificial bonds are those linkages that fail, by design, before severe damage is done to the main structure (usually the backbone of the biomacromolecule).[81] When a force is applied to bioadhesives, sacrificial bonds break and energy becomes dissipated by chain fracture. The hidden length that is protected by the sacrificial bond unravels under these circumstances. Incorporation of sacrificial bonds in bioadhesives creates a very resilient system capable of dissipating large amounts of energy. Consequentially, many naturally occurring bioadhesives are unusually tough by synthetic adhesive standards.[82] The sacrificial bond model was first demonstrated in α_2-macroglobulin (A2M) and later in the muscle protein - titin[40-44] by AFM-based single molecule force spectroscopy (SMFS) (Scheme 4.1).[83] Titin functions as a ‘damper’ to absorb most of the energy applied to its bioadhesive system.[42, 43] In fact, sacrificial bonds are abundant in nature and can be found in many biomaterials such as bone,[83-85] spider silk,[80] natural adhesives from algae,[64, 86, 87] diatom mucilage[60-63] and adult barnacle cement.[65, 66, 88] We anticipated that sacrificial bonds would also be present in cyprid temporary adhesive as this secretion has been shown to be related to the settlement-inducing protein complex - an α2M-like protein - of *B. amphitrite*.[31, 34]

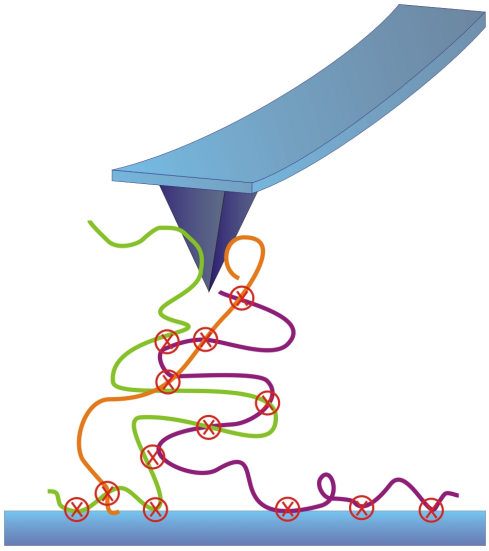

Scheme 4.1. The pickup of footprint molecules with interconnected sacrificial bonds by an AFM tip.

In previous Chapter, the morphology of barnacle, *Semibalanus balanoides*, cyprid footprints was studied by AFM.[32] The study suggested that the footprint deposits of that species are composed of bundles of proteinaceous nanofibrils with heights varying between 7 nm and 150 nm. Macro-morphology of the footprints differed on glass surfaces treated with silanes depending on substrate wettability. This Chapter focuses on the fine morphology and nanomechanical behavior of footprint protein deposits of *B. amphitrite*. Once the footprints were located, force extension curves of protein nanofibrils were recorded. When the footprint proteins were attached to the AFM tip, they could be stretched in a reversible way, allowing us to study related dynamic properties. Force-extension curves were recorded until contact failure occurred at the weakest point in the system. Different pulling rates and delay times were applied between pulling cycles to study the reforming ability of sacrificial bonds. The worm-like chain polymer elasticity model was used to determine the persistence length and contour length of the footprint fibrils.

4.2 Results

4.2.1 Morphology of Balanus amphitrite footprints

AFM for surface imaging was used to observe the morphology of the adhesive footprints of *B. amphitrite* cyprids. Footprints of the glycoproteinaceous secretion deposited by cyprids during surface exploration were probed under ASW on silane-modified glass surfaces. Typically, footprint images (Figure 4.2A) were taken using tapping mode in air (height image, z-range 100 nm). Footprints were elliptical in shape, as has been described

previously, with diameters of about 30 μm.[32, 89] The total surface coverage of an average footprint was 4.1±0.6 x 10^{-10} m^2 (n = 19). The footprint size roughly corresponded to the diameter of the antennular disc of the cyprid (Figure 4.1C).[32] The microtexture of the footprint was porous in nature with individual nanofibrils observable across the contacted surface as shown in Figure 4.2. In Figure 4.2A-D, a series of AFM micrographs, of increasing magnification, are presented to show the morphological details of footprint deposits. A high resolution AFM image (Figure 4.2B) (magnified section labeled by the blue color box in Figure 4.2A) shows the conformation of the nanofibrils. Figure 4.2C shows a high resolution scan of the boxed region in Figure 4.2B. Several extended fibrils, as identified by the white arrows, likely correspond to single adhesive protein chains or bundles of a small number of chains.

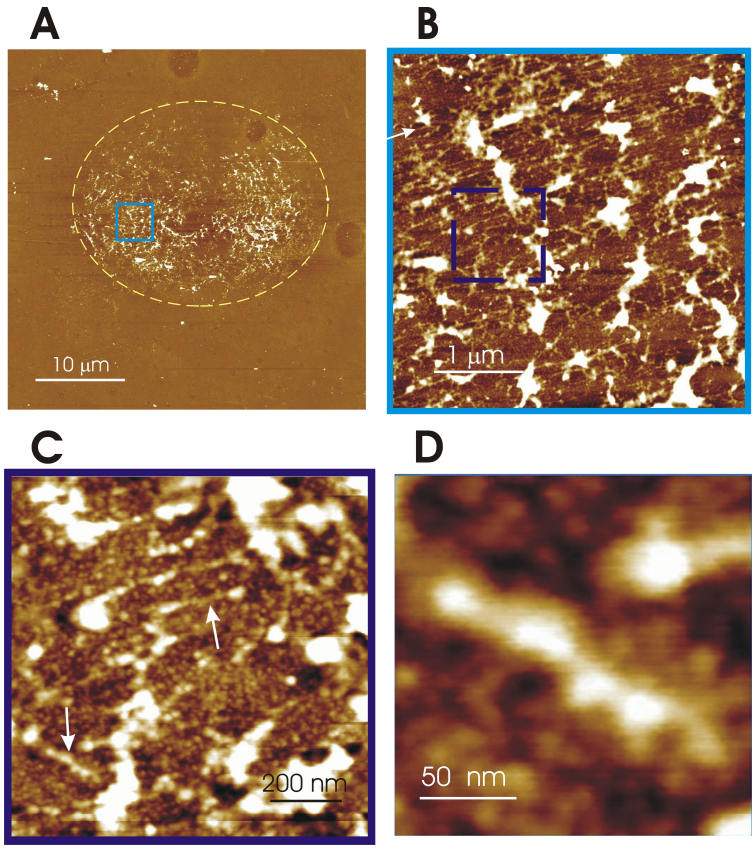

Figure 4.2. AFM micrograph (tapping mode amplitude image) of a cyprid, *Balanus amphitrite*, footprint on NH_2 terminated silanized glass (A). High magnification image of highlighted area in Figure 4.2(A) which shows the extended conformation of nanofibrils across the surface (B) and high magnification images of single nanofibrils (C [highlighted area in Figure 4.2B] & D).

As shown in Figure 4.2B, the individual fibrils of the footprint protein adhesive (thickness approximately 20 nm, including broadening by tip convolution) exhibited anisotropic properties across the area of the footprint deposit. The fibrils generally exhibited circumferential orientation (parallel with the footprint circumference; Figure 4.2A). These nanofibrils were connected in their perpendicular direction by thicker fibrous proteins (Figure 4.2B). Several possibilities can be suggested to explain this morphology. It is likely that during attachment of the antennules, the proteinaceous footprint material was forced, under pressure, into the interface between the adhesive disc and the surface resulting in radial shear of the deposited proteins. In addition, when the walking larvae detach from a surface there is likely some cohesive failure within the footprint material. Thus a new protein-water interface is created and this process may govern the morphology of the resulting deposits. The larger protein aggregates, arising vertically from the surface of the deposit, probably corresponded to the areas of adhesive failure between the deposit and the antennular disc (see Figure 4.2B). Similar fiber-like adhesives are commonly found in nature, as in spiders, silkworms, diatoms and flies larvae.[63, 84, 90, 91]

4.2.2 Reversible unfolding-refolding, elasticity and dynamics of footprint nanofibrils

In order to understand the nanomechanical properties of footprints under tensile deformation, AFM-based force spectroscopy was used to stretch footprint proteins. Corresponding experiments were carried out by first allowing the tip to be ‘immersed’ in the footprint. Once the footprint molecules were attached to the tip, the cantilever was retracted from the surface. The force-extension curves of microfibrils ‘picked up’ by the tip (Figure 4.3), exhibited typical ‘saw-tooth’ fingerprints.[42, 44] The force curves consisted of sections of gradually increasing force, separated by sharp drops in the force. Similar force-extension curves can also be observed in single protein AFM force spectroscopy, where the sharp drops in force correspond to the breaking up of domains within single proteins.[42, 43, 74] However, in the present case, the initial force extension curves did not represent single protein pulling. Rather, it is likely that we observed the stretching of bundles of protein aggregates and nanofibers, connected via sacrificial bonds.[81-85] Once a sacrificial bond was broken, the shielded polypeptide chain of the protein unfolded, resulting in a sharp reduction in tension. The rupture forces of the sacrificial bonds ranged between 220 pN to 580 pN. At a given maximum extension, without breaking tip-protein-surface contact, the relative motion of the tip was reversed and the fibrils were allowed to relax by fully removing the stress. As the tip re-approached the surface, nanofibrils exhibited a monotonic relaxation (black curve in

Figure 4.3A) showing entropic-elastic behavior. The shaded area under the force separation curves represents the energy required to break the sacrificial bonds (~ 120 x 10^{-18} J). This process was designed to simulate the interactions that take place when an external force separates sections of the footprints from the surface. The rupture of sacrificial bonds functions as a natural damping process to dissipate large quantities of energy.[92] Some of the observed 'sawteeth' could be related to breaking up of the protein internal superstructure (the mechanical denaturing of footprint protein). However, due to the complex unfolding pathway, it is not possible to assign such intermolecular events with certainty.

The response of footprint proteins to different magnitudes of mechanical strain (extension) was examined by subjecting the attached footprint nanofibrils to different stretch lengths in successive elongation-relaxation experiments. Figure 4.3B (1) shows three force separation curves for the same protein bundle with saw-tooth characteristics. The peak forces varied from 250 pN to 1000 pN, possibly due to stretching two or more protein chains in parallel. When the fibrils were extended to the contour length of 560 nm in the first cycle, a sharp drop in force was observed, probably due to complete unfolding or detachment of segments of proteins from the nanofibrils. The reforming of footprint domains during the retraction cycle occurred quickly. Reforming of footprint domains was indicated by repeated unfolding peaks observed (orange color line; Figure 3B) in the subsequent cycles of the same protein(s). Figure 4.3B (Curve 3) shows the third stretching-relaxation cycle, with a sharp increase in force at the end of a 1100 nm extension. The force-extension curves showed that the footprint nanofibrils could be stretched and relaxed in a repetitive manner. The pull-off force curves showed similar features, after repeated extend-retract cycles, to those in first cycle. Footprint nanofibrils underwent bond reformation when allowed to relax as the tip moved towards the surface. In the next force separation curve, the rupturing of sacrificial bonds was again observed, suggesting that footprint protein(s) possesses 'self-healing' ability, similar to those reported in titin, silk, diatom adhesives and other proteins.[42, 60-62, 80, 85] The network appearance observed in Figure 4.2 supported the idea that the fibrils are composed of complex and interconnected smaller macromolecular subunits. Hence, it is not surprising that several molecules were stretched simultaneously in pulling experiments. Due to the complexity of the system, force-separation experiments did not yield regular and reproducible curves with uniform unfolding force as have been produced for rabbit muscle titin molecules and engineered proteins.[43, 92]

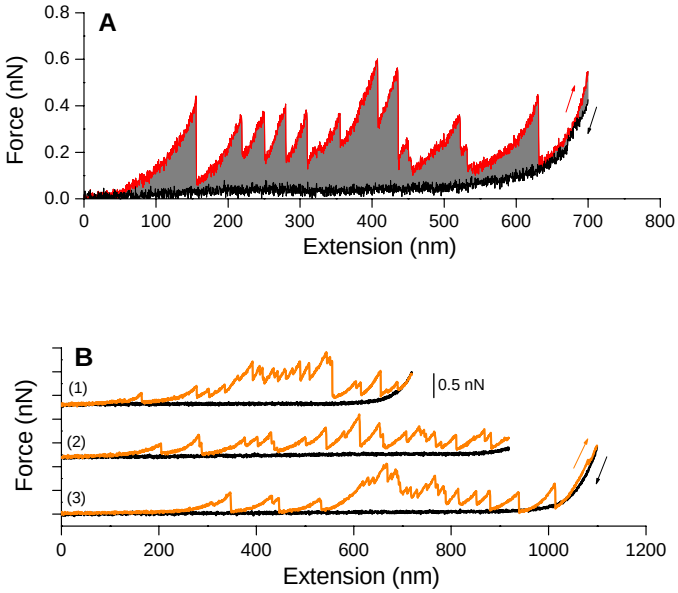

Figure 4.3. Force spectra recorded from a footprint of a *Balanus amphitrite* cyprid. Mechanical unfolding of footprint nanofibrils, which shows a saw-tooth characteristic with multiple progressive unfolding peaks (red arrow) and monotonic entropic elasticity in the relaxation curve (A). The footprint response under different mechanical strains (extension) (B).

In the experiments described so far, the piezoelectric scanner eventually reached its vertical z-direction limit (~ 2600 nm) during stretching of the nanofibrils. In order to further increase elongation, the scanner was raised manually by 2 preset values of 278 nm and 556 nm. Figure 4 shows the corresponding force-extension curves. Curve 1 in Figure 4.4 displays a force-separation curve with two distinct patterns, namely, saw-tooth characteristics at low extension (up to 700 nm) and predominantly elastic behavior at high extension (> 700 nm). Once all sacrificial bonds were broken, the tensile energy was stored elastically at higher extension.[84] When the tip was moved away from the surface, the saw-tooth characteristic gradually disappeared (see Figure 4.4, curve 5). Curve 5 showed a monotonic chain elasticity type behavior throughout the entire stretched length in the extension and retraction cycles. A transition flattening (plateau) force was observed at a stretch length of 3000 nm. This transition remained visible in Figure 4.4, curve 5, until the final detachment of the nanofibrils (at curve 16). The inset in Figure 4.4 shows another plot of such a transition found in another footprint. We suggest that this transition has a similar origin to that of chair-boat transitions of pyranose rings in polysaccharides.[69, 77, 93-96] The value of the transition force was approximately 1000 pN. This force corresponds to conformational change equivalent to a

single dextran ring, or deformation of three parallel amylose rings where the transition force is around 300 pN. The maximum force values observed in subsequent curves varied due to variation in segment detachment, rupture of sacrificial bonds and structure break-up in the complex molecular bundles. At curve 16, complete rupture of contact was observed. This rupture, presumably, took place at the weakest point, which could be anywhere between the tip and the surface. Prior to rupture, the pull-off force rose sharply to about 2000 pN followed by a sharp drop of tension to the baseline. In the next cycle, no signal from the stretching of footprint molecules was observed in the force-separation curve. Thus the nanofibrils detached completely before a total stretching length of 10 μm.

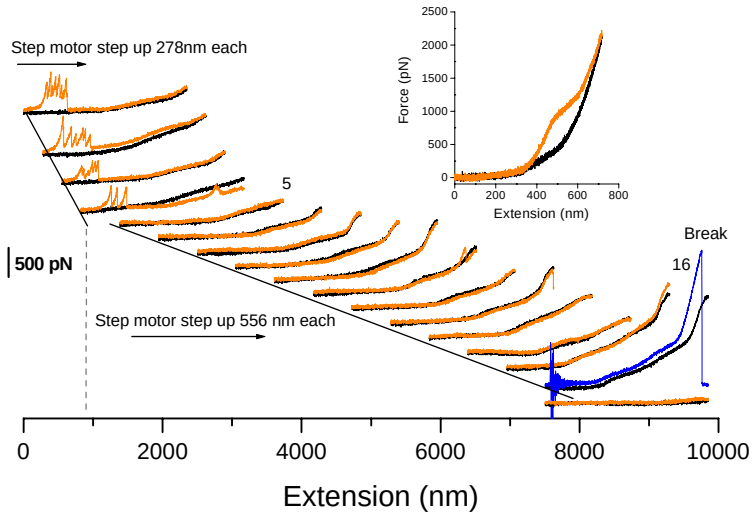

Figure 4.4. Force spectra recorded from a footprint of a *Balanus amphitrite* cyprid. Mechanical unfolding of footprint nanofibrils, which shows a saw-tooth characteristic with multiple progressive unfolding peaks (red arrow) and monotonic entropic elasticity in the relaxation curve (A). The footprint response under different mechanical strains (extension) (B).

Comparison of these results to those from α-macroglobulin[40, 41] may prove to be particularly enlightening given the similarities of this molecule to the barnacle settlement-inducing protein complex (SIPC); a glycoprotein complex (α_2-macroglobulin-like protein) known to be present in, or comprise entirely, barnacle cyprid footprint material.[33] Therefore, it is possible that both stretched α_2-macroglobulin molecules and footprint proteins possess similar mechanical responses. Ikai et al. first reported the use of AFM-FS to investigate the mechanical unfolding of α_2-macroglobulin (725 kDa) purified from human blood serum on a

gold surface.[40, 41] Force curves from the stretched α_2-macroglobulin molecule showed a saw-tooth characteristic with irregular force peaks. The stretched forces varied from 0.25 nN to 2.5 nN, with a maximum peak at 0.75 nN. The sacrificial bond unfolding force of footprints is 0.53 nN ± 0.18 nN. The difference in stretched force here may due to the gold-coated tip used in the previous study, where the formation or influence of Au-sulfide bonds is inevitable.[97, 98] The maximum stretched length of α_2-macroglobulin from human blood serum is distributed between 100 - 200 nm, for pulling of a single subunit and 400 nm, for pulling of 2 subunits connected in serial. The stretched length of footprints varied from a few hundreds of nanometers to > 2 μm, dependent on the quantity of footprint protein that was picked up by cantilever. Despite the difference in materials used in both cases, i.e. purified individual molecules vs. nanofibrils in footprint protein, the similarity in their respective stretching behaviors may allow direct comparison of the nanomechanical properties of these proteins. More significantly, it could provide further insight into the composition of the cyprid footprint.

4.2.3 Refolding dynamic of footprint protein segments

During the period of dependence on temporary attachment, the cyprid experiences significant mechanical stress in the form of hydrodynamic shear. The mechanical pulses invoked in this way apply a corresponding stress on the sacrificial bonds in footprints and eventually may detach the cyprid from the surface if their magnitude is sufficient. However, it is likely that the periodicity of these forces and their irregular application allows sacrificial bonds to reform in the footprint material before failure occurs at the substratum-protein or protein-cyprid interface. To mimic the stress-relaxation behavior of footprint nanofibrils, isolated nanofibrils were subjected to repeated AFM extension-relaxation cycles and allowed to relax over different delay periods. Figure 4.5A shows a series of force separation curves with different delay times. The first force curve obtained immediately following a stretch-relax cycle, without delay, is shown at the top of the force extension diagram in Figure 4.5A. This force extension curve shows predominantly elastic behavior, with only a few force peaks during extension, and smooth relaxation to the unstretched state. When a delay of 500 μs was applied between the pulling cycles, several force peaks were observed in the resulting force-extension trace. This trend continued for longer delays, i.e. enhancement of the saw-tooth characteristic and hysteresis was observed with increasing delay time. Moreover, the maximum pull-off distance also increased with increasing delay. These observations imply

that more energy was dissipated when a longer delay time was applied. Hansma et al. reported similar observations on the stretching of collagen.[85] They proposed that the longer delay provided more time for sacrificial bonds to reform and thus more energy could be dissipated in the next pulling cycle.

Figure 4.5B shows the energy dissipated during the pull cycle calculated from the hysteresis of the force-extension curves and the length of the extension section for which hysteresis behavior was demonstrated. This length is referred to as 'hysteresis length' and is related to the break up of all sacrificial bonds during extension. When the delay time was increased from 2 s to 10 s, sharp increases in the number of local peaks showing the saw-tooth pattern, hysteresis length and amount of dissipated energy, were observed. This indicates the onset of reforming sacrificial bonds during this delay period. We noted that similar trends were observed in several extension-delay cycles obtained for different footprints. The energy dissipation for 2 s and 10 s delays were $60 \pm 30 \times 10^{-18}$ J and $230 \pm 150 \times 10^{-18}$ J, respectively. The hysteresis length varied from 540 ± 120 nm to 800 ± 300 nm for 2 s and 10 s delay, respectively. A sharp increase in energy dissipation due to force cycle delays from 2 s to 5 s indicates the recovery time for the sacrificial bonds is about 5 s. This recovery rate is faster than the reported 10 s rebonding time for bone adhesive,[84] 30 s for diatom *Eunotia sudetica* adhesive,[99] and more than 100 s for bone collagen in calcium buffer.[85] The necessity for a rapid recovery of strength in cyprid footprints is important when one considers the size of the cyprid (*B. amphitrite* = ~ 500 μm length) compared to that of a diatom or algal spore (generally an order of magnitude smaller). Even considering the streamlined 'airfoil' shape of cyprids, their coefficient of drag would likely be significantly greater than that of a smaller organism and they would, therefore, require a correspondingly stronger adhesion system. With only a tiny amount (approximately 2×10^{-18} L on NH_2-terminated glass surface) of footprint utilized in temporary attachment (for each step), the footprints must be able to reform and recover quickly. The last pulling cycle shown in Figure 5A was captured without delay immediately following the previous cycle. Although some recovery of the sacrificial bonds can be observed, these indications disappeared after several cycles and, from there onwards, the trace is qualitatively similar to that of the first pulling cycle.

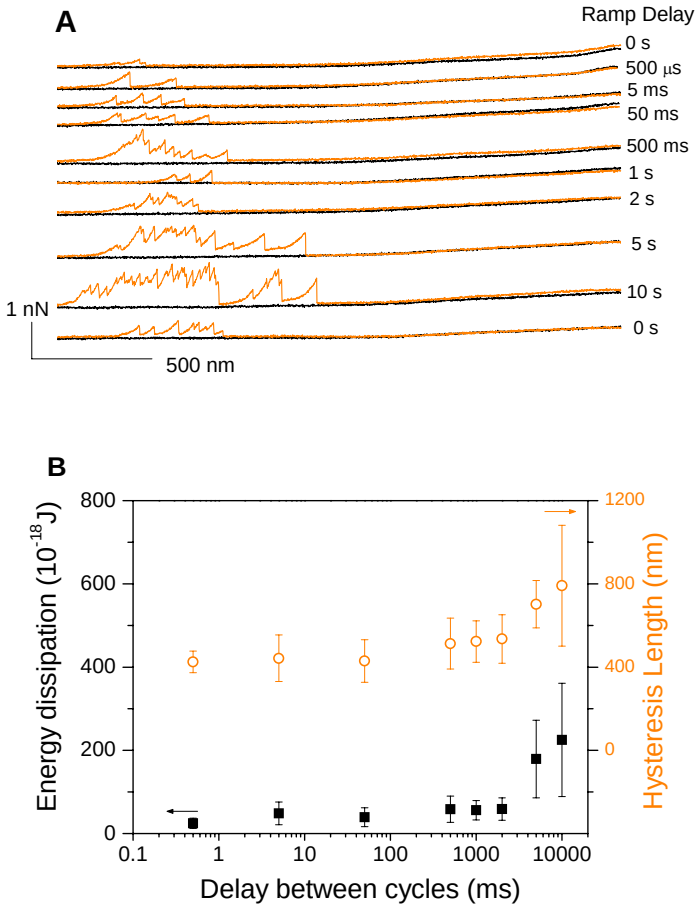

Figure 4.5. The refolding dynamics of nanofibrils allowed different relaxation times (delay time from 0 s to 10 s) (A) Energy dissipation and hysteresis length calculated from the force-extension curves with different delay time (B).

In order to check possible loading rate effects, we calculated the average rupture force observed in one pulling cycle and plotted it as a function of stretching rate (piezo retraction rate). The average rupture force is determined as the arithmetic mean of each local rupture at a sacrificial bond observed in the sawtooth pattern. Figure 4.6 shows the results of the stretch-rate experiments observed without delay and following 1 sec delay between cycles. No differences in pull-off force with respect to stretching rate could be observed. The absence of stretching rate dependence indicates that the system fluctuates between the bound and unbound states on a time scale that is much faster than that of the pulling experiment.[100-102] Again, this is a necessary scenario given the abundance of instantaneous forces that would act on an attached larva in the turbulent intertidal environment.

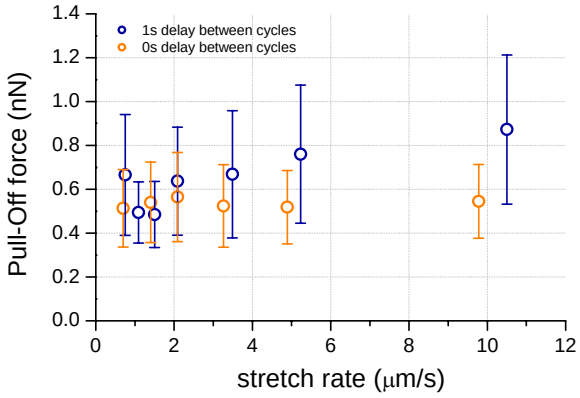

Figure 4.6. Stretch-rate dependence experiments with and without relaxation between the pulling cycles.

4.2.4 Segment elasticity of footprint protein chains

The force-extension relationship of footprint nanofibrils was described using the wormlike chain model (*WLC*)[69] in this manner (for quantitative expression see the experimental section). Fitting the *WLC* model involves the persistence length (L_P) and contour length (L_C) data of the footprint subunits which are measured under tension. We recognise that in an ideal situation this model would be applied to stretching of a single chain segment, however, the *WLC* model can also be used to describe the stretching of chain segments in parallel and this is the likely scenario in many of the present experiments. Figure 4.7 shows a representative force extension curve with saw-tooth characteristics including the fitted lines (orange) obtained from the *WLC* model. The L_P and L_C values were included in Figure 4.7to illustrate the relationship between the information obtained from the force separation curves and simulation results from the *WLC* model. The effective persistence length is shown and numbered for each curve fitted. The L_P obtained for the individual 'saw-teeth' (Figure 4.7) varied between 0.06 nm to 0.22 nm. L_P is closely related to the number of segments stretched.[61, 62] Persistence length values L_P < 0.14 nm were considered 'non-physical' since they are smaller than an atomic radius.[61, 85, 103] However, such non-physical values did occur and could be due, in this case, to the stretching and overlapping of multiple parallel molecules in the footprint nanofibrils.[61, 85, 92, 104] The unfolding peak force increased from peak 1 to peak 3 but the corresponding L_P values were reduced. In contrast, the reduction of unfolding peak forces from peaks 3 to 5 gave an increase in simulated L_P. The L_P remained relatively constant from peak 6 onwards. The unfolding force for peaks 9 to 11 is 760 pN which is higher than the 640 pN to unfold peaks 6 to 8. The L_P from peak 6 to peak

11 could imply that the stretched footprint nanofibrils were segments originating from one common backbone. The different unfolding forces could relate to the mechanical hierarchy present in the footprint nanofibrils and also to the fluctuating number of sacrificial bonds. Li et al. showed that in engineered giant titin molecules, the extension of segments proceeds from least stable to more stable domains.[43] It is likely that this sequential extension of subunits also occurs in footprint protein bundles.

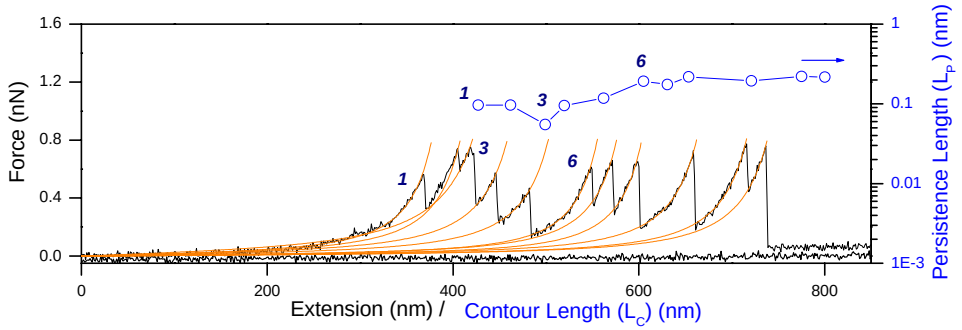

Figure 4.7. The description of saw-tooth unfolding peaks by worm-like chain (*WLC*) model (red line) and the obtained contour length (L_C) plot versus persistence length (L_P).

The number of tethered molecules (n) can be calculated from the value of the persistence length (L_P) using n = L_{P0}/L_P [92] if the longest apparent persistence length (L_{P0}) can be identified from the distribution of L_P.[61, 62] This is similar to the stretching of n-parallel springs at one time, where nF is required to stretch n individual springs with force F. Recently, Sarkar et al [104] demonstrated that the unfolding force and the persistence length value required to stretch two polyproteins in parallel was double and one half that for single polyproteins respectively.

4.3 Conclusions

Footprints of barnacle cypris larvae (*B. amphitrite*) were studied using AFM. Images revealed a network-like morphology of footprint proteins, consisting of aggregated and interconnected nanofibrils. Molecular scale mechanical properties of the fibrillar aggregates were accessed by force spectroscopy experiments. Characteristic saw-tooth force extension curves and entropic-elastic stretch behavior were observed depending on the degree of extension and deformation history. Hysteresis behavior was observed in repeated elongation-relaxation cycles. We interpreted this behavior in terms of a sacrificial bond model arising from intra/intermolecular loading and unloading. Delay/recovery time prior to testing of

individual fibrils was found to be important. For the section of force-extension curves exhibiting entropy-like spring behavior, the *WLC* model was applied to estimate the effective persistence and contour lengths. The change in persistence length with repeated testing was an indication of the breaking of sacrificial bonds between proteinaceous segments connected either in a parallel or in a serial fashion in the protein nanofibrils. The effective time needed to reform sacrificial bonds was estimated from experiments with controlled delay. Typical values were between 2 to 5 s. This behavior provides a dynamic binding mechanism for cyprids to resist water currents and instantaneous stress in a marine environment. At high elongation, following repeated stretching up to high strain, the corresponding force extension diagrams showed the signature of sugar rings within the glycoprotein which could be originated from the SIPC.

This detailed study of molecular nanomechanical properties by AFM has enabled a systematic approach to be taken towards future characterization of a large glycoprotein used in cyprid temporary adhesion. This material has properties that are desirable in synthetic adhesives, although it is likely that the actual mechanism of temporary adhesion in cyprids is more complex than reliance on a single glycoprotein deposit.[105] This material, however, must first be understood before a full understanding of how cyprids attach with such tenacity underwater can be claimed. Only when we understand this adhesion system, which facilitates initial colonization of surfaces by barnacles, will we be adequately armed to engage in hypothesis-driven development of specifically targeted antifouling marine coatings.

4.4 Experimental

Animals. *B. amphitrite* cyprids were batch cultured in the laboratory. Nauplii were released by adult *B. amphitrite* and raised on a diet of *Skeletonema costatum* according to Hellio et al.[106] Metamorphosis into cyprids occurred within 5 days. Cyprids were stored at 6°C to prevent settlement and used for AFM experiments within 5 days following the final nauplius molt to the cyprid.[107]

Surface preparation. Glass microscopy cover slips were sonicated in ethanol for 5 min and then immersed in piranha solution (a mixture of concentrated sulphuric acid and 33% hydrogen peroxide in a 3:1 ratio) for 15 mins. The surfaces were rinsed with Milli-Q water (Ultrapure Water system) and dried under N_2. Amino (NH_2-) terminated surfaces were obtained by gas-phase evaporation of 3-aminopropyl triethoxysilane (APTES) in a desiccator under vacuum.[108] APTES was obtained from Sigma Aldrich and used as received. Surfaces were incubated for several hours and then carefully rinsed with 99% ethanol and Milli-Q water.

AFM experiments. AFM measurements were carried out using a Dimension D3100 atomic force microscope equipped with a NanoScope IVa controller and a hybrid scanner (H-153) with x-, y- z-feedbacks from Veeco (Veeco / Digital Instruments (DI), Santa Barbara, CA). Triangular-shaped silicon nitride cantilevers (Veeco/Digital Instruments (DI), Santa Barbara, CA) were used throughout

the study and cantilever spring constants were calibrated using the thermal noise method.[109] The spring constant values obtained were in the range of 80 to 90 *p*N/nm. The cyprids were stored, prior to use, in 33 parts per thousand artificial seawater (ASW, Tropical Marine) and were then deposited onto prepared surfaces by micro-pipette. The modified glass cover slips were mounted in polystyrene Petri dishes prior to experiments. Typically, cyprids would attach to the glass surface and begin exploration when stimulated by small water currents. Explored areas of the modified glass were marked on the base of the Petri dishes and cyprids were then removed. Surfaces were flushed with large amounts of filtered ASW to minimize contamination. Petri dishes were then transferred to the AFM and the search for footprints was focused on the marked regions. Footprint images were obtained in contact mode with minimal force. Force-tip separation curves were subsequently obtained on preselected locations of the footprints. For imaging in air, samples were rinsed again with ASW and with Milli-Q water and dried in a stream of nitrogen gas. Silicon cantilevers, PointProbe®Plus Non-Contact High resonance frequency (PPP-NCH) from Nanosensors (Nanosensors, Wetzlar, Germany) were used for intermittent contact (tapping) mode operation to obtain high resolution images of the samples. Scan rates were varied from 0.3 Hz to 1 Hz and the free amplitude set-point value was around 1.5V. Nanoscope® software version 613b26 was used for data analysis.

Worm-like chain (WLC) polymer elasticity model. Polymer elasticity was described by the Worm-Like Chain (*WLC*) model.[32] The WLC model described the relationship between the chain extension x and entropic force $F(x)$ generated in the form: $F(x)=(kT/L_p)[0.25(1-x/L_c)^{-2} -0.25+x/ L_c]$ where k is the Boltzmann's constant; T is the temperature; L_p is the persistence length of the molecule and L_c is the contour length.[47]

4.5 Acknowledgements

Dr. Nick Aldred and Prof. Tony Clare are thanked for providing cyprid larva.

4.6 References

1. Wahl, M. *Mar. Ecol. Prog. Ser.* **1989,** *58*, 175-189.
2. Smith, A. M.; Callow, J. A., *Biological adhesives*. first ed.; Springer: Berlin, 2006.
3. Kamino, K.; Shizuri, Y., Structure and function of barnacle cement proteins. In *New developments in marine biotechnology*, LeGal, Y.; Halvorson, H. O., Eds. Plenum Press: New York, 1998; pp 77-80.
4. Kamino, K.; Inoue, K.; Maruyama, T.; Takamatsu, N.; Harayama, S.; Shizuri, Y. *J. Biol. Chem.* **2000,** *275*, 27360-27365.
5. Kamino, K. *Biochem. J.* **2001,** *356*, 503-507.
6. Mori, Y.; Urushida, Y.; Nakano, M.; Uchiyama, S.; Kamino, K. *FEBS J.* **2007,** *274*, 6436-6446.
7. Urushida, Y.; Nakano, M.; Matsuda, S.; Inoue, N.; Kanai, S.; Kitamura, N.; Nishino, T.; Kamino, K. *FEBS J.* **2007,** *274*, 4336-4346.
8. Benedict, C. V.; Waite, J. H. *J. Morphology* **1986,** *189*, 171-181.
9. Qin, X. X.; Waite, J. H. *J. Exp. Biol.* **1995,** *198*, 633-644.
10. Waite, J. H.; Qin, X. X.; Coyne, K. J. *Mat. Biol.* **1998,** *17*, 93-106.
11. Monahan, J.; Wilker, J. J. *Langmuir* **2004,** *20*, 3724-3729.
12. Lee, H.; Lee, B. P.; Messersmith, P. B. *Nature* **2007,** *448*, 338-341.
13. Waite, J. H. *Int. J. Biol. Macromol.* **1990,** *12*, 139-144.
14. Finlay, J. A.; Krishnan, S.; Callow, M. E.; Callow, J. A.; Dong, R.; Asgill, N.; Wong, K.; Kramer, E. J.; Ober, C. K. *Langmuir* **2008,** *24*, 503-510.

15. Schumacher, J. F.; Aldred, N.; Callow, M. E.; Finlay, J. A.; Callow, J. A.; Clare, A. S.; Brennan, A. B. *Biofouling* **2007,** *23*, 307 - 317.
16. Yebra, D. M.; Kiil, S.; Dam-Johansen, K. *Prog. Org. Coat.* **2004,** *50*, 75-104.
17. Townsin, R. L. *Biofouling* **2003,** *19*, 9-15.
18. Wolfson, A.; Vanblaricom, G.; Davis, N.; Lewbel, G. S. *Mar. Ecol. Prog. Ser.* **1979,** *1*, 81-89.
19. Champ, M. A. *Mar. Pollut. Bull.* **2003,** *46*, 935-940.
20. Evans, S. M.; Birchenough, A. C.; Brancato, M. S. *Mar. Pollut. Bull.* **2000,** *40*, 204-211.
21. Rosenhahn, A.; Ederth, T.; Pettitt, M. E. *Biointerphases* **2008,** *3*, IR1-IR5.
22. Clare, A. S.; Hoeg, J. T. *Biofouling* **2008,** *24*, 55-57.
23. Callow, M. E.; Callow, J. A. *Biologist* **2002**, 1-5.
24. Anderson, D. T., *Barnacles: structure, function, development and evolution*. Chapman & Hall: London, 1994; p 357.
25. Lagersson, N. C.; Hoeg, J. T. *Mar. Biol.* **2002,** *141*, 513-526.
26. Niederegger, S.; Gorb, S.; Jiao, Y. K. *J. Comp. Physiol.* **2002,** *187*, 961-970.
27. Walker, G.; Yule, A. B. *J. Mar. Biol. Ass. U. K.* **1984,** *64*, 679-686.
28. Clare, A. S.; Freet, R. K.; McClary, M. *J. Mar. Biol. Ass. U. K.* **1994,** *74*, 243-250.
29. Nott, J. A.; Foster, B. A. *Philos. Trans. R. Soc. London, Ser. B* **1969,** *256*, 115-134.
30. Yule, A. B.; Walker, G. *J. Mar. Biol. Ass. U. K.* **1984,** *64*, 429-439.
31. Dreanno, C.; Kirby, R. R.; Clare, A. S. *Biol. Lett.* **2006,** *2*, 423-425.
32. Phang, I. Y.; Aldred, N.; Clare, A. S.; Vancso, G. J. *J. R. Soc. Interface* **2008,** *5*, 397-401.
33. Dreanno, C.; Matsumura, K.; Dohmae, N.; Takio, K.; Hirota, H.; Kirby, R. R.; Clare, A. S. *Proc. Natl. Acad. Sci. U. S. A.* **2006,** *103*, 14396-14401.
34. Clare, A. S.; Nott, J. A. *J. Mar. Biol. Ass. U. K.* **1994,** *74*, 967-970.
35. Matsumura, K.; Nagano, M.; Kato-Yoshinaga, Y.; Yamazaki, M.; Clare, A. S.; Fusetani, N. *Proc. R. Soc. London, Ser. B* **1998,** *265*, 1825-1830.
36. Gerber, C.; Lang, H. P. *Nat. Nanotechnol.* **2006,** *1*, 3-5.
37. Drake, B.; Prater, C. B.; Weisenhorn, A. L.; Gould, S. A. C.; Albrecht, T. R.; Quate, C. F.; Cannell, D. S.; Hansma, H. G.; Hansma, P. K. *Science* **1989,** *243*, 1586-1589.
38. Engel, A.; Muller, D. J. *Nat. Struct. Biol.* **2000,** *7*, 715-718.
39. Bustamante, C.; Rivetti, C.; Keller, D. J. *Curr. Opin. Struct. Biol.* **1997,** *7*, 709-716.
40. Mitsui, K.; Hara, M.; Ikai, A. *FEBS Lett.* **1996,** *385*, 29-33.
41. Ikai, A.; Mitsui, K.; Tokuoka, H.; Xu, X. M. *Mater. Sci. Eng., C* **1997,** *4*, 233-240.
42. Rief, M.; Gautel, M.; Oesterhelt, F.; Fernandez, J. M.; Gaub, H. E. *Science* **1997,** *276*, 1109-1112.
43. Li, H. B.; Linke, W. A.; Oberhauser, A. F.; Carrion-Vazquez, M.; Kerkviliet, J. G.; Lu, H.; Marszalek, P. E.; Fernandez, J. M. *Nature* **2002,** *418*, 998-1002.
44. Oberhauser, A. F.; Marszalek, P. E.; Erickson, H. P.; Fernandez, J. M. *Nature* **1998,** *393*, 181-185.
45. Rief, M.; Oesterhelt, F.; Heymann, B.; Gaub, H. E. *Science* **1997,** *275*, 1295-1297.
46. Carrion-Vazquez, M.; Oberhauser, A. F.; Fisher, T. E.; Marszalek, P. E.; Li, H. B.; Fernandez, J. M. *Prog. Biophys. Mol. Biol.* **2000,** *74*, 63-91.
47. Kellermayer, M. S. Z. *Physiol. Meas.* **2005,** *26*, R119-R153.
48. Zou, S.; Hempenius, M. A.; Schonherr, H.; Vancso, G. J. *Macromol. Rapid Commun.* **2006,** *27*, 103-108.
49. Hugel, T.; Holland, N. B.; Cattani, A.; Moroder, L.; Seitz, M.; Gaub, H. E. *Science* **2002,** *296*, 1103-1106.
50. Chaudhuri, O.; Parekh, S. H.; Fletcher, D. A. *Nature* **2007,** *445*, 295-298.
51. Phang, I. Y.; Aldred, N.; Clare, A. S.; Vancso, G. J. *Nano**S*** **2007,** *01*, 35-39.
52. Pelling, A. E.; Sehati, S.; Gralla, E. B.; Valentine, J. S.; Gimzewski, J. K. *Science* **2004,** *305*, 1147-1150.
53. Zhang, Z.; Zou, S.; Vancso, G. J.; Grijpma, D. W.; Feijen, J. *Biomacromolecules* **2005,** *6*, 3404-3409.
54. Cross, S. E.; Jin, Y. S.; Rao, J.; Gimzewski, J. K. *Nat. Nanotechnol.* **2007,** *2*, 780-783.
55. Aldred, N.; Phang, I. Y.; Conlan, S. L.; Clare, A. S.; Vancso, G. J. *Biofouling* **2008,** *24*, 97-107.
56. Horber, J. K. H.; Miles, M. J. *Science* **2003,** *302*, 1002-1005.

57. Arce, F. T.; Avci, R.; Beech, I. B.; Cooksey, K. E.; Wigglesworth-Cooksey, B. *Biophys. J.* **2004,** *87*, 4284-4297.
58. Zhang, W.; Zhang, X. *Prog. Polym. Sci.* **2003,** *28*, 1271-1295.
59. Razatos, A.; Ong, Y. L.; Sharma, M. M.; Georgiou, G. *Proc. Natl. Acad. Sci. U. S. A.* **1998,** *95*, 11059-11064.
60. Dugdale, T. M.; Dagastine, R.; Chiovitti, A.; Mulvaney, P.; Wetherbee, R. *Biophys. J.* **2005,** *89*, 4252-4260.
61. Dugdale, T. M.; Dagastine, R.; Chiovitti, A.; Wetherbee, R. *Biophys. J.* **2006,** *90*, 2987-2993.
62. Dugdale, T. M.; Willis, A.; Wetherbee, R. *Biophys. J.* **2006,** *90*, L58-L60.
63. Higgins, M. J.; Molino, P.; Mulvaney, P.; Wetherbee, R. *J. Phycol.* **2003,** *39*, 1181-1193.
64. Callow, J. A.; Crawford, S. A.; Higgins, M. J.; Mulvaney, P.; Wetherbee, R. *Planta* **2000,** *211*, 641-647.
65. Phang, I. Y.; Aldred, N.; Clare, A. S.; Callow, J. A.; Vancso, G. J. *Biofouling* **2006,** *22*, 245-250.
66. Sun, Y. J.; Guo, S. L.; Walker, G. C.; Kavanagh, C. J.; Swain, G. W. *Biofouling* **2004,** *20*, 279-289.
67. Moy, V. T.; Florin, E. L.; Gaub, H. E. *Science* **1994,** *266*, 257-259.
68. Lee, G. U.; Chrisey, L. A.; Colton, R. J. *Science* **1994,** *266*, 771-773.
69. Giannotti, G. I.; Vancso, G. J. *ChemPhysChem* **2007,** *8*, 2290-2307.
70. Oberhauser, A. F.; Carrion-Vazquez, M. *J. Biol. Chem.* **2008,** *283*, 6617-6621.
71. Hinterdorfer, P.; Dufrene, Y. F. *Nat. Methods* **2006,** *3*, 347-355.
72. Stroh, C.; Wang, H.; Bash, R.; Ashcroft, B.; Nelson, J.; Gruber, H.; Lohr, D.; Lindsay, S. M.; Hinterdorfer, P. *Proc. Natl. Acad. Sci. U. S. A.* **2004,** *101*, 12503-12507.
73. Janshoff, A.; Neitzert, M.; Oberdorfer, Y.; Fuchs, H. *Angew. Chem. Int. Ed.* **2000,** *39*, 3213-3237.
74. Best, R. B.; Brockwell, D. J.; Toca-Herrera, J. L.; Blake, A. W.; Smith, D. A.; Radford, S. E.; Clarke, J. *Anal. Chim. Acta* **2003,** *479*, 87-105.
75. Beyer, M. K.; Clausen-Schaumann, H. *Chem. Rev.* **2005,** *105*, 2921-2948.
76. Bustamante, C.; Macosko, J. C.; Wuite, G. J. L. *Nat. Rev. Mol. Cell Biol.* **2000,** *1*, 130-136.
77. Marszalek, P. E.; Li, H. B.; Fernandez, J. M. *Nat. Biotechnol.* **2001,** *19*, 258-262.
78. Zhuang, X. W.; Rief, M. *Curr. Opin. Struct. Biol.* **2003,** *13*, 88-97.
79. Bustamante, C. *Q. Rev. Biophys.* **2005,** *38*, 291-301.
80. Becker, N.; Oroudjev, E.; Mutz, S.; Cleveland, J. P.; Hansma, P. K.; Hayashi, C. Y.; Makarov, D. E.; Hansma, H. G. *Nat. Mater.* **2003,** *2*, 278-283.
81. Fantner, G. E.; Oroudjev, E.; Schitter, G.; Golde, L. S.; Thurner, P.; Finch, M. M.; Turner, P.; Gutsmann, T.; Morse, D. E.; Hansma, H.; Hansma, P. K. *Biophys. J.* **2006,** *90*, 1411-1418.
82. Groshong, K. *NewScientist* **2007,** *194*, 43-45.
83. Smith, B. L.; Schaffer, T. E.; Viani, M.; Thompson, J. B.; Frederick, N. A.; Kindt, J.; Belcher, A.; Stucky, G. D.; Morse, D. E.; Hansma, P. K. *Nature* **1999,** *399*, 761-763.
84. Fantner, G. E.; Hassenkam, T.; Kindt, J. H.; Weaver, J. C.; Birkedal, H.; Pechenik, L.; Cutroni, J. A.; Cidade, G. A. G.; Stucky, G. D.; Morse, D. E.; Hansma, P. K. *Nat. Mater.* **2005,** *4*, 612-616.
85. Thompson, J. B.; Kindt, J. H.; Drake, B.; Hansma, H. G.; Morse, D. E.; Hansma, P. K. *Nature* **2001,** *414*, 773-776.
86. Mostaert, A. S.; Higgins, M. J.; Fukuma, T.; Rindi, F.; Jarvis, S. P. *J. Biol. Phys.* **2006,** *32*, 393-401.
87. Mostaert, A. S.; Jarvis, S. P. *Nanotechnology* **2007,** *18*, 044010.
88. Nakano, M.; Shen, J. R.; Kamino, K. *Biomacromolecules* **2007,** *8*, 1830-1835.
89. Yule, A. B.; Walker, G. *J. Mar. Biol. Ass. U. K.* **1985,** *65*, 707-712.
90. Holland, C.; Terry, A. E.; Porter, D.; Vollrath, F. *Nat. Mater.* **2006,** *5*, 870-874.
91. Vollrath, F.; Porter, D. *Soft Matter* **2006,** *2*, 377-385.
92. Kellermayer, M. S. Z.; Bustamante, C.; Granzier, H. L. *Biochim. Biophys. Acta* **2003,** *1604*, 105-114.
93. Kawakami, M.; Byrne, K.; Khatri, B.; McLeish, T. C. B.; Radford, S. E.; Smith, D. A. *Langmuir* **2004,** *20*, 9299-9303.

94. Marszalek, P. E.; Oberhauser, A. F.; Li, H. B.; Fernandez, J. M. *Biophys. J.* **2003,** *85*, 2696-2704.
95. Marszalek, P. E.; Pang, Y. P.; Li, H. B.; El Yazal, J.; Oberhauser, A. F.; Fernandez, J. M. *Proc. Natl. Acad. Sci. U. S. A.* **1999,** *96*, 7894-7898.
96. Li, H. B.; Rief, M.; Oesterhelt, F.; Gaub, H. E.; Zhang, X.; Shen, J. C. *Chem. Phys. Lett.* **1999,** *305*, 197-201.
97. Carl, P.; Kwok, C. H.; Manderson, G.; Speicher, D. W.; Discher, D. E. *Proc. Natl. Acad. Sci. U. S. A.* **2001,** *98*, 1565-1570.
98. Ikai, A.; Afrin, R.; Itoh, A.; Thogersen, H. C.; Hayashi, Y.; Osada, T. *Coll. Surf. B.* **2002,** *23*, 165-171.
99. Gebeshuber, I. C.; Thompson, J. B.; Del Amo, Y.; Stachelberger, H.; Kindt, J. H. *Mater. Sci. Technol.* **2002,** *18*, 763-766.
100. Bell, G. I. *Science* **1978,** *200*, 618-627.
101. Bustamante, C.; Chemla, Y. R.; Forde, N. R.; Izhaky, D. *Annu. Rev. Biochem.* **2004,** *73*, 705-748.
102. Evans, E.; Ritchie, K. *Biophys. J.* **1997,** *72*, 1541-1555.
103. Abu-Lail, N. I.; Camesano, T. A. *Langmuir* **2002,** *18*, 4071-4081.
104. Sarkar, A.; Caamano, S.; Fernandez, J. M. *Biophys. J.* **2007,** *92*, L36-38.
105. Aldred, N.; Clare, A. S. *Biofouling* **2008,** *24*, 351-363.
106. Hellio, C.; Marechal, J. P.; Veron, B.; Bremer, G.; Clare, A. S.; Le Gal, Y. *Mar. Biotech.* **2004,** *6*, 67-82.
107. Rittschof, D.; Branscomb, E. S.; Costlow, J. D. *J. Exp. Mar. Biol. Ecol.* **1984,** *82*, 131-146.
108. Ling, X. Y.; Reinhoudt, D. N.; Huskens, J. *Langmuir* **2006,** *22*, 8777-8783.
109. Hutter, J. L.; Bechhoefer, J. *Rev. Sci. Instrum.* **1993,** *64*, 3342-3342.

Chapter 5

Interfacial forces with chemical specificity of barnacle cyprid "footprints" proteins by AFM*

Cyprid larvae of the barnacle *Semibalanus balanoides* leave footprint proteins at surfaces immersed in marine environment during pre-settlement exploration. This is considered as a very essential step in biofouling processes, hence the relevant interfaces, i.e. protein-substrate and protein seawater (or other contacting body) should be understood. The nanomechanical properties of such temporary adhesive "footprints" secreted by barnacle cyprid larva were probed by atomic force microscopy (AFM). Freshly secreted footprint adhesives at hydrophilic -NH_2 terminated surfaces were studied by imaging and force spectroscopy. In this Chapter, we used commercial, hydrophilic Si_3N_4 tips and chemically functionalized tips featuring –CH_3 functional groups to mimic the interfacial interaction with hydrophobic and hydrophilic surfaces. Force-extension curves of protein bundles picked up by AFM tips exhibited a characteristic saw-tooth appearance, and showed characteristic differences for the two different tip surface chemistries. These differences were evident from the pull-off force and pull-off length plots. All pull-off force histograms showed forces in the range of 0 - 2 nN, with a maximum at ca. 0.9 nN, which was attributed to breaking "sacrificial" intermolecular bonds. Data from –CH_3 functionalized tips showed an additional pull-off force (~ 6 nN) arising from hydrophobic interactions.

*Parts of this Chapter have been submitted for publication.

5.1 Introduction

Barnacles, are perhaps the most notorious marine fouling species, being commonly found attached to the hulls of ships and other artificial structures. The accumulation of fouling on manmade surfaces has the principal effect of increasing surface roughness and, therefore, increasing the hydrodynamic drag experienced by the immersed object. Depending on the structure in question, this process can variously enhance corrosion,[1] increase greenhouse gas emissions,[2] reduce propulsion efficiency and increase fuel costs by as much as 86%.[3] In marine fouling research, most effort is currently directed towards understanding the release of adult barnacles from surfaces,[4] however, there is an alternate perspective and barnacles have historically received much attention from those wishing to exploit their adhesives commercially.[5] In the latter regard, the cyprid larvae of barnacles, which have discrete adhesives of their own, have received surprisingly little attention.

The cyprid larva of barnacles is responsible for surface exploration, selection and settlement.[6] Cyprids, in this case of the barnacle *Semibalanus balanoides* (*S. balanoides*), are capable of temporary or rapidly reversible adhesion; a process that is used during their initial exploration of surfaces.[7] Using two specialized antennules, laden with sensory structures[8] and terminated in an adhesive disc,[9] cyprids walk across surfaces in a bi-pedal fashion and at a maximum rate of two body lengths per second. During surface exploration, 'footprints' of a glycoproteinaceous material are deposited and this material has an assumed role in the temporary adhesion of the organism; in some cases being termed 'temporary adhesive'.[7] Once the cyprid commits to settlement, a rapidly curing "permanent cement"[10] is secreted through the antennules, embedding them and fixing the cyprid permanently to the surface. The permanent cement, which is not discussed any further in this study, is thought to be different in composition and function to both the temporary adhesive and the adult barnacle cement.[11] Metamorphosis from a settled cyprid to a juvenile barnacle is then completed within 5 – 8 h in *B. amphitrite*.

Understanding the adhesives of barnacles and their larvae is a necessary step in the development of biomimetic adhesives that are capable of functioning underwater. This problem includes two interfaces, i.e. protein - substrate, and protein - sea water contacts. Clearly the little known and poorly understood 'temporary' and 'permanent' adhesives of cyprids present an opportunity to study the properties and composition of adhesives that have evolved to function in a liquid medium. It is likely that inspiration from materials such as these will direct future adhesives formulation. The present study concentrates on the cyprid temporary adhesive and builds on information presented in recent publications.[12-14] We

explore, with chemical specificity, using the recently developed molecular force spectroscopy by Atomic Force Microscopy (AFM), the adherence strength of the exposed footprint surface to AFM tips bearing hydrophilic, or hydrophobic surfaces.

AFM is a simple but versatile instrument[15] and, in its most simple application, it employs a sharp probe to image surface topology on the micro-/nano-scale. Most commonly, the surface of interest is raster scanned in relation to a static tip – a process controlled by electronic feedback. Reflection of a laser beam from the AFM tip is detected and this information can be interpreted into x, y, z data, allowing real-time compilation of high-resolution three-dimensional topological maps. Force distance interactions between the tip and the surface can also be measured with high accuracy, providing that the spring constant of the cantilever (on which the tip is mounted) is known. Single chains can be stretched, and force extension curves be measured quantitatively [for a recent review see e.g. Giannotti & Vancso (2007)].[16] The advantages of AFM over other microscopic techniques have historically been exploited to measure surface topology in "quasi" 3 dimensions,[17, 18] surface physical/chemical properties[19, 20] and physical properties of (bio)macromolecules at the nano-scale and in different environments.[21-38] In particular, there is growing interest in using AFM-based techniques to measure the mechanical properties of single molecules *in singulo*, so as to study the static and dynamic molecular properties of engineered proteins, measure specific antigen-antibody interactions and determine the energy dissipation associated with bond rupturing.[23-29]

Throughout their development, the above techniques have been used extensively to study the complex nanomechanical properties of natural bio-materials. For example, measurement of the modulus of alga adhesive,[39, 40] the energy dissipation mechanisms of spider silk[41-43] or bone glue,[44, 45] and single modular protein unfolding in diatom mucilage[46-46-50] have been explored. By studying the energy dissipation mechanisms of different bioadhesives, Hansma et al. (1999) proposed that the toughness present in most bioadhesives originates from the repetitive breaking of intermediate "sacrificial bonds" that prevent severe damage of the protein backbone under applied stress. [51-53] The incorporation of sacrificial bonds in bioadhesives creates a very resilient system capable of dissipating large amounts of energy. In addition, the surface of the AFM tip can be tailored, by chemical functionalization, for applications that require experimentation using specific chemical end-groups. Chemical force microscopy (CFM) utilizes tips with different chemistries, produced through covalent attachment of thin monolayers of alkane-silane or alkane-thiols.[30-38] Moreover, by using live bioprobe such as bacteria,[54-56] live ditaom[57] attached to the tip, which term biological force

microscopy, has been used to measure the adhesion force of the respective species respect to different surfaces.

Study of the nanomechanical properties of barnacle cyprid (*S. balanoides*) footprints by AFM aimed to further elucidate the role of this material in the reversible adhesion of cyprids. We have carried out similar work previously[13, 58] and some preliminary data pertaining to footprints was gleamed, however the majority of analytical work of this type (in the sphere of barnacles) has focused on the adult stage. For example, Sun et. al. (2004) studied the elastic modulus of adult barnacle cement by indenting the adhesives with an AFM tip. They concluded that the barnacle adhesive plaque is a multilayered structure.[59]

The cyprids deposited footprints of a glycoproteinaceous secretion while exploring on chemically functionalized surfaces. Footprints of *S. balanoides* (Figure 5.1A-B) have been observed previously on -NH_2 and -CH_3 functionalized glass surfaces.[13] Representative AFM height images of the footprint morphology are shown in Figure 5.1. Figure 5.1A displays a single footprint on an –NH_2, while Figure 5.1B captures a footprint on a –CH_3 substrate. High-resolution imaging revealed that the adhesive is porous and fibrillar in nature on -NH_2 glass. The dimensions of the footprints depend on the polarity (water contact angle) of the substrate and vary between 50-60 microns, which were noted to be significantly larger on the hydrophobic surface than on -NH_2 glass. Isolated chains and bundles of protein aggregates were observed in the network structure of footprints (Figure 5.1C).[39, 41, 48] Figure 5.1C exhibits a perspectivic view of a section of a footprint. It can be seen that footprints have an oval appearance, and consist of thin fibrils with a variation in their diameter, which were identified as protein chain bundles, or even single chain proteins.[13] However, a quantitative understanding of the interactions between footprint proteins and surfaces still remains unknown. Data of this type are necessary before biomimetic adhesives akin to the cyprid FP can be formulated.

With this in mind, the aim of this Chapter is to probe the relevant interfacial forces of footprints at the protein-substrate and protein-seawater (or protein surface-contacting body) interfaces with chemical specificity. This Chapter reports on the results of the protein deposits on the hydrophilic substrates featuring –NH_2 groups tested using commercial untreated, and chemically modified AFM probes at the seawater-protein side of the relevant interfaces. This allows us to better understand the interactions of footprint proteins with different chemically terminated surfaces.

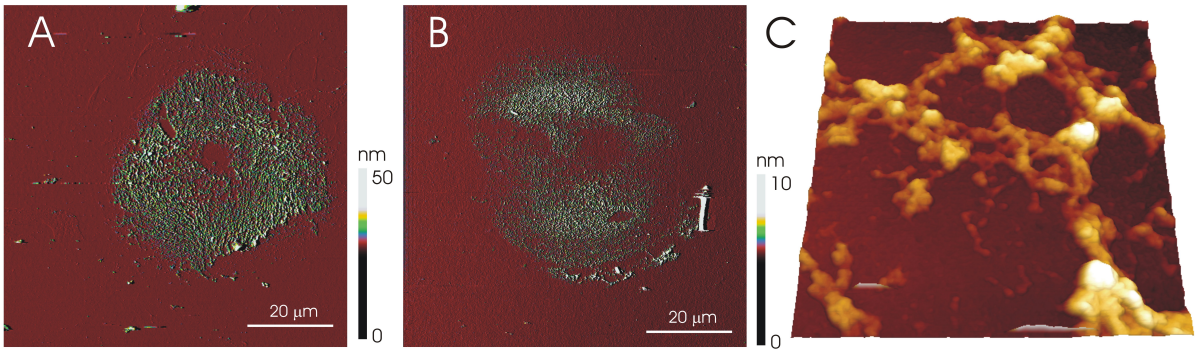

Figure 5.1. Atomic force microscopy (AFM) micrographs (deflection) of cyprid larva footprints deposited on (A) NH_2- and (B) CH_3-chemically functionalized surfaces. (C) High resolution 3D AFM micrograph of protein adhesive in an aggregated fibrillar structure (scan size: 1 µm × 1 µm and z-range = 50 nm).

5.2 Results and discusssion

Figure 5.2 shows typical force-extension curves obtained from AFM force measurements of footprints on -NH_2 functionalized glass surfaces (abbreviated as FP-NH_2) using either commercial, untreated Si_3N_4 tips, or tips featuring an alkanethiol monolayer, terminated by -CH_3 functions (CH_3-tip hereafter). Force spectroscopy measurements were performed by allowing the AFM tip to contact and subsequently withdraw from the footprint surface. The appearance of force-extension curves (Figure 5.2A and B) showed marked differences depending on the tip surface chemistry. For example, in Figure 5.2, when footprint proteins adhered to the AFM tip, pull-off events were observed in the retraction cycle, which rendered a saw-tooth appearance to the force-extension curve. Representative force curves consisted of sections of gradually increasing upward slopes, as the protein chains experienced an increasing elongation towards their maximum extension. Eventually a sacrificial bond, presumably involved in maintaining the tertiary structure of the protein, would yield and, as a consequence, the tension within the stretched chain dropped to minimum, manifesting a ‘pull-off’ event in the force extension curve.[58] The sacrificial chain “hidden length” within the folded proteins unraveled as the sacrificial bond was broken, which contributed to an increase in total extension of the protein. As the piezoelectric scanner was retracted further from the surface, the tip continued to stretch and unravel more sacrificial bonds.[53] Thus, as the stretching process continued, distinctive saw-tooth force curves were obtained, which are known to be diagnostic of this type of unfolding behavior. This process of sacrificial bond rupturing continued until the last bond was broken. The saw-tooth characteristic was observed in both force extension curves obtained from Si_3N_4 and

CH_3-tip, respectively. However, for hydrophobic tips, initially large pull-off forces were typically observed with a pull-off length of 100-200 nm, prior to the onset of the saw-tooth pattern with pull-off peaks at much more moderate forces. The pull-off force of CH_3-tip experienced larger pull-off events with adhesion forces measured up to several nanoNewton (nN, 10^{-9} N) at the first part of the force-extension curve, followed by the saw-tooth characteristic with pull-off force of several hundreds of picoNewton (pN, 10^{-12} N). The force and length recorded for each individual pull-off event (as shown in Figure 5.2A, labels 1-6) were considered as individual pull-off force and pull-off length events in the subsequent analysis.

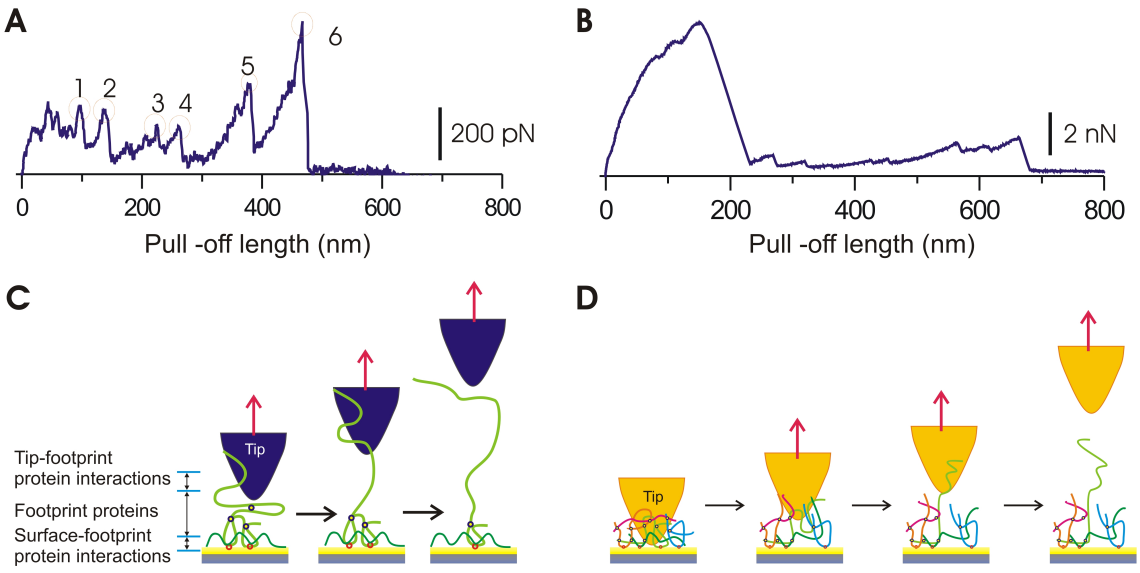

Figure 5.2. Representative force-separation curves between FP-NH_2 and Si_3N_4-tip (A) and CH_3-tip (B). Only retraction cycle is shown in this figure. Note the difference in the scale of the pull-off force axis. Schematic of Si_3N_4 tip (C) and CH_3-tip (D) interacted with footprints found in NH_2- glass.

In our study, the footprint proteins were freshly secreted by cyprids with neither additional treatment nor purification. Thus, it is likely that at least some of the observed stretching events were the result of bundles of protein aggregates binding to the AFM tip, connected to each other via sacrificial bonds. In the present context, therefore, 'sacrificial bond' refers to all of the possible supramolecular intra- and intermolecular (non-covalent) bonds within the footprint material that maintain its conformation in native conditions. [41, 44, 45, 47, 51-53]

The pull-off force measurements from control experiments on NH_2-glass (without footprints) were obtained by using CH_3-tip as well as Si_3N_4 tip. All the force-distance curves showed a single adhesion pull-off peak in the control experiments. The respective histograms of the pull-off forces (see supporting information) indicated adhesion forces of 1.1 ± 0.2 nN and 2.2 ± 0.4 nN, for Si_3N_4 and CH_3-tips, respectively. This trend is in line with CFM in water [see review by Noy et al. (1997)].[36] As these single-peaked adhesion-force curves were observed at very low pull off lengths (in comparison with the footprint proteins), tip-surface pull-off contributions can be neglected in the following discussion.

Figure 5.2C-D shows the mechanism that is believed to operate during pulling of FP proteins with the Si_3N_4 and CH_3-tip, respectively. For a hydrophilic tip the nonspecific pull-off forces are moderate, and the pull-off cycle is dominated by rupturing sacrificial bonds. We believe (see later) that when hydrophobic tips are used, first large, non-specific hydrophobic-hydrophobic forces in water should be broken between tip and hydrophobic sections of the FP protein.[36] Then, remaining fibrils, or chains should be broken up following the sacrificial rupture model, until contact between FP protein and tip is disconnected. Eventually, in the final rupture event (in Figure 5.2A, e.g. 6) the weakest link gets ruptured. If this is between protein-tip, then the tip will break loose of the protein surface. However, depending on the number and strength of the supramolecular bonds between tip-protein and protein-substrate, also the protein-substrate contact may also yield (adhesive rupture). The force of the physisorption can range from hundreds of piconewtons (pN) to as strong as several nanonewtons (nN) before the molecule detaches from the tip (or from the surface).[60-62] As Figure 5.2A-B shows, the footprint proteins were securely anchored to the tip prior to detachment; hence the individual sacrificial bond strength and the interactions between footprint proteins and substratum can be examined. As the pulling process continued, the sacrificial bonds broke (blue open circle) and the chain is stretched further until it is finally detached from the tip (Figure 5.2C-D).

The force curves displaying the nanomechanical properties of footprint proteins are statistically analyzed and summarized in Figure 5.3. Figure 5.3A-C shows the histograms of the pull-off force, the pull-off length and pull-off force versus pull-off length measured from Si_3N_4 tip from FP-NH_2, respectively. The pull-off forces required to stretch proteins for FP-NH_2 substrates as shown in Figure 5.3A were broadly distributed centered at one *Lorentzian* peak, at 0.7 nN, using a single *Lorentzian* fit. The corresponding pull-off lengths presented in Figure 5.3B showed a narrowly distributed population, with an average length at 40 nm and a very broad population peaked at ~280 nm, respectively. The force histograms obtained with

CH_3-tips showed in Figure 5.3D exhibit a distribution with two Lorentzian peaks with maxima at 0.9 nN and 6 nN, respectively. In particular, the high pull-off force peak exhibited a very broad distribution, ranging from 2 - 8 nN. The histogram of the pull-off length from CH_3-tips is shown in Figure 5.3E. Again, a sharp maximum at short pull-off lengths (ca. 40 nm), and a broad distribution centered around 400 nm can be observed.

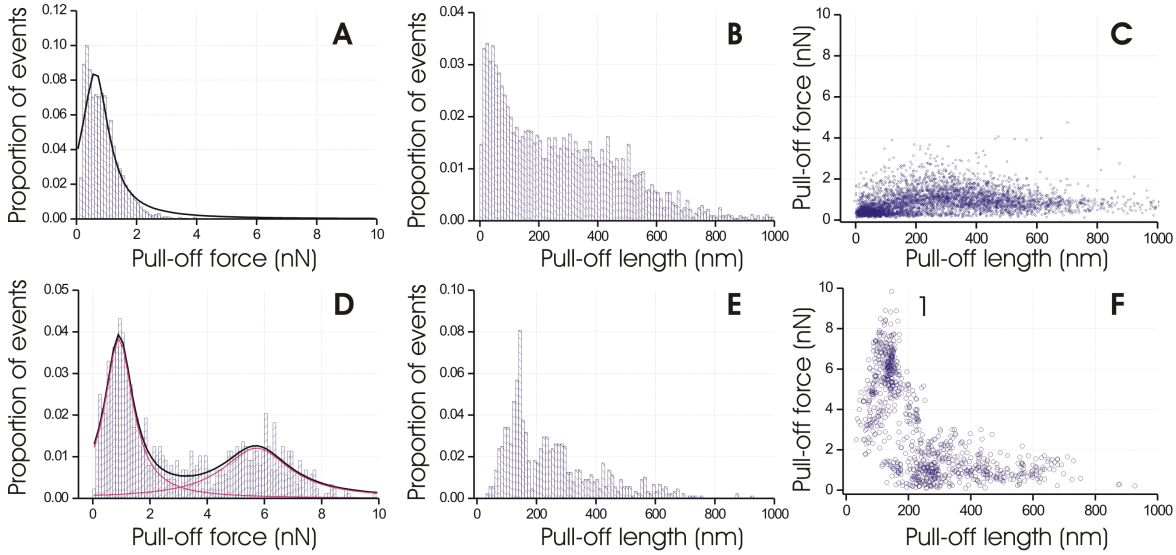

Figure 5.3. Histograms of pull-off force, pull-off length and pull-off force versus pull-off length correlation plots from footprints found in NH_2-SAMs glass with Si_3N_4 tip (A - C) and CH_3-tip (D - E). All peaks were fitted with Lorentzian functions.

The study of the correlation between pull-off force and pull-off length provided better understanding to footprint proteins as adhesives that bind to the surface. In one single force cycle several pull-offs can be observed at different rupture lengths, until the final pull-off event. It is interesting to display pull-off forces and the corresponding statistical pull-off lengths in form of "cross-correlation" plots. Figure 5.3C shows that the rupture forces observed are between 0 - 2 nN while for all corresponding rupture the pull-off length is varied between 0 - 800 nm. This means that there is no preferencial length at which rupture should take place for Si_3N_4 tip and FP protein. This gives us support to assume that the corresponding molecular rupture events belong to breaking sacrificial bonds. Figure 5.3F shows the correlation diagram of pull-off force versus pull-off length with respect to the -CH_3 functionalized tips on the FP-NH_2. Here we see clearly two populations, i.e. a horizontal band similar to the Si_3N_4 tip (Figure 5.3C) and a vertical one at short pull-off lengths, however to very high rupture forces (up to 8 - 10 nN). This large population of high pull-off forces are

related to the high adhesion forces observed in Figure 5.3B. The low pull-off force observed in both CH_3-tip (0.9 nN) are in the same order of magnitude of pull-off force observed in Si_3N_4 (0.7 nN) and hence we ascribe these to the stretching of sacrificial chains and breaking of sacrificial bonds.[63]

The correlation plot of pull-off force vs. pull-off length showed that high pull-off force events were mostly concentrated at low pull-off length. The high adhesion force at low pull off length, i.e. population "1" in Figure 5.3F, hints at a different and additional interaction between the hydrophobic and the FP proteins. The average pull-off force of CH_3-tip (~ 6 nN) observed is approximately one order of magnitude higher than the average pull-off force of hydrophilic tip (Si_3N_4 tip). This strong adhesion from the CH_3-tip could not arise from the specific interactions between the disulfide groups in the footprint proteins and the gold surface because the tip is densely covered by the hydrophobic self-assembled molecules.[64] We explain this by assuming that when CH_3-tip is in contact with footprint proteins in aqueous environment, the surrounding water molecules must be excluded from the footprint proteins and CH_3-tip interface as a result of the presence of hydrophobic tip. This change of water distribution in the local environment does consequently affect the footprint protein conformation, resulting in higher adhesion forces via strong hydrophobic-hydrophobic interactions in water observed in Figure 5.3F. [30, 36, 65-68] In support of this observation, in a review on CFM of chemically functionalized surfaces pull-off forces between -CH_3 terminated surfaces in water were reported to be 10 - 20 times higher as compared to pull-off forces between two –CH_2OH terminated surfaces.[36, 66]

5.3 Conclusions

The mechanical behavior of barnacle cyprid (*Semibalanus balanoide*) footprint proteins were probed from specific surfaces. Footprints deposited on the CH_3-glass and NH_2-glass were imaged *in situ* by AFM. Footprint proteins deposited on the NH_2-glass were measured by force spectroscopy with hydrophilic, as well as chemically functionalized hydrophobic tips in order to determine the chemically specific tip surface- footprint protein interaction in aqueous media (artificial seawater). The different chemically functionalized tips provide an important pathway to investigate *in situ* the interface of the footprint and surface. While the footprint proteins experienced elongation between the AFM tip and the different surfaces, the individual sacrificial bond strength and the interactions between footprint proteins and substratum were examined. The rupture force of sacrificial bonds was independent on the tip surface chemistry. When the CH_3-tip is separating from the footprint

protein, the effect of water exclusion in the local environment resulted in a higher adhesion force than that observed for hydrophilic tips. The use of AFM force measurements with chemically specificity would be beneficial for future studies in in situ characterization of bioadhesives - interface interactions.

5.4 Experimental

Animals. *S. balanoides* cyprids were collected by plankton tow from the wild population at Cullercoats, UK (55.1N 1.26W) during April 2006 and were stored in 2*l* glass containers, at 1 cyprid/ml, filled with artificial sea water (ASW; Tropic Marin™) at 6^{o}C prior to use. Feeding was not necessary as cyprids are lecithotrophic.

Chemicals. 1-Octadecanethiol (ODT, $CH_3(CH_2)_{17}SH$) and 3-aminopropyl triethoxysilane (APTES) were purchased from Sigma Aldrich. All chemicals were used as received, unless otherwise stated.

Surface preparation. Glass microscopy cover slips were sonicated in ethanol for 5 min and then immersed in piranha solution (a mixture of concentrated sulphuric acid and 33% hydrogen peroxide in a 3:1 ratio) for 15 mins. The surfaces were rinsed with nanopure water and dried under N_2. Amino (NH_2) terminated surfaces were obtained by gas-phase evaporation of 3-aminopropyl triethoxysilane (APTES) in a desiccator under vacuum. All chemicals were used as received, unless otherwise stated. Surfaces were incubated for several hours and then carefully rinsed with 99% ethanol and nanopure water. Contact angle measurements were carried out to characterized the functionalized surfaces immediately after completion of the silanization. The values of contact angles for NH2-functionalized glass was 60°.

Preparation of functionalized tips. Triangular shaped silicon nitride tips and silicon nitride tips (Digital Instruments (DI), Santa Barbara, CA) were coated with ca. 2 nm Ti and ca. 50 nm Au in high vacuum (SSENS b.v. Hengelo NL). The cantilever functionalization was carried out as described earlier [69]. Briefly, the tips were sonicated in ethanol solution and rinse with excess ethanol and DI water to remove contamination. Then, the tips were rinsed overnight in the thiolated solution containing 1mM of 1-octadecanethiol. The functionalized tips were rinsed thoroughly with ethanol and DI water under nitrogen stream. The surfaces ranged in wettability as defined using advancing water contact angles (θ_{AW}) from 11-mercapto-1-undecanol is 15^{o} and from 1-octadecanethiol is 107^{o}.

Atomic force microscopy (AFM). AFM measurements were carried out using a Dimension D3100 atomic force microscope equipped with a NanoScope IVa controller and a hybrid scanner (H-153) with x-, y- z- feedbacks from Veeco (Veeco / Digital Instruments (DI), Santa Barbara, CA). Triangular-shaped silicon nitride cantilevers (Veeco/Digital Instruments (DI), Santa Barbara, CA) were used throughout the study and cantilever spring constants were calibrated using the thermal noise method.[70] The cantilevers used for acquisition of the present results had a spring constant range from 0.062 to 0.100 Nm^{-1}. Cyprids were stored, prior to use, in 33 parts per thousand artificial sea

water (ASW) and were then deposited onto prepared surfaces by micro-pipette. Surfaces were mounted in glass Petri-dishes prior to experimentation. Typically, cyprids would attach and begin exploration of the surfaces when stimulated by small water currents. Explored areas of the glass were marked on the base of the cover slip and cyprids were then removed from the Petri-dishes. Surfaces were flushed with large amount of filtered ASW to minimize contamination. Petri-dishes were then transferred to the AFM and the search for footprints was focused on the marked regions. Custom programmed software for LABVIEW™ was used for data analysis throughout to transform the raw data to force-separation curves according to method described by Janshoff *et al.* [25] There were a total of 3860 pull-off events detected in 899 force extension curves from FP-NH_2 and 880 events were detected in 295 force-separation curves for statistical histogram presented in Figure 3. Different chemically modified tips were used to measure the adhesion force of footprints deposited on NH_2-glass. All peaks were fitted with Lorentzian functions.

5.5 Acknowledgements

Dr. Nick Aldred and Prof. Tony Clare are thanked for providing cyprid larva.

5.6 References

1. Yebra, D. M.; Kiil, S.; Dam-Johansen, K. *Prog. Org. Coat.* **2004,** *50*, 75-104.
2. Townsin, R. L. *Biofouling* **2003,** *19*, 9-15.
3. Schultz, M. P. *Biofouling* **2007,** *23*, 331-341.
4. Anderson, D. T., *Barnacles: structure, function, development and evolution*. Chapman & Hall: London, 1994; p 357.
5. Kamino, K. *Mar. Biotechnol.* **2008,** *10*, 111-121.
6. Crisp, D. J.; Walker, G.; Young, G. A.; Yule, A. B. *J. Colloid Interface Sci.* **1985,** *104*, 40-50.
7. Walker, G.; Yule, A. B. *J. Mar. Biol. Ass. U. K.* **1984,** *64*, 679-686.
8. Clare, A. S.; Nott, J. A. *J. Mar. Biol. Ass. U. K.* **1994,** *74*, 967-970.
9. Nott, J. A.; Foster, B. A. *Philos. Trans. R. Soc. Lond., Ser. B* **1969,** *256*, 115-134.
10. Walker, G. *J. Adhes.* **1981,** *12*, 51-58.
11. Yule, A. B.; Walker, G., Adhesion in barnacles. In *Crustacean Issues 5: Barnacle Biology*, Southward, A. J., Ed. A. A. Balkema: Rotterdam, 1987; pp 389-402.
12. Aldred, N.; Phang, I. Y.; Conlan, S. L.; Clare, A. S.; Vancso, G. J. *Biofouling* **2008,** *24*, 97-107.
13. Phang, I. Y.; Aldred, N.; Clare, A. S.; Callow, J. A.; Vancso, G. J. *J. R. Soc. Interface* **2008,** *5*, 397-401.
14. Phang, I. Y.; Aldred, N.; Clare, A. S.; Vancso, G. J. *Nano**S*** **2007,** *01*, 35-39.
15. Gerber, C.; Lang, H. P. *Nat. Nanotechnol.* **2006,** *1*, 3-5.
16. Giannotti, G. I.; Vancso, G. J. *ChemPhysChem* **2007,** *8*, 2290-2307.
17. Engel, A.; Muller, D. J. *Nat. Struct. Biol.* **2000,** *7*, 715-718.
18. Radmacher, M.; Tillmann, R. W.; Fritz, M.; Gaub, H. E. *Science* **1992,** *257*, 1900-1905.
19. Butt, H. J.; Cappella, B.; Kappl, M. *Surf. Sci. Rep.* **2005,** *59*, 1-152.
20. Cappella, B.; Dietler, G. *Surf. Sci. Rep.* **1999,** *34*, 1-104.
21. Ginger, D. S.; Zhang, H.; Mirkin, C. A. *Angew. Chem. Int. Ed.* **2004,** *43*, 30-45.
22. Jaschke, M.; Butt, H. J. *Langmuir* **1995,** *11*, 1061-1064.
23. Carrion-Vazquez, M.; Oberhauser, A. F.; Fisher, T. E.; Marszalek, P. E.; Li, H. B.; Fernandez, J. M. *Prog. Biophys. Mol. Biol.* **2000,** *74*, 63-91.
24. Hinterdorfer, P.; Baumgartner, W.; Gruber, H. J.; Schilcher, K.; Schindler, H. *Proc. Natl. Acad. Sci. U. S. A.* **1996,** *93*, 3477-3481.

25. Janshoff, A.; Neitzert, M.; Oberdorfer, Y.; Fuchs, H. *Angew. Chem. Int. Ed.* **2000,** *39*, 3213-3237.
26. Lee, G. U.; Chrisey, L. A.; Colton, R. J. *Science* **1994,** *266*, 771-773.
27. Mitsui, K.; Hara, M.; Ikai, A. *FEBS Lett.* **1996,** *385*, 29-33.
28. Moy, V. T.; Florin, E. L.; Gaub, H. E. *Science* **1994,** *266*, 257-259.
29. Schonherr, H.; Beulen, M. W. J.; Bugler, J.; Huskens, J.; van Veggel, F.; Reinhoudt, D. N.; Vancso, G. J. *J. Am. Chem. Soc.* **2000,** *122*, 4963-4967.
30. Frisbie, C. D.; Rozsnyai, L. F.; Noy, A.; Wrighton, M. S.; Lieber, C. M. *Science* **1994,** *265*, 2071-2074.
31. Noy, A. *Surf. Interface Anal.* **2006,** *38*, 1429-1441.
32. Noy, A.; Vezenov, D. V.; Kayyem, J. F.; Meade, T. J.; Lieber, C. M. *Chem. Biol.* **1997,** *4*, 519-527.
33. Hudson, J. E.; Abruna, H. D. *J. Am. Chem. Soc.* **1996,** *118*, 6303-6304.
34. McKendry, R.; Theoclitou, M. E.; Rayment, T.; Abell, C. *Nature* **1998,** *391*, 566-568.
35. Vezenov, D. V.; Noy, A.; Rozsnyai, L. F.; Lieber, C. M. *J. Am. Chem. Soc.* **1997,** *119*, 2006-2015.
36. Noy, A.; Vezenov, D. V.; Lieber, C. M. *Annu. Rev. Mater. Sci.* **1997,** *27*, 381-421.
37. Sheng, X. X.; Jung, T. S.; Wesson, J. A.; Ward, M. D. *Proc. Natl. Acad. Sci. U. S. A.* **2005,** *102*, 267-272.
38. Hillborg, H.; Tomczak, N.; Olah, A.; Schonherr, H.; Vancso, G. J. *Langmuir* **2004,** *20*, 785-794.
39. Mostaert, A. S.; Jarvis, S. P. *Nanotechnology* **2007,** *18*, 044010.
40. Walker, G. C.; Sun, Y. J.; Guo, S. L.; Finlay, J. A.; Callow, M. E.; Callow, J. A. *J. Adhes.* **2005,** *81*, 1101-1118.
41. Becker, N.; Oroudjev, E.; Mutz, S.; Cleveland, J. P.; Hansma, P. K.; Hayashi, C. Y.; Makarov, D. E.; Hansma, H. G. *Nat. Mater.* **2003,** *2*, 278-283.
42. Oroudjev, E.; Soares, J.; Arcdiacono, S.; Thompson, J. B.; Fossey, S. A.; Hansma, H. G. *Proc. Natl. Acad. Sci. U. S. A.* **2002,** *99*, 9606-9606.
43. Shulha, H.; Po Foo, C. W.; Kaplan, D. L.; Tsukruk, V. V. *Polymer* **2006,** *47*, 5821.
44. Fantner, G. E.; Hassenkam, T.; Kindt, J. H.; Weaver, J. C.; Birkedal, H.; Pechenik, L.; Cutroni, J. A.; Cidade, G. A. G.; Stucky, G. D.; Morse, D. E.; Hansma, P. K. *Nat. Mater.* **2005,** *4*, 612-616.
45. Thompson, J. B.; Kindt, J. H.; Drake, B.; Hansma, H. G.; Morse, D. E.; Hansma, P. K. *Nature* **2001,** *414*, 773-776.
46. Crawford, S. A.; Higgins, M. J.; Mulvaney, P.; Wetherbee, R. *J. Phycol.* **2001,** *37*, 543-554.
47. Dugdale, T. M.; Dagastine, R.; Chiovitti, A.; Mulvaney, P.; Wetherbee, R. *Biophys. J.* **2005,** *89*, 4252-4260.
48. Dugdale, T. M.; Dagastine, R.; Chiovitti, A.; Wetherbee, R. *Biophys. J.* **2006,** *90*, 2987-2993.
49. Dugdale, T. M.; Willis, A.; Wetherbee, R. *Biophys. J.* **2006,** *90*, L58-L60.
50. Higgins, M. J.; Molino, P.; Mulvaney, P.; Wetherbee, R. *J. Phycol.* **2003,** *39*, 1181-1193.
51. Groshong, K. *NewScientist* **2007,** *194*, 43-45.
52. Smith, B. L.; Schaffer, T. E.; Viani, M.; Thompson, J. B.; Frederick, N. A.; Kindt, J.; Belcher, A.; Stucky, G. D.; Morse, D. E.; Hansma, P. K. *Nature* **1999,** *399*, 761-763.
53. Fantner, G. E.; Oroudjev, E.; Schitter, G.; Golde, L. S.; Thurner, P.; Finch, M. M.; Turner, P.; Gutsmann, T.; Morse, D. E.; Hansma, H.; Hansma, P. K. *Biophys. J.* **2006,** *90*, 1411-1418.
54. Razatos, A.; Ong, Y. L.; Sharma, M. M.; Georgiou, G. *Proc. Natl. Acad. Sci. U. S. A.* **1998,** *95*, 11059-11064.
55. Bowen, W. R.; Lovitt, R. W.; Wright, C. J. *J. Colloid Interface Sci.* **2001,** *237*, 54-61.
56. Lower, S. K.; Hochella, M. F.; Beveridge, T. J. *Science* **2001,** *292*, 1360-1363.
57. Arce, F. T.; Avci, R.; Beech, I. B.; Cooksey, K. E.; Wigglesworth-Cooksey, B. *Biophys. J.* **2004,** *87*, 4284-4297.
58. Phang, I. Y.; Aldred, N.; Ling, X. Y.; Huskens, J.; Clare, A. S.; Vancso, G. J. **2008**, submitted.
59. Sun, Y. J.; Guo, S. L.; Walker, G. C.; Kavanagh, C. J.; Swain, G. W. *Biofouling* **2004,** *20*, 279-289.
60. Rief, M.; Oesterhelt, F.; Heymann, B.; Gaub, H. E. *Science* **1997,** *275*, 1295-1297.
61. Grandbois, M.; Beyer, M.; Rief, M.; Clausen-Schaumann, H.; Gaub, H. E. *Science* **1999,** *283*, 1727-1730.

62. Kellermayer, M. S. Z. *Physiol. Meas.* **2005,** *26*, R119-R153.
63. Monahan, J.; Wilker, J. J. *Langmuir* **2004,** *20*, 3724-3729.
64. Carl, P.; Kwok, C. H.; Manderson, G.; Speicher, D. W.; Discher, D. E. *Proc. Natl. Acad. Sci. U. S. A.* **2001,** *98*, 1565-1570.
65. Singh, S.; Houston, J.; van Swol, F.; Brinker, C. J. *Nature* **2006,** *442*, 526-526.
66. Sinniah, S. K.; Steel, A. B.; Miller, C. J.; ReuttRobey, J. E. *J. Am. Chem. Soc.* **1996,** *118*, 8925-8931.
67. Skulason, H.; Frisbie, C. D. *Langmuir* **2000,** *16*, 6294-6297.
68. Meyer, E. E.; Rosenberg, K. J.; Israelachvili, J. *Proc. Natl. Acad. Sci. U. S. A.* **2006,** *103*, 15739-15746.
69. Schonherr, H.; Hruska, Z.; Vancso, G. J. *Macromolecules* **1998,** *31*, 3679-3685.
70. Hutter, J. L.; Bechhoefer, J. *Rev. Sci. Instrum.* **1993,** *64*, 1868-1873.

Chapter 6

Marine biofouling field tests, settlement assay and footprint morphology by AFM, of cyprid larvae of *Balanus amphitrite* on model surfaces*

In this Chapter, AFM, settlement assay and field tests were used to correlate the morphology of cyprid footprints with the settlement behaviour of cyprids on different substrates. AFM imaging under laboratory conditions revealed that footprints found on glass coated with alkane silane, exposing a CH_3- surface, are more porous and larger than the footprints observed on aminosilane, NH_2-functionalized surfaces. The overall footprint volume secreted on both substrates is found to be the same (2.1 - 2.6 μm^3). In addition to AFM imaging, laboratory cyprid larva settlement assays and marine field tests were used to study the settlement behavior of cyprid larvae. In these studies three substrates were used: untreated clean glass and the two silanized glass surfaces used in AFM experiments, featuring CH_3- and NH_2- terminal groups. The results distinguish a settlement preference on the NH_2-glass and untreated glass, as compared to CH_3- terminated surfaces. This result suggests that barnacle cyprid larvae favor settlement on hydrophilic over hydrophobic surfaces. Combining the observations from all experiments at different length scales, we speculate that the confined footprint size on NH_2-glass may contribute to a higher concentration of the settlement inducing protein complex (SIPC). Settlement may be further facilitated by stronger adherence of FP adhesives to the NH_2-surface via Coulombic interactions.

*Parts of this Chapter have been accepted as: I. Y. Phang, K. C. Chaw, S. S. H.Choo, R. K. C. Kang, S. S. C. Lee, W. R. Birch, S. L. M. Teo, G. J. Vancso. *Biofouling,* **2008,** *accepted.*

6.1 Introduction

Earlier in this Thesis various aspects of the biofouling of barnacles, at the early stages of the fouling process, have been discussed. It has been shown, that cypris larvae explore surfaces in a bipedal walking prior to settlement. During this process they extract glycoproteinaceous material in contact with substrates, in form of "footprints". We investigated the morphology of these footprint proteins by AFM imaging, and their micro/nanomechanical properties by AFM based force spectroscopy. We have also looked at the influence of the surface chemistry of the substrates on the footprint characteristics. These results provided new insights into the cyprid attachment process from a fundamental point of view. In order to make the first steps towards utilization, we have undertaken "real" field test studies, using model substrates which possess the same types of functional groups, as used in our fundamental AFM work. The field studies have been performed in Singapore, in close collaboration with scientists of the Tropical Marine Science Institute of the National University of Singapore, jointly with colleagues from the Institute of Materials Research and Engineering (IMRE, A*STAR). We believe that the combination of this field test study, together with the outcome of our fundamental AFM experiments of the footprints, will provide industries with additional concepts for future materials design to obtain new and advanced antifouling coatings. In the forthcoming Chapter the corresponding results of this field test research are summarized.

Marine biofouling is a long-standing issue with economic and environmental impact. Biofouling on ship hulls costs billions of dollars in fuel consumption and maintenance. This increased fuel consumption contributes to greenhouse gas emissions.[1] The undesirable attachment of marine organisms, such as barnacles, green algae, diatoms, and mussels compromises the functioning of man-made structures immersed in sea water. This fouling degrades the performance of high added-value marine structures, such as buoy sensors and harbour installations. Among fouling organisms, barnacles represent a significant nuisance, due to their size and gregarious nature.[2] A barnacle evolves through planktotrophic nauplius stages, leading to a non-feeding cypris stage, which metamorphoses into adulthood. Cyprids have sole mission to explore and select the permanent settling site, where the adult barnacle will remain fixed.[3] Cyprids use a temporary adhesion, generated by a protein extract to facilitate their reversible attachment to surfaces.[4-7] As they explore the surface, they leave "footprints." The exact physiochemical nature of the footprint adhesive material remains largely unknown. However, a settlement inducing protein complex (SIPC), which functions as a conspecies settlement cue, can be found in footprint adhesive.[5-7]

Significant efforts are being made to design new, environmentally benign solutions that prevent and tackle marine fouling. Concerted action is needed by materials scientists, biologists, chemists, and coatings specialists to deliver significant improvements. Despite our need to understand the settlement process to implement coating design, the relevant behavior of marine organisms remains poorly understood.[8-21]

The antifouling performance characteristics of current antifouling coatings are generally evaluated by settlement assays of bacteria or macrofoulers. These tests are corroborated by field tests that evaluate the performance of the coatings in marine environments. While the majority of barnacle biofouling studies focus on the settlement of adult barnacles from field tests, studies on the exploration stage of cyprid larvae remain elusive. We note that permanent, cured proteinaceous adhesives (barnacle "cement") used by adult barnacles for attachment are intriguing materials. They exhibit a very high adhesion strength and consist of initially water-soluble proteins, which cure underwater.[22] It is generally considered that footprint proteins are different from those in the permanent cement[23, 24] and that their adhesive performance is also different. Although they may be inferior adhesives, the role they play in the settlement process is crucial. We believe that if progress is to be made in designing and preparing new antifouling surfaces, the first steps of the fouling process, including the deposition of footprint proteins at the microscopic larval stage, must be understood. This understanding would then help to devise antifouling strategies as opposed to making empirical efforts to optimize antifouling coating formulations by "hit-or-miss" or "empirical" approaches.

Previously, we studied the morphology of the footprints of barnacle (*Semibalanus balanoide*) cyprid larva by atomic force microscopy (AFM) at the micro- and nanoscopic length scales.[25-27] Our studies find that footprint adhesives deposited in situ at hydrophobic and hydrophilic surfaces show significant differences in footprint size and morphology, consisting of thin nanofibrils and protein fibers. Studies of footprint morphology and settlement behaviour of cyprids may provide information on the relationship between the spreading and adhesion of footprint adhesive and settlement behaviour.

In this Chapter, we examine the morphology of cyprid footprints using AFM, comparing it with laboratory cyprid settlement tests and marine biofouling field tests. AFM provides detailed morphological information on individual footprints with micron and nano scale resolution. Settlement assays and field tests determine the settlement preferences of single species cyprid larvae. Field tests generate quantitative species population data in a marine environment. Comparing AFM-based studies with larval settlement and marine

biofouling may provide an indication of how footprint adhesive interactions with model surfaces may be used to regulate the recruitment of barnacles and other macrofouling organisms.

6.2 Results

6.2.1 Footprint morphology by AFM imaging

The morphology of barnacle cyprid footprints (FPs) was studied by AFM on different substrates, including hydrophobic and hydrophilic surfaces (CH_3-glass NH_2-glass, respectively). Figure 6.1 shows representative AFM height images of FPs obtained from different surfaces (CH_3- and NH_2-glass) in air by tapping mode AFM (TM-AFM). Entire footprints and sections of footprints at higher magnification were imaged. The morphology and size of FPs on the CH_3- and NH_2- terminated surfaces exhibit significant differences. The footprints on CH_3-glass are generally larger in size and have a broader shape variations. They exhibit an oval shape and a porous structure (Figure 6.1). At the edge of the FPs fiber-like structures can be seen. These are spread in a radial pattern and probably represent adhesive material, as shown in Figure 6.1(B - C). The size of a typical FP on CH_3-glass (CH_3-FP) is approximately 60 μm in length by 50 μm wide. In contrast, footprints deposited on NH_2-glass (NH_2-FP) have a well-defined size and shape. The three NH_2-FPs shown in Figure 6.1D are imaged with lower magnification. The NH_2-FPs are less porous than CH_3-FPs. Large areas of the NH_2-FPs are densely covered with a homogeneous layer of adhesive, composed of fibres. Their layer thickness (Figure 6.1(E - F)), is much thinner than that on CH_3-glass. The shape of these footprints was also oval. However, as stated earlier, the size of the NH_2-FPs is smaller, typically 30 μm in length by 20 μm wide.

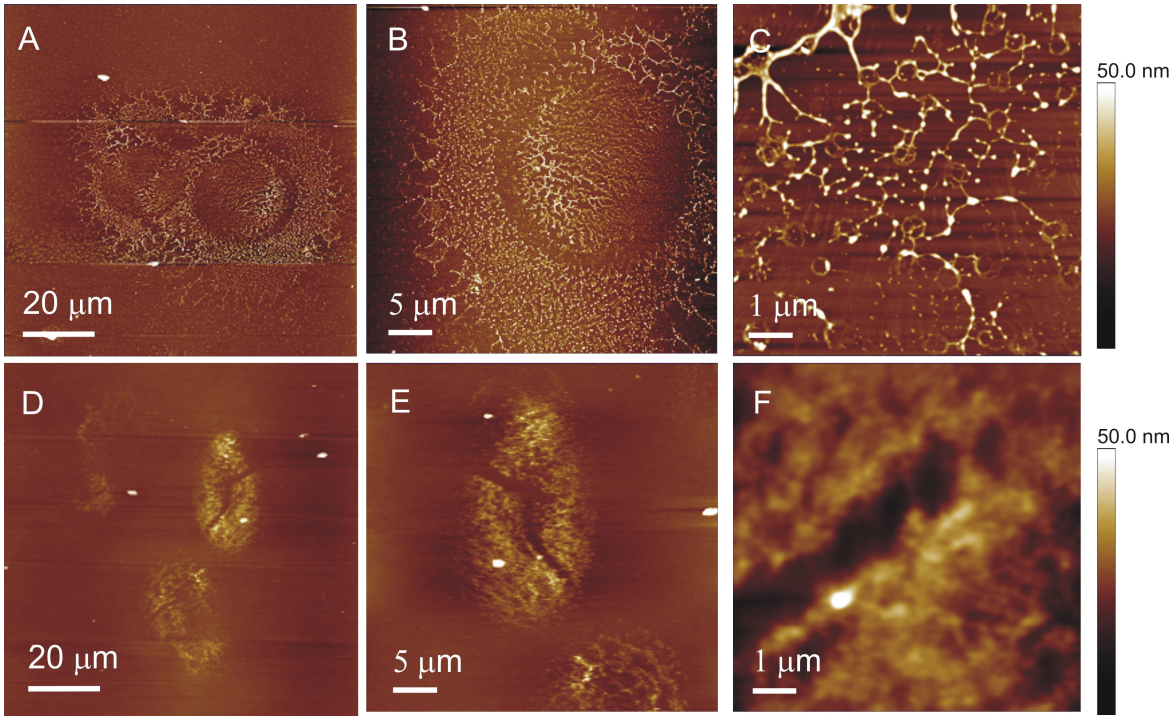

Figure 6.1. The morphogies of footprints secreted by barnacle cyprid larva on CH_3- (A – C) and NH_2-(D – F) functionalized glass surfaces.

The outlines of all FPs collected over an 18 month period on CH_3- and NH_2-glass are compiled in Figure 6.2. There were more FPs obtained on NH_2-glass (19 FPs) than on CH_3-glass (6 FPs). Table 6.1shows the geometrical data extracted from the footprint contours on NH_2- and CH_3-glass. The average surface area of CH_3-FPs is 5 times larger than NH_2-FPs. The size of the NH_2-FPs is similar to that of the attachment pad, reported to be about 20 μm in diameter.[25] The thickness and volume of the FP adhesive layer deposited on the two surfaces also differs. FP adhesive spread on CH_3-glass consisted of thick nano-fibers, with a height of 15 - 40 nm. On NH_2-glass, the thickness ranged from 5 to 15 nm. However, the average thickness for the FPs is similar if the porous area on the footprints is factored into the total volume (6.5 nm for CH_3-FPs and 8.4 nm for NH_2-FPs, respectively). The porosity of CH_3-FPs is 80 %, and that of NH_2-FPs is 40%. Taking this porosity into account, the footprints deposited on CH_3-glass and NH_2-glass have similar volumes, of 2.6 μm^3 and 2.0 μm^3, respectively.

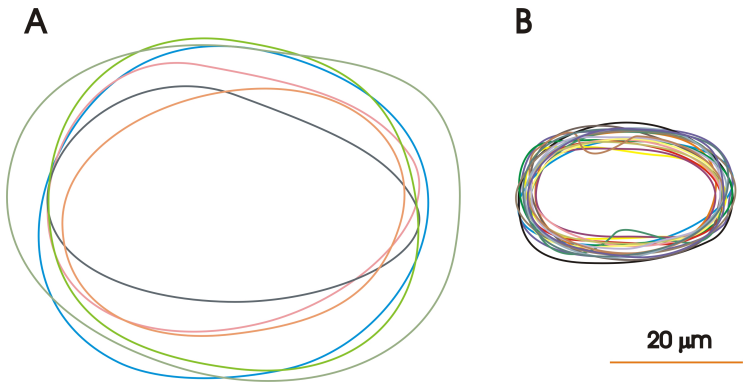

Figure 6.2. The outline of all FPs collected over a period of 18 months on (A) CH_3- and (B) NH_2-terminated glass surfaces.

Table 6.1. The morphological information of footprints obtained by AFM.

Glass surface functionalization	*Mean footprint area (μm^2)*	*Average thickness (nm)*	Porosity	Volume (μm^3)
CH_3 (θ_{Adv} = 106°)	1980 ± 500	6.5	0.8	2.6 ± 0.7
NH_2 (θ_{Adv} = 60°)	410 ± 60	8.4	0.4	2.1 ± 0.3

6.2.2 Cyprid larvae settlement assay

In addition to the morphology observations of footprints, a laboratory scale settlement choice assay was performed using *Balanus amphitritae* larvae on CH_3-glass and NH_2-glass, respectively. The settlement assay provides a preliminary study of the settlement preferences of barnacle cyprid larva under see water in a single fouling species environment. Cyprid larvae were incubated in the trough containing glasses, NH_2-glasses and CH_3-glasses, respectively where clean glass slides were used as reference. There were a total of 5 slides for each substrates tested for the respective settlement assay. Cyprid larvae were allowed to explore freely on the surfaces in the trough for 24 h. The number of settled cyprids found on each surfaces were counted and the statistics were shown in Figure 6.3. The highest number of settled cyprid larva was found on untreated borosilicate glass, with 14 ± 16 settlements, followed by 8 ± 5 settlements on NH_2-glass and the least settlements found on CH_3-glass surfaces with 1 ± 1 settlements. The large standard variation observed is probably due to the gregarious settlement nature of cyprid larvae. Once the cyprid started to settle on the surface, it fouls relatively quicker than those surfaces without settlement,[28] resulting in a large variation in certain samples. Hence, a statistical analysis, i.e. Wilcoxon 2 sample test is used

to differentiate the samples. The Wilcoxon-Mann-Whitney test (Wilcoxon test) in statistics is a non-parametic test for assessing whether two statistical samples of observations originate from the same distribution. A statistical parameter p can be calculated to characterize the overlap between two distributions. P can have values between 0 and 1. Both extreme values represent complete separation of the distributions, while a ρ of 0.5 represents complete overlap.

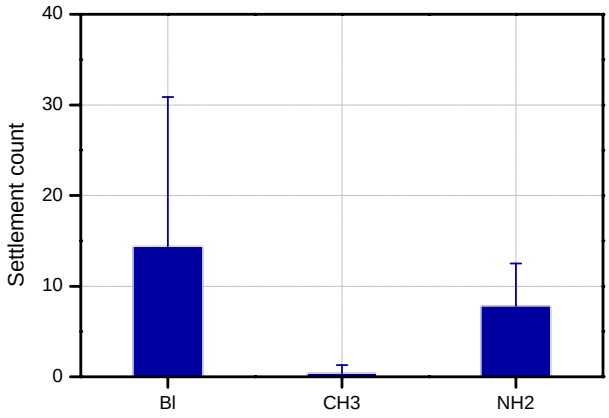

Figure 6.3. The 24 h laboratory settlement assay of barnacle cyprid larva on blank glass surface (Bl), CH_3- and NH_2-glass surfaces.

Wilcoxon 2 sample tests performed on the CH_3-glass and NH_2-glass yielded a $p < 0.008$, which showed a clear difference in cyprid settlement preferences on these surfaces. In addition, CH_3-glass and borosilicate glass also lead to differences in the settlement, with $p < 0.02$, whereas the settlement of cyprid on glass and NH_2-glass surfaces are not distinguishable ($p < 0.81$). The results of settlement assay suggest the preference of cyprid to settle on the hydrophilic surfaces (glass, NH_2-glass) over the hydrophobic surface (CH_3-glass).

6.2.3 Field assessment

Panel immersion tests were carried out to assess the fouling conditions on CH_3- and NH_2-surfaces, as well as untreated glass, in a macroscopic marine environment. The aim was to compare the result from panel immersion to the choice settlement assays, and to try to correlate these with AFM observations. We prepared alkyl- (CH_3-) and amino-terminated monolayers (NH_2-) on glasses and silicon surfaces, i.e. CH_3-glass, NH_2-glass, CH_3-SiO_2 and NH_2-SiO_2 by vapour phase deposition for panel immersion test. There were 4 silicon substrates and 5 glass slides for each type of surface. Glass slides and silicon wafers were

subjected to the panel immersion test simultaneously for comparison. All the test samples were accessed and recorded by photography twice per week. The field assessment was completed when 40% of the surface was covered with fouling organisms. Prior to the evaluation, we trimmed away 2.5 cm and 0.5 cm from the edge of the images taken from the silicon and glass samples, respectively to remove the edge effect. The evaluation of the surfaces was performed by commercial software Photogrid 1.0. The pictures obtained from the panel immersion test were imported to Photogrid and 100 points were randomly assigned across the surface. Fouling species found on these points was identified manually.

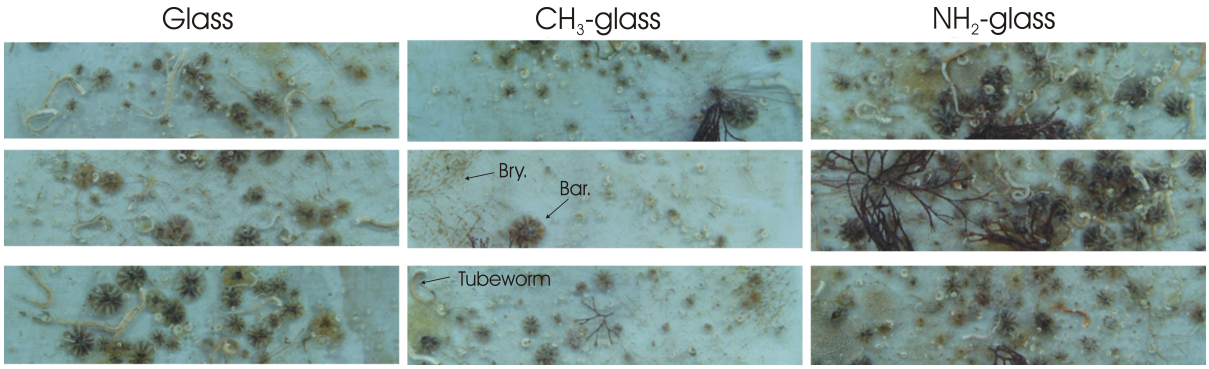

Figure 6.4. Representative photographs of three microscope slides from each of the model surfaces: glass, CH_3-glass, and NH_2-glass. Slides were exposed to a tropical marine environment for 25 days.

The glass slides exposed to marine environment after 25 days were fouled with species like barnacle, (soft and hard) tubeworm, cnidaria (hydroids) and bryozoan. From the optical micrographs presented in Figure 6.4, the field test results show a similar trend in macrofoulers recruitment, i.e. less fouling observed in CH_3-glass than glass and NH_2-glass surfaces. Image analysis and statistical evaluation provide a quantitative foundation to differentiate the behavior of the surface with different functionalities. To compare with the laboratory settlement choice assay, the quantity of barnacle on the test surface was illustrated separately in comparison to total macrofoulers. Figure 6.5 shows the number of scores of fouling organisms obtained from the respective fouled glass surfaces. The results show that the NH_2-glass has the highest score in barnacle with 30 ± 6, followed by glass with 19 ± 11 and CH_3-glass score the least of 6 ± 4 barnacles, respectively. Similar trend was observed for other macrofouler organisms where NH_2-glass attracted the highest surface coverage of macrofoulers, followed by glass and CH_3-glass, with NH_2-glass have the highest score of 50 ± 8, followed by glass with score of 26 ± 13 and CH_3-glass with the score of 13 ± 6. The

analysis on the barnacle settlement behavior in marine environment clearly indicates a sharp differentiation between NH_2-glass and CH_3-glass, with $p < 0.0001$. Glass and CH_3-glass are barely distinct, with $p < 0.04$. Glass and NH_2-glass are not distinguishable ($p < 0.11$). The tubeworms (not shown) did not show significant differences in recruitment on glass, CH_3-glass and NH_2-glass surfaces. Bryozoan settlement is low on all but NH_2-glass. The total settlements by other macrofoulers were considerably higher for NH_2-glass over CH_3-glass ($p < 0.0001$) and glass ($p < 0.007$).

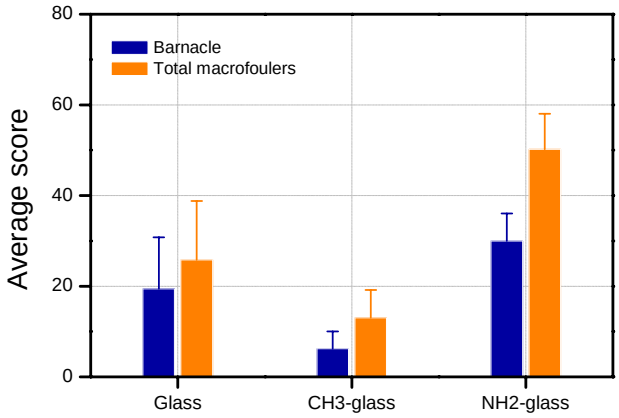

Figure 6.5. The fouling of barnacles and total macrofoulers on different glass surfaces over a 25-days marine field test.

Panel immersion test of different silicon (wafer) surfaces were performed together with the glass slides. The results of fouling assessment from silanized silicon samples after 25 days were shown in Figure 6.6. Similar trend was found on the fouling condition on the silicon surfaces as to glass. No barnacle was found on the SiO_2 and CH_3-SiO_2 surfaces. Barnacle was only found on the NH_2-SiO_2 surfaces with the score of 1 ± 1. The total macrofoulers mostly fouled on NH_2-SiO_2 with the average scored of 10 ± 5, followed by SiO_2 with score of 6 ± 1 and the least on 1 ± 2 for CH_3-SiO_2. The difference in settlement quantity on silicon and glass surfaces could be attributed by the difference in surface area. Silicon surface has a larger surface compared to glass slides. Hence, cyprid larvae and other macrofoulers may spend more time to explore on the silicon surfaces before settlement, resulting in lower settlement counts within the experimental time scale. The fouling on silicon surfaces has similar outcomes as that from glass, i.e., CH_3-SiO_2 samples have the lowest score on all fouling species. In general, barnacle prefers to settle on the hydrophilic

surface than hydrophobic surface. The results from panel immersion test are consistent with the results from choice settlement assay.

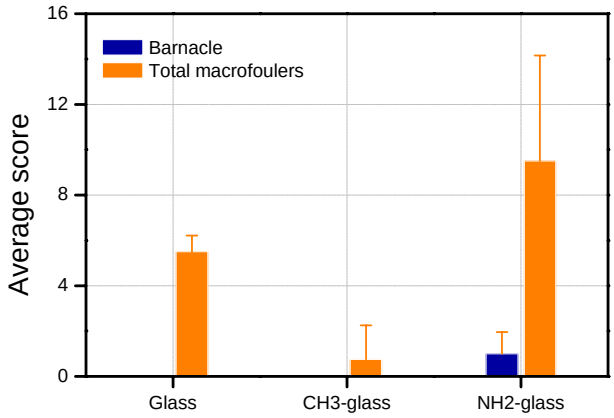

Figure 6.6. The fouling of barnacles and total macrofoulers on different silicon surfaces over a 25-days marine field test.

6.3 Discussion

The observed differences in footprint morphology on model hydrophobic and hydrophilic surfaces may explain the lower ability of hydrophobic surfaces to recruit macrofoulers in a marine environment. The AFM morphological study of cyprid footprints provides insight into the interaction of the footprint adhesive material with model surface chemistries. The size of the footprints found on CH_3-glass is systematically larger than on NH_2- glass, which have dimensions comparable to those of the antennule's attachment pad.[29-34] The larger size observed on CH_3-glass indicates an additional spreading of this material or a possible sliding of the antennule while in contact with the substrate. The estimated volume of the material composing a footprint on NH_2-glass and CH_3-glass is approximately the same, implying that the larger surface area is generated a spreading of the footprint adhesive. This observation is in agreement with Crisp *et al.*,[2] who suggested that a highly charged bioadhesive can displace water and spread more easily on a hydrophobic surface.[2, 9, 35] Moreover, the thick micrometer adhesive fiber observed on CH_3-glass (Figure 6.1) may indicate a different conformation, adopted from a reorganization and self-assembly of the molecules in the footprint adhesive material. Footprint proteins are expected to interact with the hydrophobic surface by excluding water between their hydrophobic segments and the substrate. Studies have shown that the configuration of the adsorbed protein molecules can be altered by their interactions with the substrate.[36, 37]

The morphology of the adsorbed footprint protein and the size of the footprints combine to suggest an enhanced protein adsorption to the NH_2-glass surface, as compared to hydrophobic glass. This surface has been shown to expose a high density of both positively charged $–NH_3^+$ and negatively charged $–SiO^-$ moieties in the vicinity of neutral pH.[38] The surface charge present on the target surface is important, leading to a strong adsorption from the aggregated influence of multiple Coulombic interactions with the substrate.[39]

We should note that not all proteins are able to induce the conspecies settlement of barnacle larva. It is generally accepted that conspecies surface-bound chemical cues, as isolated from barnacle adult extract, are responsible for inducing and mediating the gregarious settlement of cyprids.[40] These cues are referred to as the settlement inducing protein complexes (SIPC),[5-7, 40, 41] They consist of glycoprotein complexes (α_2-macroglobulin-like protein) found in the cyprid adhesive material. Studies have shown SIPC to be present in footprint proteins adsorbed to the substrate following cyprid exploration.[6] We may surmise that the spreading of footprints on CH_3-glass contributes to a lower concentration of settlement cue (SIPC) per unit area than in footprints found on NH_2-glass. This, in turn, may reduce the ability of cyprid larva to settle on hydrophobic surfaces, accounting for the observed trends in the settlement assay and field test.

Settlement behavior distinguishes surfaces of different wettabilities, as proven in the settlement assay and marine field test. Results show a clear preference for NH_2-glass, as compared to a hydrophobic glass surface. Similar settlement preferences were observed for other macrofouling species, with a higher macrofouler colonization on NH_2-glass versus hydrophobic CH_3-glass.

The settlement assay and field test observations suggest that barnacle cyprid larva settlement behavior may correlate with the difference in FP morphology observed by AFM. These morphologies may give rise to differences in the surface density of conspecies settlement cues (SIPC). It has been established that footprints function as settlement cue for conspecies settlement. Thus, the preferred settlement of barnacle cyprids on NH_2-glass could be explained by the higher concentration of SIPC, facilitated by an enhanced adsorption of footprint proteins on NH_2-glass. This would attract other cyprid larvae for settlement. In contrast, a hydrophobic surface with its reduced SIPC surface density may be less attractive to Cyprid settlement. The lower concentration of settlement cues may also contribute to lower recruitment in the settlement assay and generate slower fouling in the field test. The combined AFM, settlement assay, and field test results indicate a direct correlation of surface wettability with the settlement behaviour of barnacle cyprid larvae.

6.4 Conclusions

The microscopic morphology of the cyprid footprints on surfaces with different wettabilities was examined. This is compared with the settlement behaviour of cyprids of *Balanus amphitritae*. Results show a correlation between the bioadhesive interface, which is determined by surface characteristics, and the settlement behaviour of cyprid larvae, both in the laboratory and in a marine field test. The footprint morphology on CH_3-glass obtained by AFM was larger in size and porous, with thick microsized fibers spreading across the surface. The footprints on NH_2-glass were found to be more confined and rather densely packed with proteinaceous fibers at the micrometer and naometer length scales. This morphological difference may result in a difference in concentration of the chemical cues on differing surface chemistries. The clearly distinguishable settlement behaviour from the laboratory settlement assay and panel immersion test showed that the barnacle cyprids prefer to settle on hydrophilic surfaces than on hydrophobic substrates. By combining the observations from all experiments at different length scales, we speculate that higher concentrations of settlement-inducing cues (SIPC) present on the NH_2-surface may contribute to barnacle fouling behaviour on this surface. Charge adsorption enhances the adhesion of footprint proteins on a hydrophilic surface. Thus, the limited settlement behaviour found on CH_3-glass might be induced by a lower concentration of SIPC per unit area. We anticipate, that by studying the bioadhesive morphology of cyprids (or of other macrofoulers), one could deduce the physiochemical properties of the adhesive and better understand the settlement behaviour on different chemically functionalized surfaces. In the future, chemical force microscope (CFM) with different, chemically functionalized tips will be applied to probe specific protein-surface interactions.[42-44] A library of these physiochemical properties of macrofoulers should be established and utilized in the design of new antifouling surfaces.

6.5 Experimental

Surface preparation. Glass microscopy cover slips (24 mm x 24 mm, Menzel-Glaser) were sonicated in ethanol for 5 min and then immersed in piranha solution (a mixture of concentrated sulphuric acid and 33% hydrogen peroxide in a 3:1 ratio) for 15 mins. The surfaces were rinsed with nanopure water and dried under a stream of compressed nitrogen gas. Amino (NH_2) and alkyl (CH_3) - terminated surfaces were obtained by gas-phase evaporation of 3-aminopropyl triethoxysilane (APTES) and dodecyltriethoxysilane (DTES) in a desiccator under vacuum, respectively.[45] These glass microscopy cover slips were used for footprint deposition in AFM microscopy studies. APTES was obtained from Sigma Aldrich and used as received. Surfaces were incubated for several hours and then carefully rinsed with 99% ethanol and nanopure water.

Microscope slides (75 mm x 25 mm, Sail Brand reference 7101) were stripped of adsorbed organic contaminants with pyrolysis, by heating them to 500 °C followed by cooling to room temperature. Vapour deposition of aminosilane (Fluka reference 09324) was performed by enclosing liquid silane with the clean slides and heating to 60 °C for two hours. n-Octadecyltriethoxy silane, OTE, (Alfa Aesar reference 230-995-9) was deposited in solution using a procedure adapted from Peanasky *et al.*.[46] A pre-hydrolysis solution of OTE was prepared by mixing 0.42 g of OTE and 0.25 g of 1.31 N aqueous hydrochloric acid into 50ml of tetrahydrofuran (Sigma). This solution was left at room temperature for four hours and then stored in a refrigerator at 4 °C. Silanisation was achieved by immersing the clean slides in cyclohexane (Aldrich, reference 34855) and then adding the pre-hydrolysis solution in a ratio of 1.11 g per 18.6 grams of cyclohexane. The slides were incubated overnight in the silanisation solution and then rinsed by ultrasonication in cyclohexane.

To check the surface properties of these model surfaces, one glass slide from every ten was subjected to a basic quality control. For the bare glass, cleanliness was verified by the wetting and spreading, including zero degree recede contact angle, of a two microlitre water drop. Aminosilane-coated glass was stained overnight using colloidal gold (Bio-Rad reference 170-6527). After rinsing, blow-drying, and cleaning off the lower surface, the presence and uniformity of the stain indicated the presence of aminosilane on the glass surface. The wettability of these slides gave sessile water drop contact angles in the range between 21 to 23 degrees. For OTE, ten sessile water drops were measured. The criteria for acceptance were an average in the range 107 to 110 degrees and standard deviation of one degree across each slide. As for aminosilane-coating contact angle measurements, at least three sessile drops of water were applied for each sample.

Cyprid culture. Barnacle larvae from field-collected adults were reared on an algal mixture of 1: 1 *v/v* of *Tetraselmis suecica* and *Chaetoceros muelleri* at 25°C, at approximately 5 x 10^5 cells per ml density. On this regime, larvae metamorphose to cyprids in 5 days. These cyprids were aged at 4° C for 2-3 days prior to use and 45-70% settlement observed after 24 hours.[47]

Cyprid settlement assay. The settlement assay for Cypris larvae of *B. amphitrite*, referred to as Cyprids, was conducted in laboratory conditions. Glass slides with NH_2-terminated and CH_3-terminated chemical functionalities were used for cyprid settlement assays. The glass slides were cut in half, yielding pieces of 2.5 x 3.5 cm. Glass slides were suspended vertically using steel paper clip in small trough (15x15x3 cm^3) containing filtered seawater. Area of slide immersed in the filter seawater was approximately 2.5 x 2 cm^2. Glass slides were arranged in rows with 5 slides per row and each row was approximated 1 cm apart. Five replicates were used for each surfaces. Approximately seven hundred cyprids were introduced into the trough in 1 liter of filtered seawater and incubated for 24 hrs in the dark. The Cyprids attached to each glass surface were counted, classifying them as exploring (lying on their side) or settled/metamorphosed (perpendicular to the glass surface). The latter ones were counted and subjected to a Wilcoxon Sum of Rank (Wilcoxon-Mann-Whitney) statistical analysis. This is a non-parametric test for assessing whether two statistical samples of observations originate from the same distribution.[48] The parameter output from this calculation, p, represents the probability of overlap between two data sets. Its value ranges from 0 to 1, with a value of 0.05 representing the cutoff point, above which the data sets are not considered as distinguishable.

Atomic force microscopy (AFM). AFM measurements were carried out using a Dimension D3100 atomic force microscope equipped with a NanoScope IVa controller and a hybrid scanner (H-153) with x-, y- z- feedbacks, housed at the University of Twente. A Dimension D3100 with

NanoScope IV controller and a 188CL scanner in NUS-SNI, were used in Singapore. Both instruments are manufactured by Veeco (Veeco / Digital Instruments (DI), Santa Barbara, CA). Triangular-shaped silicon nitride cantilevers (Veeco/Digital Instruments (DI), Santa Barbara, CA) were used throughout the study and cantilever spring constants were calibrated using the thermal noise method. The cantilevers used had spring constants in a range from 48 to 54 pN/nm. Cyprids used in experiments were stored in 33 parts per thousand artificial sea water (ASW, Tropic Marin). They were deposited onto prepared silanized glass surfaces by micro-pipette. Glass samples with different surface functionalities (CH_3-glasses and NH_2-glasses) were fixed to the bottom of polystyrene petri-dishes with double-sided carbon tape prior to experimentation. Cyprid larvae were introduced into a Petri dish containing artificial seawater (ASW), with glass substrates at the bottom, facing up. The larval exploration was monitored visually by an optical stereo microscope. When a FP was deposited, its location was marked. The cyprid was subsequently removed and the surface was transferred to AFM for measurement in air or under ASW. Typically, cyprids would attach and begin exploration when stimulated by small water currents. Explored areas of the glass were marked on the base of the cover slip and cyprids were then removed from the petri-dishes. The surfaces used were rinsed with filtered ASW to minimize surface contamination. The Petri-dishes were transferred to the AFM and its search for footprints was focused on the marked regions. Once the footprint was located, imaging was performed in contact mode, using a minimal force. The footprint samples were rinsed with ASW and dried under stream of nitrogen. AFM images were taken in air using the intermittent-contact mode with Silicon cantilevers (PointProbe®Plus Non-Contact High resonance frequency (PPP-NCH) from Nanosensors, Wetzlar, Germany). The porosity of deposited footprint adhesive material is estimated using a filling-box construct. A grid is superposed onto the AFM footprint and each grid box is evaluated. If the grid box is covered by less than 50 % FP adhesives, it is marked as a void. The porosity is estimated by summing all the void boxes and dividing by total number of boxes.

Field test by panel immersion. The marine biofouling field test was run by placing samples at constant depth on a raft moored at a test site on the West Coast of Singapore, situated in a tropical estuarine marine coastal environment. The area is relatively protected, with waves primarily generated by ferries accessing a nearby harbor and recreational boats. Test samples were immersed from 20th July 2007 to 14th Sept 2007. The water temperature, pH, salinity, oxygen level was monitored every fortnight. Water temperature varied from 27.9°C to 31.7°C and pH fluctuated between 7.81 and 8.15. Five glass slides of each type: bare glass (B), amino-silane (N) coated glass and hydrophobic (C) glass were held with their surfaces horizontal in a PVC frame, laid out in sequence (BCNBCN etc.) in two parallel rows (Figure 6.7). All the test samples were accessed and recorded by photography twice per week. After the field test, the slides were rinsed in fresh water and dried and then photographed. Evaluation of surfaces was done by commercial software Photogrid 1.0. The pictures obtained from the panel immersion test were imported to Photogrid. To avoid edge effects, a 0.5 cm wide border was excluded for each slide. The central portion was subjected to analysis with PhotoGrid software using 100 points per slide. Briefly, one hundred points are placed at random over the image. The fouling species present at each of these points was identified visually by the operator. At each point, if a macrofouler is present, it is scored into one of the following categories: barnacle, tubeworm (serpulid and spirorbid), and bryozoa (arborescent and encrusting). The raw data were processed using the Student's t Test, determining the statistical probability of differentiating between surface chemistries. For the Wilcoxon Sum of Rank and the Student's t Test, the analysis compares two sets of data,

providing the probability that the two sets (over all samples) are independent. Following convention, we consider $p < 0.05$ as indicating that the two data sets are distinguishable. Conversely $p > 0.05$ indicates that the two data sets are not statistically differentiated by this analysis.

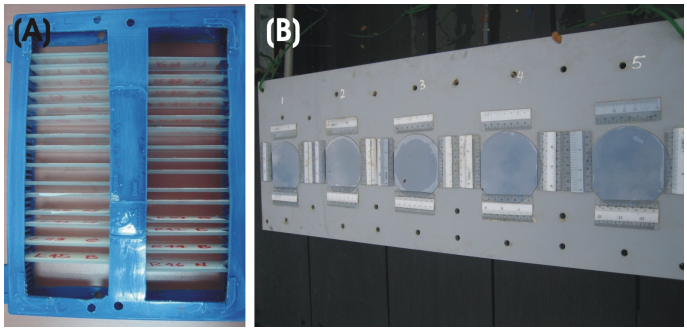

Figure 6.7. Sample holders for (A) glass slides and (B) silicon wafers.

6.6 Acknowledgements

NUS-SNI and Dr. Wan Xin Sun from Veeco Asia are thanked for kindly providing instrumental support for AFM experiments. I would like to thank the team working in biofouling project in IMRE and TMSI, Singapore; especially Dr. Serena Teo, Dr. Ryan Chaw, Ms. Sue Choo, Mr. Ryan Kang, Dr. William Birch, Mr. Chin Sing Lim, Mr. Md Razali Bin Duriat, and Dr. Dominik Janczewski for substantial supports.

6.7 References

1. Yebra, D. M.; Kiil, S.; Dam-Johansen, K. *Prog. Org. Coat.* **2004,** *50*, 75-104.
2. Crisp, D. J.; Walker, G.; Young, G. A.; Yule, A. B. *J. Colloid Interface Sci.* **1985,** *104*, 40-50.
3. Aldred, N.; Clare, A. S. *Biofouling* **2008,** *24*, 351-363.
4. Yule, A. B.; Walker, G. *J. Mar. Biol. Ass. U. K.* **1985,** *65*, 707-712.
5. Dreanno, C.; Matsumura, K.; Dohmae, N.; Takio, K.; Hirota, H.; Kirby, R. R.; Clare, A. S. *Proc. Natl. Acad. Sci. U. S. A.* **2006,** *103*, 14396-14401.
6. Matsumura, K.; Nagano, M.; Kato-Yoshinaga, Y.; Yamazaki, M.; Clare, A. S.; Fusetani, N. *Proc. R. Soc. Lond. Ser. B.* **1998,** *265*, 1825-1830.
7. Dreanno, C.; Kirby, R. R.; Clare, A. S. *Biol. Lett.* **2006,** *2*, 423-425.
8. Fusetani, N. *Nat. Prod. Rep.* **2004,** *21*, 94-104.
9. Aldred, N.; Ista, L. K.; Callow, M. E.; Callow, J. A.; Lopez, G. P.; Clare, A. S. *J. R. Soc. Interface* **2006,** *3*, 37-43.
10. Schumacher, J. F.; Aldred, N.; Callow, M. E.; Finlay, J. A.; Callow, J. A.; Clare, A. S.; Brennan, A. B. *Biofouling* **2007,** *23*, 307-317.
11. Fratzl, P. *J. R. Soc. Interface* **2007,** *4*, 637-642.
12. Autumn, K.; Liang, Y. A.; Hsieh, S. T.; Zesch, W.; Chan, W. P.; Kenny, T. W.; Fearing, R.; Full, R. J. *Nature* **2000,** *405*, 681-685.
13. Huber, G.; Gorb, S. N.; Hosoda, N.; Spolenak, R.; Arzt, E. *Acta Biomaterialia* **2007,** *3*, 607-610.
14. Lee, H.; Lee, B. P.; Messersmith, P. B. *Nature* **2007,** *448*, 338-341.
15. Chaudhury, M. K.; Finlay, J. A.; Chung, J. Y.; Callow, M. E.; Callow, J. A. *Biofouling* **2005,** *21*, 41-48.

16. Holm, E. R.; Kavanagh, C. J.; Meyer, A. E.; Wiebe, D.; Nedved, B. T.; Wendt, D.; Smith, C. M.; Hadfield, M. G.; Swain, G.; Wood, C. D.; Truby, K.; Stein, J.; Montemarano, J. *Biofouling* **2006,** *22*, 233-243.
17. Finlay, J. A.; Krishnan, S.; Callow, M. E.; Callow, J. A.; Dong, R.; Asgill, N.; Wong, K.; Kramer, E. J.; Ober, C. K. *Langmuir* **2008,** *24*, 503-510.
18. Callow, J. A.; Callow, M. E., The *Ulva* spore adhesive system. In *Biologival Adhesives*, Smith, A.; Callow, J. A., Eds. Springer: New York, 2006; pp 63-78.
19. Chiovitti, A.; Dugdale, T. M.; Wetherbee, R., Diatom adhesives: molecular and mechanical properties. In *Biological Adhsives*, Smith, A.; Callow, J. A., Eds. Springer: New York, 2006; pp 79-104.
20. Krishnan, S.; Wang, N.; Ober, C. K.; Finlay, J. A.; Callow, M. E.; Callow, J. A.; Hexemer, A.; Sohn, K. E.; Kramer, E. J.; Fischer, D. A. *Biomacromolecules* **2006,** *7*, 1449-1462.
21. Kavanagh, C. J.; Quinn, R. D.; Swain, G. W. *J. Adhes.* **2005,** *81*, 843-868.
22. Kamino, K. *Mar. Biotechnol.* **2008,** *10*, 111-121.
23. Odling, K.; Albertsson, C.; Russell, J. T.; Martensson, L. G. E. *J. Exp. Biol.* **2006,** *209*, 956-964.
24. Phang, I. Y.; Aldred, N.; Clare, A. S.; Callow, J. A.; Vancso, G. J. *Biofouling* **2006,** *22*, 245-250.
25. Phang, I. Y.; Aldred, N.; Clare, A. S.; Callow, J. A.; Vancso, G. J. *J. R. Soc. Interface* **2008,** *5*, 397-401.
26. Phang, I. Y.; Aldred, N.; Ling, X. Y.; Huskens, J.; Clare, A. S.; Vancso, G. J. **2008**, Submitted.
27. Aldred, N.; Phang, I. Y.; Conlan, S. L.; Clare, A. S.; Vancso, G. J. *Biofouling* **2008,** *24*, 97-107.
28. Pawlik, J. R. *Oceanogr. Mar. Biol.* **1992,** *30*, 273-335.
29. Yule, A. B.; Walker, G. *J. Mar. Biol. Ass. U. K.* **1984,** *64*, 147-156.
30. Yule, A. B.; Walker, G. *J. Mar. Biol. Ass. U. K.* **1984,** *64*, 429-439.
31. Yule, A. B.; Walker, G., Adhesion in barnacles. In *Crustacean Issues 5: Barnacle Biology*, Southward, A. J., Ed. A. A. Balkema: Rotterdam, 1987; pp 389-402.
32. Berglin, M.; Gratenholm, P. *Colloids Surf. B* **2003,** *28*, 107-117.
33. Wiegemann, M.; Watermann, B. *J. Adhes. Sci. Tech.* **2003,** *17*, 1957-1977.
34. Wiegemann, M.; Watermann, B. *Biofouling* **2004,** *20*, 147-153.
35. Callow, J. A.; Callow, M. E.; Ista, L. K.; Lopez, G.; Chaudhury, M. K. *J. R. Soc. Interface* **2005,** *2*, 319-325.
36. Meadows, P. Y.; Walker, G. C. *Langmuir* **2005,** *21*, 4096-4107.
37. Luong-Van, E.; Grondahl, L.; Nurcombe, V.; Cool, S. *Biomaterials* **2007,** *28*, 2127-2136.
38. Carre, A.; Lacarrriere, V.; Birch, W. *J. Colloid Interface Sci.* **2003,** *260*, 49-55.
39. Arima, Y.; Iwata, H. *Biomaterials* **2007,** *28*, 3074-3082.
40. Crisp, D. J.; Meadows, P. S. *Proc. R. Soc. Lond. Ser. B.* **1962,** *156*, 500-520.
41. Knightjones, E. W. *J. Exp. Biol.* **1953,** *30*, 584-598.
42. Frisbie, C. D.; Rozsnyai, L. F.; Noy, A.; Wrighton, M. S.; Lieber, C. M. *Science* **1994,** *265*, 2071-2074.
43. Noy, A.; Vezenov, D. V.; Lieber, C. M. *Annu. Rev. Mater. Sci.* **1997,** *27*, 381-421.
44. Schonherr, H.; Hruska, Z.; Vancso, G. J. *Macromolecules* **2000,** *33*, 4532-4537.
45. Ling, X. Y.; Reinhoudt, D. N.; Huskens, J. *Langmuir* **2006,** *22*, 8777-8783.
46. Peanasky, J.; Schneider, H. M.; Granick, S.; Kessel, C. R. *Langmuir* **1995,** *11*, 953-962.
47. Willemsen, P. R.; Overbeke, K.; Suurmond, A. *Biofouling* **1998,** *12*, 133-147.
48. Sokal, R. R.; Rohlf, F. J., *Biometry*. 2nd ed.; W. H. Freeman and Co.: San Francisco, 1981.

Chapter 7

The effect of a serine protease, Alcalase®, on the adhesives of barnacle cyprids (*Balanus amphitrite*)*

Barnacles are a persistent fouling problem in the marine environment, however their effects (e.g. reduced fuel efficiency, increased corrosion) can be reduced through the application of antifouling or fouling-release coatings to marine structures. It is necessary to develop future fouling resistant coatings that are more facile, cost-effective and that are not deleterious to the marine environment. The incorporation of proteolytic enzymes into coatings has been suggested as one potential option. In this Chapter, we assess the efficacy of a commercially available serine endopeptidase, Alcalase®, as an antifoulant and investigate its mode of action on barnacle cypris larvae. *In situ* atomic force microscopy (AFM) of barnacle cyprid adhesives during exposure to Alcalase® supported the hypothesis that Alcalase® reduces the effectiveness of the cyprid adhesives, rather than deterring the organisms from settling. Quantitative behavioural tracking of cyprids, using Ethovision™ 3.1, further supported this observation. Alcalase® removed cyprid 'footprint' deposits from glass surfaces within 26 min, but cyprid permanent cement became resistant to attack by Alcalase® within 15 h of expression, acquiring a crystalline appearance in its cured state. It is concluded, on the basis of its effects on cyprid footprints, un-cured permanent cement and its non-toxic action, that Alcalase® has real antifouling efficacy providing that it can be successfully incorporated into a commercial coating.

*This Chapter has been published as: N. Aldred, I. Y. Phang, S. L. Conlan, A. S. Clare, G. J. Vancso. *Biofouling* **2008,** *24,* 97-107.

7.1 Introduction

Protease enzymes have a multitude of commercial uses, ranging from their incorporation in common detergents to industrial processes. Significant effort has been directed towards immobilization of enzymes in PDMS films[1-5] since, in that form, they can be used as reactive surfaces or catalysts in industrial applications. Although controllable release of biologically active compounds from coatings remains a challenge, the incorporation of such catalysts into synthetic coatings is becoming routine in industry. Production of coating films containing delicate macromolecules must currently involve 'sol-gel' processes and low temperature hydrolysis of the necessary biological monomers.[1, 6] This method has become commonplace for coatings containing sensitive biological materials since it tends to preserve large, fragile molecules such as enzymes more effectively than the traditional melting of silica[5] in silica-based film production. Although cost-effective, enzyme-based industrial coatings have not yet reached the market place, the efficacy of enzymes as cleaning agents against strongly adhered protein films has been demonstrated repeatedly.[7] It has been suggested[8-10] that serine proteases could be included in novel fouling-resistant coatings to prevent the attachment of marine fouling organisms, such as *B. amphitrite* [11] through lysis of their adhesive proteins on contact with the active surface. In fact, the efficacy of enzymes in this role has already been alluded to in the antifouling strategy of pilot whales.[12]

Effective fouling resistant coatings, whether they are based on antifouling[13-15] or fouling release technology,[16-18] are high value commodities since the international ban on the use of TBT (tributyltin) based paints.[13] The economic costs associated with marine fouling run into billions of U. S. dollars annually[19] and barnacles[20] are particularly pervasive foulers[21] due to their relatively large size, hard-calcareous form[22] and gregarious nature.[23, 24] Removal of large adult barnacles has historically been the focus of antifouling studies with regard to these species, however more attention is now being given to the dispersal and settlement stages of barnacles - the planktonic larvae.

The settlement stage of barnacles is a cypris larva (= cyprid) that actively explores immersed surfaces using a poorly understood method of reversible attachment known as temporary adhesion. Temporary adhesion is facilitated, at least in part,[25-28] by the secretion of a glycoproteinaceous material from glands within specialised antennular structures that cyprids use for walking.[29] This material has often been referred to in the literature as the cyprid temporary adhesive. During exploration, cyprids deposit 'footprints' of glycoprotein that act as a conspecific settlement cue for subsequently exploring larvae.[26, 28, 30, 31] Once a suitable settlement location has been selected, cyprids use a second, discrete, adhesive for

permanent attachment.[32, 33] This permanent adhesive, or cement, is derived from a pair of specialised glands within the cyprid's body where it is stored in secretory granules. Following neurotransmitter stimulation,[34] two cement precursors are released via exocytosis and expressed by an unknown control mechanism through the antennules.[29] The precursors cure, when mixed,[33, 35, 36] into a globular disc embedding the cyprid's antennules and attaching it permanently to the selected surface.[32] Metamorphosis into a juvenile occurs within hours in *B. amphitrite* and the adult adhesive develops some time thereafter.

Pettittt et al.[8] screened twenty-five enzymes for antifouling activity including lipases, cellulases, glucoamylases and multi-enzyme complexes. Of these, the serine-proteases (specifically the enzyme preparation, 'Alcalase®') were found to be most effective in preventing settlement of spores of *Ulva* sp. and cyprids of *Balanus amphitrite*. Alcalase® (Novozymes, Denmark) is a commercial preparation of the serine endopeptidase Subtilisin, an enzyme initially obtained from *Bacillus subtilis* and the Alcalase® formulation is marketed as offering, "Increased savings due to less fouling and the need to clean equipment". It is this putative antifouling action that is of interest to the present study.

Unpublished data[37] suggested that the reduction of barnacle cyprid settlement in response to Alcalase® was due, at least in part, to the effects of the enzyme on the adhesives of barnacle cyprids. Serine proteases catalyse hydrolysis of the covalent peptide bonds between amino acids within proteins.[38] Although modes of action vary, these enzymes generally facilitate proteolytic cleavage through nucleophilic attack of the targeted peptide bond by a serine; aligned side chains of serine, histidine and aspartate are common to most serine proteases.[39, 40] It appears from Pettitt et al.,[8] and from personal observation, that Alcalase® directly affects the *ability* of cyprids to attach rather than reduce their willingness to attach. No direct evidence for this was presented, however Pettitt et al.[8] demonstrated a weakening effect of Alcalase® on the permanent adhesive of cyprids.

This Chapter examines the hypothesis that the principal mode of action of Alcalase®, in its role as an antifoulant, is its ability to attack the adhesive proteins of barnacle cyprids. This is explored using a combination of settlement assays, behavioural assays and direct observation of the cyprid temporary and permanent adhesives. Atomic force microscopy (AFM) was used to study the cyprids' adhesives in response to proteolytic attack. AFM is able to measure nano-scale properties of natural bioadhesive materials and adhesive interfaces in native conditions,[41] i.e. hydrated in a saline solution, making it well suited to studies of this type. In fact, AFM has been used previously in similar studies, for example, to observe the enzymatic degradation of spin-coated poly(trimethylene carbonate) films by

lipase solutions from *Thermomyces lanuginosus*.[42] Zhang et al.[42] observed a reduction in the thickness of their films using AFM and also demonstrated that the enzyme significantly affected film roughness over the duration of their study. The AFM results presented here demonstrate the fine structure of both types of barnacle cyprid adhesive on the nano-scale and report modulation of adhesive force and corresponding changes in morphology for 'footprint' deposits exposed to Alcalase®.

7.2 Results

7.2.1 Settlement and behaviour of cyprids

Previous work by Pettitt et al. were exposed to concentrations of Alcalase® between 1: 400 and 1: 30 000 of the original stock solution.[8] The concentration at which Alcalase® was found to be acutely toxic to cyprids of *B. amphitrite* was in excess of 1: 400. Pettitt et al.[8] did not, however, determine the effects of Alcalase® on pre-settlement behaviour in cyprids. Here, remote video tracking of day 3 cyprids in 1: 800 and 1: 400 dilutions of Alcalase® demonstrated no significant differences in any behavioral parameter (see experimental details) between cyprids in Alcalase® and those in ASW or heat denatured Alcalase® (Figure 7.1). Exposure to non-toxic concentrations of Alcalase®, which elicited significantly reduced settlement, did not, therefore, alter the general behaviour of *B. amphitrite* cyprids when measured in this way.

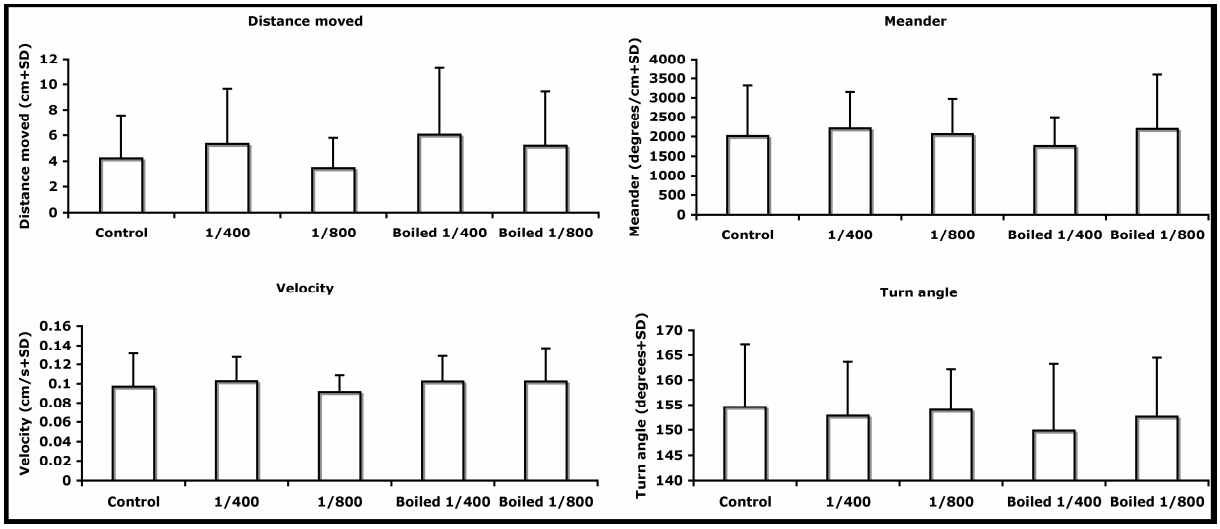

Figure 7.1. Behavioural data acquired by remote video tracking of *B. amphitrite* cyprids in Alcalase® solutions. 1: 400 and 1: 800 dilutions Alcalase® do not significantly affect the overall behaviour of cyprids

7.2.2 Temporary adhesion of cyprids

Footprints were enumerated on nitrocellulose membrane that had been explored by cyprids and subsequently washed with either 1: 400 Alcalase®, heat denatured Alcalase® or ASW. No significant reduction in footprint density was detected after treatment with ASW (mean density = 9.1 ± 1.2 SE footprints cm^{-2} (n = 30)) and heat denatured Alcalase® (mean density = 11.6 ± 1.4 SE footprints cm^{-2} (n = 30)), however, no footprints were observed on membrane that had been treated with active 1: 400 Alcalase®.

To determine whether enzymic removal of footprints negated their inductive (pheromonal) effect on settlement of cyprids, a choice assay was performed between clean (control) and previously explored (footprint-treated) surfaces that had been exposed either to Alcalase® or ASW. When 3-day-old *B. amphitrite* cyprids were used, there was a significant bias towards settlement on footprint-treated surfaces that had not been exposed to Alcalase® (χ^2 = 10.89 P = 0.012). Settlement on the other test surfaces appeared equal (Figure 7.2).

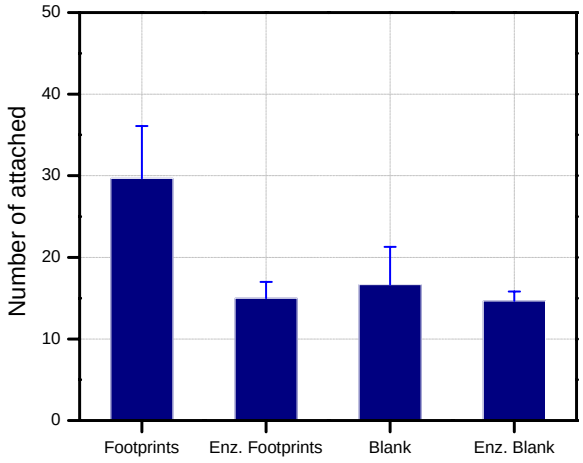

Figure 7.2. The number of *B. amphitrite* day 3 cyprids settled in a 24 h choice assay. Cyprids were allowed a choice between nitrocellulose surfaces with previously deposited footprints ("footprints"), blank control nitrocellulose surfaces ("blank") and those two types of surface that had also been exposed, prior to the assay, to 1: 400 Alcalase® (namely "enz. Footprints" and "enz. Blank" respectively).

AFM provided direct evidence for enzymic proteolysis of cyprid footprints. In ASW individual footprints could be scanned in contact mode for hours consecutively and their nanomechanical properties investigated both before and after the introduction of a 1: 400 Alcalase® solution. The technical difficulty of locating and scanning footprint deposits with AFM precluded the desired replication, nevertheless, on three occasions footprints were

noted to be entirely removed from a glass substratum twenty to twenty-five minutes after the introduction of 1: 400 Alcalase® (Figure 7.3). No morphological changes were detected in footprints exposed to ASW or heat denatured Alcalase® for the duration of the experiments. AFM observation of footprints on glass suggested that in the absence of external influence, footprints would persist unmodified for days in either ASW or hear denatured Alcalase®.

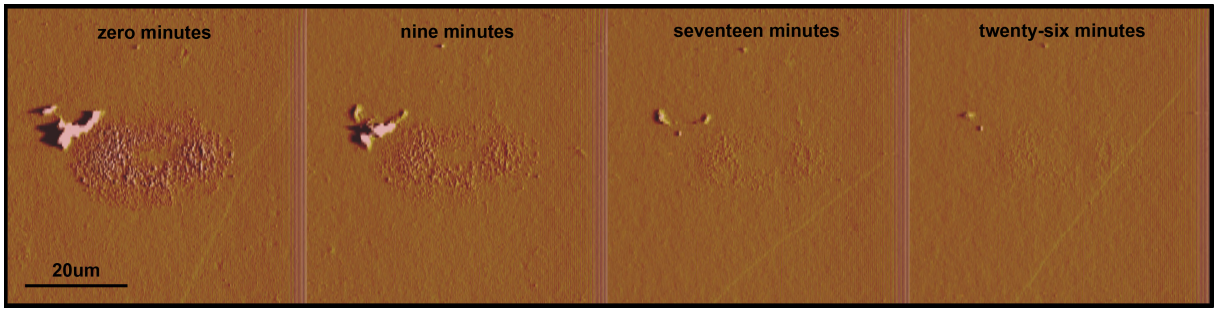

Figure 7.3. The proteolytic removal of a *B. amphitrite* footprint from a glass surface over the course of 26 min. Images are AFM cantilever deflection traces.

Figure 7.4 shows the effect of Alcalase® on the morphology of the cyprid footprint in Figure 7.3. Before addition of Alcalase®, *B. amphitrite* footprints deposited on glass were of the order of 30 μm diameter and 5 nm thick. The thickness of the footprint deposits varied depending on surface chemistry/hydrophobicity.[43] From Figure 7.3 and Figure 7.4, it is clear that footprint deposits were 'doughnut' shaped, with a central circular area of ~10 μm diameter that contained very little glycoprotein secretion.[43] The surface structure of the footprints suggested that the proteinaceous material was drawn into fibrils on removal of the antennular disc from the surface.

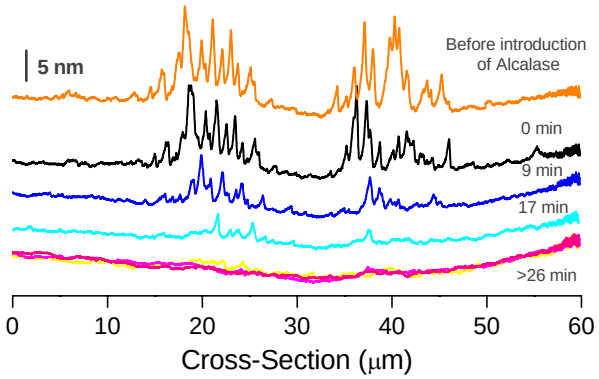

Figure 7.4. AFM cross section height profiles of the footprint in Figure 7.3 recorded over the course of 26 min.

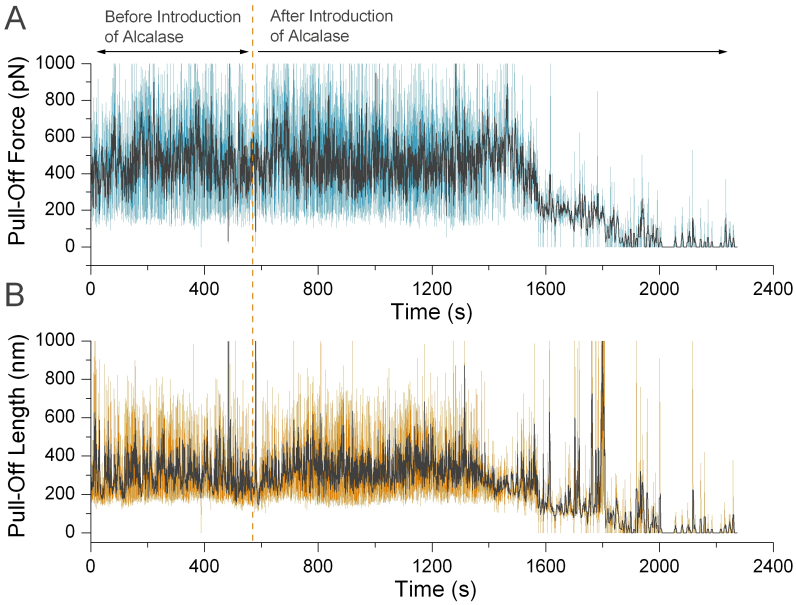

Figure 7.5. Data from AFM analysis of *B. amphitrite* footprints before and during exposure to Alcalase®. A, a plot of pull-off force between the AFM tip and the footprint over time, B. a plot of pull-off length – the distance from the footprint over which proteins remained attached to the AFM tip, over time. The dark line in both curves is a 5-point average and the blue rectangle highlights a series of unusually high pull-off length events around 1800 s (30 min).

Figure 7.5 presents data acquired from one cyprid footprint during enzymic proteolysis. The pull-off force of individual protein fibrils (Figure 7.5A) that had adhered to the cantilever tip and the length that fibrils reached before detaching from the tip (Figure 7.5B) were highly variable, but constant over the duration of testing in ASW. Although only 10 minutes of ASW control period are presented in Figure 7.5, this control period lasted, in reality, for several hours. Only after the introduction of Alcalase® was there any change in either of these two parameters. Even though Figure 7.3 and Figure 7.5 represent different footprints, the time frame in which the enzyme solution acts is similar for both. Three minutes after the addition of Alcalase® (at 1450 s in Figure 7.5A & B), the pull-off force began to decrease with a concurrent reduction in variability of the pull-off force distribution (Figure 7.5A). The variability of pull-off length data also decreased. There was, however, a series of unusually high pull-off length events throughout the time course of the experiment that suggested some fibrils were still being drawn out to considerable lengths until the footprint had been removed completely (highlighted blue in Figure 7.5B). After a 16 min exposure to Alcalase®, only a trace of the footprint shown Figure 7.5 remained on the substratum with few pull-off events evident from 2000 s onwards in Figure 7.5A & B.

Alcalase®, introduced at 564 s, reduced the pull-off force (Figure 7.7A) in a step-wise manner. The pull-off force dropped from 340 pN (between 600 and 1400 s) to a plateau at 150 pN before dropping again to virtually zero – the native force of the glass substratum.

7.2.3 Permanent adhesion of cyprids

After 48 h in ASW, *B. amphitrite* permanent cement appeared to be totally resistant to Alcalase®. The AFM tip did not pick up any proteins at the surface of the cement plaque either before or after addition of the enzyme. Adhesion of surface proteins to the tip was common in uncured cement.[33, 41] Figure 7.6 shows the structure of cured permanent cement from *B. amphitrite* prior to Alcalase® exposure and this surface structure remained unchanged after 3 h Alcalase® exposure. High resolution scans of the permanent cement were possible in this cured state where they were not possible for newly deposited cement in Phang et al.[33]

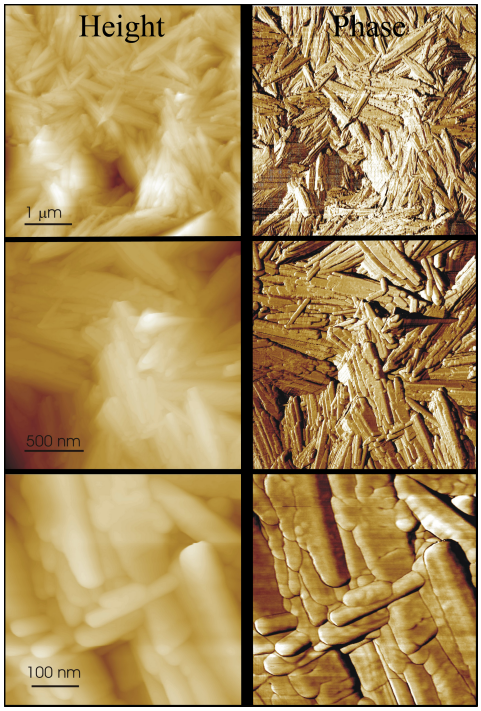

Figure 7.6. AFM images of cured (3-d-old) and hydrated *B. amphitrite* cyprid permanent cement. This cement had not been exposed to Alcalase®. Cement of the same age that was exposed to Alcalase® appeared identical when viewed by AFM suggesting that cured cement is resistant to Alcalase® attack.

In contrast, uncured cement (~1 h old) was highly susceptible to Alcalase® (Figure 7.7), as in Pettitt et al.,[8] and was visibly thinned over the course of 5-h exposure. If the cyprid was attached to the cement plaque during this period then its movements invariably

caused it to dislodge from the surface. Only when the cyprid had been manually removed did the adhesive plaque remain attached to the surface on exposure to Alcalase®. This thinning of the adhesive plaque did not occur if the cement was first stained with a fixing protein dye such as Coomassie Brilliant Blue (acetic acid and methanol preparation).

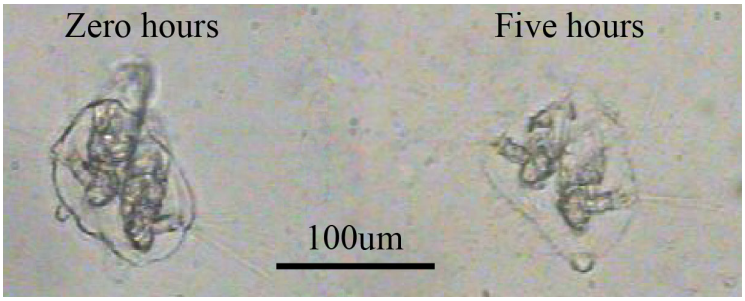

Figure 7.7. Cyprid permanent cement that is not fully cured visibly thins during exposure to a 1: 400 solution of Alcalase®.

7.3 Discussion

The present study aimed to extend the scope of Pettitt et al.,[8] using surface topology imaging and nanomechanical probing by AFM, to provide a mechanistic understanding of the non-toxic inhibitory action of Alcalase® on barnacle cyprid settlement. It is important to mention that since Alcalase® is a commercial preparation of Subtilisin it is impossible to attribute the findings of this study entirely to the action of Subtilisin. There remains a possibility, albeit unlikely, that another undisclosed element of Alcalase®, which can also be heat inactivated, is responsible for the present observations. Therefore replication using pure Subtilisin will be the next phase of study. Alcalase® was used here only to further illustrate and directly expand upon previous observations.[8]

The hypothesis that modulation of cyprid settlement by the enzyme was principally driven by its proteolysing effect on cyprid adhesives seemed to be vindicated by AFM analysis and immunostaining. It was shown that the cyprid antennular secretion (in the form of footprints), critical to surface exploration, did not persist for more than a few minutes in a concentrated solution of Alcalase®. Although antibody staining of explored surfaces appeared to show total removal of cyprid footprints by Alcalase®, it is recognised that the enzyme could interfere with the immunostaining technique by blocking the binding sites of the 76 kDa peptide-specific antibody. The ability of Alcalase® to completely remove cyprid footprints however, as demonstrated by AFM (Figure 7.3), suggests that the disappearance of footprints from nitrocellulose membrane was a result of Alcalase® exposure rather than a failure of the staining method. Dissolution of the cyprids' glycoproteinaceous antennular

secretion would reduce the attachment tenacity of cyprids during exploration[43] and, therefore, the likelihood of their settlement;[44] even if the cyprids were still physically capable of settling. Remote video tracking suggested that an aqueous solution of Alcalase®, of a sufficiently high concentration to reduce settlement, did not affect pre-settlement behaviour of cyprids in any measurable way. This result suggests that the inhibitory action of Alcalase® on cyprid settlement is via non-toxic action – an important environmental consideration.

Interestingly, the material properties of cyprid footprints did not change over the duration of exposure to ASW and the inductive properties of footprints are known to persist for days to weeks in the natural environment.[26] An implication is that the adhesive/de-adhesive "duo-gland" hypothesis proposed by some for temporary adhesion in starfish[45] is unlikely to be applicable to cyprid antennule detachment. If the cyprid secreted its own enzymes to break down the antennular secretion and facilitate release, the progressive effects of those enzymes would be detected by AFM. Moreover, the glycoprotein that is thought to comprise footprints[28, 30, 31] had significant topography (Figure 7.4) after removal of the cyprid antennule from the surface, suggesting that the adhesive was still connected to the antennular disc during detachment. It was not possible to discern whether the adhesive failure was cohesive within the cyprid footprint itself, or adhesive between the footprint and the antennular disc. However, maintaining as much material on the adhesive disc as possible would reduce the necessity for costly production and would be an advantageous evolutionary trait for cyprids.

The reductions in both pull-off force and pull-off length of footprint proteins after the addition of Alcalase® (Figure 7.5) may be directly linked. If a protein fibril was not effectively attached to the AFM tip, if it was removed by Alcalase® during extension, or lysed along its length, it would predictably have a low pull-off length and force. The drawing out of footprint protein fibrils by the AFM tip[41] would have exposed more sites to Alcalase® making proteolysis more likely. The longer the footprint was exposed to Alcalase® the more proteolysis events would have occurred, continually reducing the mean length of protein fibrils in the deposits and also reducing the mean pull-off length. The high pull-off length events (Figure 7.5B) that persisted until the end of the experiment suggested that even until late in the time series some full-length protein fibrils remained.

It was not the intention of the present study to provide a mechanistic explanation for cyprid temporary adhesion. An interesting observation, however, was that cyprid footprints were 'hollow' (Figure 7.4) when viewed from above by AFM. The authors certainly do not propose suction to be important to cyprid attachment[46] - Nott and Foster[29] and Yule and

Walker[47] disproved that hypothesis - but this void may still play an important role in attachment or detachment. Alternatively it could provide an uncontaminated area for surface sensation by the axial sense organ[29] in the centre of the adhesive disc.

Pettitt et al.[8] noted that fresh permanently attached cyprids (Figure 7.8) became quickly detached from their settlement surface after exposure to 1: 400 Alcalase®. After ~15 h post-settlement, however, Pettitt et al.[8] observed that Alcalase® no longer facilitated removal and suggested that either a new, Alcalase®-resistant adhesive was produced at this time, or that the cyprid cement had fully cross-linked[35] and was therefore impervious to attack by the enzyme. Further evidence for curing of cyprid cement was provided here in that no effect of exposure to Alcalase® was detectable in 48-h old cement. This result suggests that in the early post-metamorphosis stage of barnacles it is the fully cross-linked cyprid cement that mediates attachment rather than a discreet juvenile adhesive system. The cyprid cement persists, viewable from beneath the basis, throughout adulthood in barnacles.[47] It was something of a surprise, in the light of previous results,[33] that cement curing, as defined by Alcalase® resistance, should take up to 15 h from the time of expression. Phang et al.[33] provided evidence that *B. amphitrite* cyprid cement cures within 70 min of release to the substratum. The measurements in the first study were made, however, only on the outermost layer of cement, where curing may be catalyzed by available trace metals, oxygen or water. Both observations are, therefore, valid.

The permanent cyprid cement (Figure 7.6) had a distinctly crystalline appearance when cured that had not been observed in the only other AFM study by Phang et al.[33] It is not known if these features were crystals in the true sense, only close study using X-ray techniques could confirm that hypothesis, however it is known that the cement likely self-assembles via quinone tanning from the peptide monomers kept in granular form within α and β cells in the cyprid cement glands.[35] The permanent adhesive apparatus of cyprids could, hypothetically, be similar in this regard to the silk production system of spiders, albeit simplified. Silk-spinning in spiders[48] works by a mechanism of storage and secretion, from specialised glands, of a water-soluble material (the ‘spinning-dope’) that is added to during extrusion to form a water resistant crystalline-matrix thread. Much of the spider’s elaborate silk-spinning machinery is involved in formation of a usable thread. This is not required by cyprids, so their mechanism for simply expressing a volume of cured crystal-matrix material need not be so complex. Requisites would be water-soluble precursors,[35] a collecting duct where curing agents could be added[29] and the ability to express the material before it cures.[33]

The cyprid cement in Figure 7.6 is morphologically different to the adult barnacle cement,[49-51] allaying the debate surrounding whether or not the two may be the same or related. Walker (pers. com.) first observed that material from the cyprid cement glands migrates during metamorphosis and is included in the adult cement glands, although it seems that the product of the adult adhesive machinery is quite distinct from that of its cyprid counterpart. Further, Kamino et al.[52] demonstrated that genes encoding adult cement production were not expressed in the cyprid, making any biochemical similarity in the adhesives unlikely.

The exact mechanisms by which artificial chemical fixation (shown here using Coomassie Brilliant Blue) and putative quinone cross-linking (a natural process in cyprid cement curing) invoke Alcalase® resistance in cyprid permanent cement are unknown, but are probably similar in effect since artificial fixation generally occurs via covalent cross-linking of proteins. Covalent bonds formed during fixation are not the common peptide bond that Alcalase® acts on and, therefore, remain unaffected by the presence of Alcalase®. Quinone cross-linking is highly variable and not completely understood. Bonds formed during the tanning of insect cuticle, for example, are highly complex. Quinones of N-acylated catecholamines, such as N-acetyldopamine (NADA) or N-b-alanyldopamine (NBAD) are known to undergo nucleophilic addition with amino acids such as histidine, resulting in bonds that would also be resistant to Alcalase®.[53] Given the potent effects of Alcalase® on barnacle cyprid adhesives, as well as on the adhesives of algae and diatoms,[8] it would seem that proteolytic enzymes of this type have considerable antifouling potential. Now that their efficacy has been proven, it is the task of coatings manufacturers to incorporate enzymes into affordable systems that maintain their biological activity over a long operational period (at least 1 yr). If this is accomplished, enzyme-based coatings could find wide application wherever underwater fouling is an issue.

7.4 Conclusions

In this Chapter, AFM was used to provide direct evidence for enzymic proteolysis of cyprid footprints. Typically entirely footprints were removed from a glass substratum twenty to twenty-five minutes after the introduction of 1: 400 Alcalase®. Force extension curves obtained after the introduction of Alcalase® showed change in the pull-off force and pull-off length events. After a 16 min exposure to Alcalase®, only a trace of the footprint remained on the substratum with few pull-off events evident from 2000 s onwards. The effect of Alcalase® was shown with no effect on cured *B. amphitrite* permanent cement. However, in contrast, uncured cement was highly susceptible to Alcalase®.

7.5 Experimental

Cyprid culture. *B. amphitrite* cyprids were cultured as described by Hellio et al..[54]

Preparation of Alcalase® solutions. The Alcalase®solution (4.4 % protein, specific activity: 0.057 μmoles glycine.μg protein^{-1} h^{-1}; [8]) was provided by Novozymes and was stored at 6^{o}C. This starting solution was then diluted 1: 400 (equivalent to 100 μg ml^{-1} pure Subtilisin) or 1: 800 in artificial seawater for use in assays. Alcalase® retained 90 % of its original activity after 48 h at 28 ^{o}C, although all assays presented here were completed within 24 h. Total protein content was determined by the Bradford method,[55] although estimated protein content of the stock solution differed considerably from the quoted concentration. This discrepancy was probably due to the lack of an appropriate control solution (i.e. the carrier solution with no enzyme) in the total protein assay. As a result, all enzyme solutions are referred to as dilutions of the stock. Heat denatured Alcalase® was produced by boiling 500 μl aliquots of the stock enzyme solution in a water bath for 1 h, followed by cooling to 4 ^{o}C and 1 h centrifugation at 8000 *g*. The supernatant was removed and diluted for assays as described above.

Cyprid settlement and tracking assays. Behavioural tracking of cyprids using Noldus Ethovision 3.1 followed the protocol of Marechal et al..[56] The parameters used in analysis are defined in Table 7.1.

Table 7.1. The definitions of parameters used to compare the behaviour of cyprids in different experimental treatments.

Parameter	*Unit*	*Definition*
Total distance moved	cm	Cumulative distance travelled by a cyprid in 5 minutes
Mean meander	degrees cm^{-1}	Sinuosity of the track – deviation from linear movement
Mean velocity	cm s^{-1}	Mean directional speed over 5 minutes
Total turn angle	degrees	Cumulative directional change taken 12 times/second

The effects of Alcalase® on cyprid footprints as a settlement cue were ascertained using settlement assays. Nitrocellulose membrane (0.45 μm pore size, Advantec MFS Inc., USA) was fixed to both sides of acid-washed (10% Nitric) microscope slides (Fisherbrand, Fisher Scientific) using high modulus, aquarium-grade silicone sealant. Slides prepared in this way were used in sets of two. One side of each slide was conditioned with cyprid footprints by allowing ~100 *B. amphitrite* cyprids to explore over the surface for 6 h in the dark at 28 ^{o}C. This time period varied slightly between replicate experiments since cyprids needed to be removed from the nitrocellulose surfaces as soon as they were likely to begin settlement. Following footprint deposition, one slide of each pair was exposed to a 1: 400 dilution of Alcalase® for 1 h with gentle agitation, followed by a brief rinse with distilled water. The other slide of the pair was treated in the same way but using artificial seawater (ASW; Tropic Marin™) rather than Alcalase® solution.

Slides were arranged vertically using plastic-coated steel wire in polypropylene Hi-Pack (As One corp., Japan) containers - a surface that inhibits cyprid settlement when new. Two hundred cyprids were introduced into each Hi-Pack container in 300 ml ASW and incubated for 24 h in the dark at 28 ^{o}C. Three replicate containers were used. Mean numbers of settled cyprids on: a) footprint-treated b) blank c) Alcalase®-treated blank and d) Alcalase®-treated footprints were calculated and compared to a control distribution using χ^2 analysis.

For footprint enumeration studies, cyprids were allowed to explore a 10 x 5 cm piece of 0.45 μm pore size nitrocellulose membrane, adhered to the base of a Hi-Pack container using conductive carbon tape. Two hundred cyprids were used in 100 ml ASW. These assays were incubated for 16 h at 22°C in the dark. Following incubation the membrane was removed and rinsed for 1 h in either nanopure water, 1: 400 Alcalase® or heat denatured 1:400 Alcalase®. The membrane was then immunoblotted following the protocol of Matsumura et al..[30] Briefly, the membrane was rinsed in Tris-buffered saline (TBS), immersed in blocking buffer (3% gelatine in TBS) and incubated with a 1% solution of the antibody to the 76 kDa subunit of *B. amphitrite* settlement-inducing protein complex (SIPC). Incubation with a secondary goat anti-mouse antibody (alkaline phosphatase conjugate) was followed by staining with a BCIP/NBT solution until footprints became obvious. The membrane was allowed to dry out before footprint enumeration, which greatly enhanced the contrast of the stained footprints.

Collection of cyprid permanent cement. Three-day-old cyprids (*B. amphitrite*) were settled in 1 ml beads of 33 parts per thousand (ppt) ASW onto acetone-washed glass microscopy cover-slips (2 cm × 2 cm). Typically, they would begin to settle in numbers after ~ 8 h at 28 °C [33] and permanent cement was then expressed over the course of a few minutes (Figure 7.8). The adhesive was allowed to cure for 2 h before the cyprid's body was excised using fine tungsten needles and the remaining cement mass, with embedded antennules, was stored at 4 °C in ASW during delivery from Newcastle to Twente. In Twente, the cement samples were loaded into the AFM 'wet-cell' and probed in artificial seawater. Imaging and force measurements were conducted for at least 1 h before addition of Alcalase®. After Alcalase® had been introduced, AFM probing continued for up to 5 h.

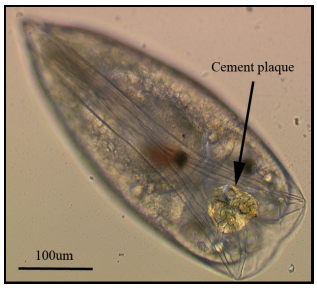

Figure 7.8. A settled *B. amphitrite* cyprid viewed from beneath. Note that the cement plaque with embedded antennules has been artificially accentuated.

Atomic force microscopy. AFM measurements were carried out using a Dimension D3100 atomic force microscope equipped with NanoScope IVa controller and a hybrid scanner (H-153) with x-, y- and z- feedbacks from Veeco (Veeco / Digital Instruments (DI), Santa Barbara, CA). Triangular-shaped silicon nitride cantilevers (Veeco / Digital Instruments (DI), Santa Barbara, CA) were used throughout the study and cantilever spring constants were calibrated using the thermal noise method. The cantilever used for acquisition of the present results had a spring constant range from 48 to 54 pN nm^{-1}. For experiments, cyprids were stored, prior to use, in 33 ppt ASW and were then deposited onto prepared silanized glass surfaces by micro-pipette. Amine-functionalized glass samples[43] were adhered with carbon tape in polystyrene Petri dishes prior to experiments. Typically, cyprids would attach and begin exploration when stimulated by small water currents. Explored areas of the glass were marked on the base of the cover slips and cyprids were then removed from the Petri dishes. Surfaces were flushed with filtered ASW to minimize surface contamination. Petri dishes were

then transferred to the AFM and the search for footprints was focused on the marked regions. Once footprints were located, the ASW was replaced with a 1: 400 Alcalase® or heat denatured 1: 400 Alcalase® solution. Images were taken in contact mode at 1 Hz scan rate. Nanoscope software v6.13b25 was used to transform the raw data to force-separation curves. Pull-off events occurred on these curves whenever individual proteins/protein fibrils adhered to the AFM tip on its retraction cycle. When the protein chain reached maximum extension or, alternatively, when the energy stored by extension of the protein exceeded the energy in the adhesive interaction between the tip and the protein, sharp 'pull-off' events manifested on the force-separation curve. The location of these events on the force-separation curve allowed estimation of the adhesive force between tip and substrate protein. The data (pull-off force and pull-off length) obtained from the corresponding peaks of the force-separation curves were plotted in a time-lapse fashion to demonstrate the effects of Alcalase®.

7.6 Acknowledgements

Ms. Xing Yi Ling is gratefully acknowledged for providing functionalized glass surfaces, Dr Michala Pettittt for providing Alcalase/Subtilisin calibration data. Dr. Nick Aldred for supplying cyprid larva and tracking experiments.

7.7 References

1. Avnir, D.; Braun, S.; Lev, O.; Ottolenghi, M. *Chem. Mater.* **1994,** *6*, 1605-1614.
2. Wu, S. G.; Lin, J.; Chan, S. I. *Appl. Biochem. Biotechnol.* **1994,** *47*, 11-20.
3. Gill, I.; Pastor, E.; Ballesteros, A. *J. Am. Chem. Soc.* **1999,** *121*, 9487-9496.
4. Gill, I.; Ballesteros, A. *Biotechnol. Bioeng.* **2000,** *70*, 400-410.
5. Kim, Y. D.; Dordick, J. S.; Clark, D. S. *Biotechnol. Bioeng.* **2001,** *72*, 475-482.
6. Dave, B. C.; Dunn, B.; Valentine, J. S.; Zink, J. I. *Anal. Chem.* **1994,** *66*, 1120-1127.
7. Turner, K.; Serantoni, M.; Boyce, A.; Walsh, G. *Proc. Biochem.* **2005,** *40*, 3377-3382.
8. Pettitt, M. E.; Henry, S. L.; Callow, M. E.; Callow, J. A.; Clare, A. S. *Biofouling* **2004,** *20*, 299-311.
9. Olsen, S. M.; Pedersen, L. T.; Laursen, M. H.; Kiil, S.; Dam-Johansen, K. *Biofouling* **2007,** *23*, 369-383.
10. Leroy, C.; Delbarre, C.; Ghillebaert, F.; Compere, C.; Combes, D. *Biofouling* **2008,** *24*, 11-22.
11. Clare, A. S.; Hoeg, J. T. *Biofouling* **2008,** *24*, 55-57.
12. Baum, C.; Simon, F.; Meyer, W.; Fleischer, L. G.; Siebers, D.; Kacza, J.; Seeger, J. *Biofouling* **2003,** *19*, 181-186.
13. Evans, S. M.; Birchenough, A. C.; Brancato, M. S. *Mar. Pollut. Bull.* **2000,** *40*, 204-211.
14. Omae, M. *Chem. Rev.* **2003,** *103*, 3431-3448.
15. Statz, A.; Finlay, J.; Dalsin, J.; Callow, M.; Callow, J. A.; Messersmith, P. B. *Biofouling* **2006,** *22*, 391-399.
16. Adkins, J. D.; Mera, A. E.; RoeShort, M. A.; Pawlikowski, G. T.; Brady, R. F. *Prog. Org. Coat.* **1996,** *29*, 1-5.
17. Stein, J.; Truby, K.; Wood, C. D.; Stein, J.; Gardner, M.; Swain, G.; Kavanagh, C.; Kovach, B.; Schultz, M.; Wiebe, D.; Holm, E.; Montemarano, J.; Wendt, D.; Smith, C.; Meyer, A. *Biofouling* **2003,** *19*, 71-82.
18. Chaudhury, M. K.; Finlay, J. A.; Chung, J. Y.; Callow, M. E.; Callow, J. A. *Biofouling* **2005,** *21*, 41-48.
19. Yebra, D. M.; Kiil, S.; Dam-Johansen, K. *Prog. Org. Coat.* **2004,** *50*, 75-104.
20. Wendt, D. E.; Kowalke, G. L.; Kim, J.; Singer, I. L. *Biofouling* **2006,** *22*, 1-9.
21. Otani, M.; Oumi, T.; Uwai, S.; Hanyuda, T.; Prabowo, R. E.; Yamaguchi, T.; Kawai, H. *Biofouling* **2007,** *23*, 277-286.

22. Anderson, D. T., *Barnacles: structure, function, development and evolution*. Chapman & Hall: London, 1994; p 357.
23. Crisp, D. J.; Meadows, P. S. *Proc. R. Soc. Lond. Ser. B.* **1962,** *156*, 500-520.
24. Clare, A. S.; Matsumura, K. *Biofouling* **2000,** *15*, 57-71.
25. Yule, A. B.; Walker, G. *J. Mar. Biol. Ass. U. K.* **1984,** *64*, 429-439.
26. Yule, A. B.; Walker, G. *J. Mar. Biol. Ass. U. K.* **1985,** *65*, 707-712.
27. Clare, A. S.; Freet, R. K.; McClary, M. *J. Mar. Biol. Ass. U. K.* **1994,** *74*, 243-250.
28. Dreanno, C.; Kirby, R. R.; Clare, A. S. *Biol. Lett.* **2006,** *2*, 423-425.
29. Nott, J. A. *Mar. Biol.* **1969,** *2*, 248-&.
30. Matsumura, K.; Nagano, M.; Kato-Yoshinaga, Y.; Yamazaki, M.; Clare, A. S.; Fusetani, N. *Proc. R. Soc. Lond. Ser. B.* **1998,** *265*, 1825-1830.
31. Dreanno, C.; Matsumura, K.; Dohmae, N.; Takio, K.; Hirota, H.; Kirby, R. R.; Clare, A. S. *Proc. Natl. Acad. Sci. U. S. A.* **2006,** *103*, 14396-14401.
32. Walker, G. *J. Adhesion* **1981,** *12*, 51-58.
33. Phang, I. Y.; Aldred, N.; Clare, A. S.; Callow, J. A.; Vancso, G. J. *Biofouling* **2006,** *22*, 245-250.
34. Okano, K.; Shimizu, K.; Satuito, C. G.; Fusetani, N. *J. Exp. Biol.* **1996,** *199*, 2131-2137.
35. Walker, G. *Mar. Biol.* **1971,** *9*, 205-212.
36. Odling, K.; Albertsson, C.; Russell, J. T.; Martensson, L. G. E. *J. Exp. Biol.* **2006,** *209*, 956-964.
37. Aldred, N.; Conlan, S. L. Pers. Commun.
38. Hunkapiller, M. W.; Smallcombe, S. H.; Richards, J. H. *Org. Magnet. Reson.* **1975,** *7*, 262-265.
39. Voet, D.; Voet, J. G., *Biochemistry*. 3rd edition ed.; John Wiley & Sons: New York, 2004.
40. Olivieri, M. P.; Wollman, R. M.; Hurley, M. I.; Swartz, M. F. *Biofouling* **2002,** *18*, 149-159.
41. Phang, I. Y.; Aldred, N.; Clare, A. S.; Vancso, G. J. *Nano**S*** **2007,** *01*, 35-39.
42. Zhang, Z.; Zou, S.; Vancso, G. J.; Grijpma, D. W.; Feijen, J. *Biomacromolecules* **2005,** *6*, 3404-3409.
43. Phang, I. Y.; Aldred, N.; Clare, A. S.; Callow, J. A.; Vancso, G. J. *J. R. Soc. Interface* **2007**, submitted.
44. Neal, A. L.; Yule, A. B. *Biofouling* **1992,** *6*, 33-38.
45. Flammang, P.; Demeulenaere, S.; Jangoux, M. *Biol. Bull.* **1994,** *187*, 35-47.
46. Lindner, E., The attachment of macrofouling invertebrates. In *Marine biodeterioration: An interdisciplinary study.*, Castlow, J. D.; Tipper, R. C., Eds. Naval Institute Press: Annapolis, 1984; pp 183-201.
47. Yule, A. B.; Walker, G., Adhesion in barnacles. In *Barnacle Biology. Crustacean Issues, 5.*, Southward, A. J., Ed. AA Balkema: Rotterdam, 1987; pp 389-402.
48. Vollrath, F.; Knight, D. P. *Nature* **2001,** *410*, 541-548.
49. Berglin, M.; Gratenholm, P. *Colloids Surf. B.* **2003,** *28*, 107-117.
50. Sun, Y. J.; Guo, S. L.; Walker, G. C.; Kavanagh, C. J.; Swain, G. W. *Biofouling* **2004,** *20*, 279-289.
51. Nakano, M.; Shen, J. R.; Kamino, K. *Biomacromolecules* **2007,** *8*, In pressed.
52. Kamino, K.; Shizuri, Y., Structure and function of barnacle cement proteins. In *New developments in marine biotechnology*, LeGal, Y.; Halvorson, H. O., Eds. Plenum Press: New York, 1998; pp 77-80.
53. Bittner, S. *Amino Acids* **2006,** *30*, 205-224.
54. Hellio, C.; Marechal, J. P.; Veron, B.; Bremer, G.; Clare, A. S.; Le Gal, Y. *Mar. Biotechnol.* **2004,** *6*, 67-82.
55. Bradford, M. M. *Anal. Biochem.* **1976,** *72*, 248-254.
56. Marechal, J. P.; Hellio, C.; Sebire, M.; Clare, A. S. *Biofouling* **2004,** *20*, 211-217.

Chapter 8

An *in situ* study of the nanomechanical properties of barnacle (*Balanus amphitrite*) cyprid cement using AFM*

Cyprids are the final planktonic stage in the larval dispersal of barnacles and are responsible for surface exploration and attachment to appropriate substrata. The nanomechanical properties of barnacle (*Balanus amphitrite*) cyprid permanent cement were studied *in situ* using atomic force microscopy (AFM). Force curves were recorded from the cement disc continually over the course of its curing and were subsequently analysed using custom software. Results showed a narrowing of the pull-off force distribution with time, as well as a reduction in molecular stretch length over time. In addition, there was a strong correlation between maximum pull-off force and molecular stretch length for the cement, suggesting 'curing' of the adhesive; some force curves also contained a 'fingerprint' of modular protein unfolding. This Chapter provides the first direct experimental evidence in support of a putative 'tanning' mechanism in barnacle cyprid cement.

*This Chapter has been published as: I. Y. Phang, N. Aldred, A. S. Clare, G. J. Vancso. *Biofouling* **2006,** *22***,** 245-250**.**

8.1 Introduction

Sessile marine organisms such as barnacles,[1] mussels [2,3] and green algae,[4] cause serious damage to the protective coatings of man-made marine structures,[5, 6] the consequences of which have an economic impact running into billions of U.S. dollars annually.[7] This is a direct result of their accumulation in a process referred to generally as "biofouling". Barnacles are of particular concern because their large size causes vastly increased hydrodynamic drag on vessels; significantly increasing fuel costs and the necessity for costly cleaning procedures.[8, 9] Further, the cypris larvae of barnacles such as *Semibalanus balanoides* and *Balanus amphitrite* (the species discussed here) readily attach to moving objects and settle gregariously,[10] exacerbating their impact. It is hoped that, by studying the bioadhesion of barnacles, mussels, algae and diatoms, technology-based solutions to this problem will be forthcoming, such as the development of non-toxic, fouling-resistant marine coatings.[8]

A generalized barnacle life-history incudes six planktotrophic nauplius stages, a non-feeding cypris stage and the adult. It is the cyprid that is of most interest to anti-biofouling studies, as this is the stage that explores submerged surfaces in search of appropriate settlement sites. This surface exploration is thought to be facilitated by the use of a glycoproteinaceous secretion originating from unicellular glands within the antennules.[11] The secretion is commonly referred to as the "temporary adhesive"[12] and also acts as a settlement cue to subsequently exploring larvae.[13, 14] Once settled, the cyprid uses another distinct proteinaceous cement, originating from glands within its body, to attach permanently.

Although the adult cement system has been well studied,[15, 16] the cyprid system has been somewhat neglected. There is presently no evidence to suggest that either the apparatus used in the production and delivery of cyprid and adult permanent cements, or the adhesives themselves, are in any way related. Given the economic importance of these processes it is, perhaps, surprising that dedicated studies of the cyprid permanent cement amount to one paper, now in excess of 30 years old, studying its composition[17] and two studying its delivery.[18, 19] The former used basic histological techniques to ascertain that the cement originated from two different cell types within the cement glands, where it is stored in secretory granules[20] and released to collecting ducts under neurotransmitter control.[18] From this observation, it was postulated that the adhesive was probably dual-component in nature - a hypothesis substantiated somewhat by the identification of diphenols and the enzyme polyphenoloxidase in the cement apparatus, suggesting a dual component adhesive that cures, when mixed, via quinone cross linking (tanning). The present study is, therefore, designed as

a logical extension from this conclusion since, at present, no convincing case has been proposed in support of any mechanism other than quinone tanning.

On expression, this adhesive is delivered through the antennular cement ducts[21] and is deposited in a globular disc measuring <100 μm in diameter (*B. amphitrite*). From this moment, the antennules are embedded and the cyprid permanently attached during metamorphosis into an adult; at which point the adult adhesive systems take over. It is likely that permanent adhesion in cyprids is a single, irreversible event, resulting in total release of all the organism's store of adhesive.[20] Observation of secretory granules with partial content loss[19] suggests, however, that failed adhesion attempts or some involuntary stimulus may result in partial secretion of the permanent adhesive prior to settlement.

Since its development in 1986, Atomic Force Microscopy (AFM) has become a widely used tool for the characterization of materials and polymer structures. Moreover, AFM has an advantage over conventional "optical" microscopic techniques (SEM, ESEM, TEM) since it also enables the study of processes *in situ*, providing information about surface chemical composition and nanomechnical properties. Force spectroscopy has been used widely for the study of bond-rupturing and to quantify the unfolding forces of modular proteins.[22-25] However, due to the technical difficulty of using the AFM 'wet cell' to image fresh and hydrated samples, only recently has it become widely embraced for the study of biological materials. Dedicated studies have used AFM to investigate the properties of natural bio-materials and bio-adhesives as varied as abalone shell,[26] spider silk,[27] adult barnacle cement,[28] gecko spatulae,[29] algae[30] and diatoms.[31] Presented here are the results from a recent AFM study intended to provide preliminary data describing the post-expression curing of cyprid permanent cement, thus, beginning the elucidation of this complex system in *B. amphitrite*. The nanomechanical properties of the permanent cement were recorded over the course of its curing and the findings support the hypothesis that cyprid permanent cement indeed hardens over time, putatively via a quinone tanning mechanism.

8.2 Results and discussion

The results of this Chapter present statistically significant trends, as well as considerable anecdotal evidence to support previous observations.[20] The frequency of observed pull-off events taken over the 45 min time course is presented in Figure 8.1. This frequency distribution consists of 2800 tip-adhesive interaction events in total, with 523 allowing the acquisition of a clear and reliable force curve, therefore termed 'successful'. It

appears from Figure 8.1 that the frequency of successful events decreased over time, anecdotally suggesting curing of the permanent cement.[32]

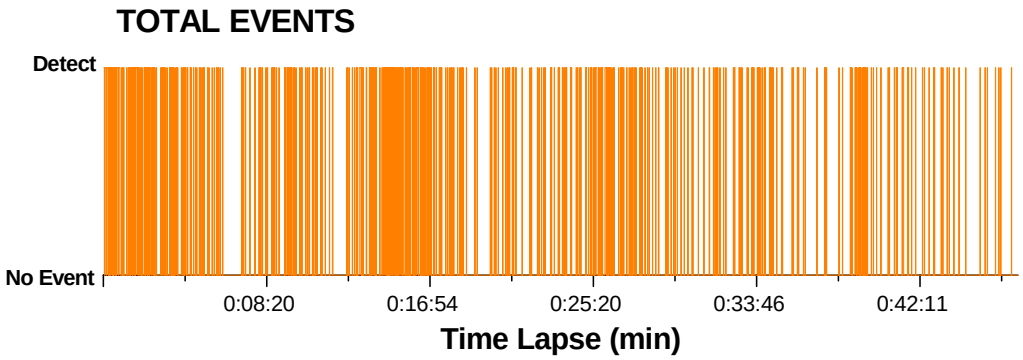

Figure 8.1. The distribution of total pull off events detected over the course of the investigation.

All 523 successful pull-off curves were subsequently analysed individually and the resulting information is presented in Figure 8.2B - D. A typical pull-off curve is shown in Figure 8.2A, displaying a force profile containing information related to force experienced during pull off and molecular pull-off length. The data extracted from each of these force-separation curves were plotted onto graphs to demonstrate trends in pull off force and length independently. Figure 8.2B and C summarize the information obtained and analyzed from AFM force curves over the curing period. Maximum force fluctuated between the ranges of few hundred picoNewtons (pN) to a few nanoNewtons (nN) during the experiment as shown in Figure 8.2B and this heterogeneity presents the likelihood that the putative dual-component cement is not thoroughly mixed on expression, with different constituents presenting different pull off characteristics. No significant trend of either increasing or decreasing force with time was obvious.

Over all strong pull-off forces suggest that, on expulsion from the glands, native cement is very sticky and adheres strongly to the cantilever. In addition, this range begins to narrow as curing progresses, although accurate quantification of this narrowing is difficult. The significant reduction of maximum pull-off length with time (regression ANOVA $F = 132.43$ $P = < 0.001$ Figure 8.2C) provided further evidence that molecular chain cross-linking was occurring in the permanent cement.

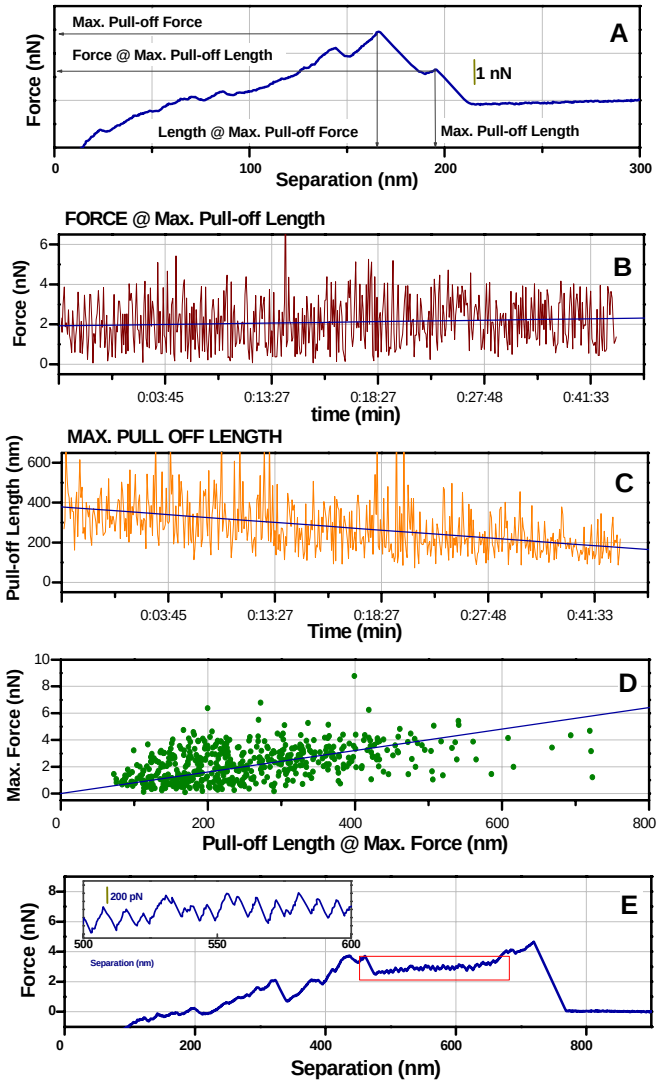

Figure 8.2 (A) A typical force–separation curve from barnacle cyprid permanent cement showing multiple pull-offs. (B) Pull-off force at maximum pull-off length. (C) Maximum pull-off length. (D) The correlation between the maximum force and length. (E) An example of a force curve demonstrating a "saw-tooth" modular protein unfolding characteristic (inset).

From Figure 8.2C, extrapolation of the molecular pull-off length to zero suggested that cement would be totally cured ~71 min after the on set of data acquisition. This suggested a total curing time of ~116 mi and, from that, we estimate that fully cured cement would require a pull-off force of ~2.5 nN. Note that these numbers are, however, only valid for the outer layer of cement, and that it is not yet clear what effects factors such as salinity and the availability of oxygen may have on cement curing[20] and the properties of the bulk adhesive.

Finally, Figure 8.2D demonstrates a significant linear increase of pull-off force with pull-off length (regression ANOVA F = 128.82 P = < 0.001), suggesting that the observed "curing" of the adhesive is directly related to changes in protein conformation. Analysis of individual force curves revealed an unusual characteristic in individual curves, and this is highlighted in Figure 8.2E.

In summary, this study takes a first step forwards towards better understanding the nanomechanical properties of barnacle cyprid adhesives through the use of atomic force microscopy. It was clear from the results that the properties of this proteinaceous adhesive change significantly with time, providing the first experimental evidence of a curing process in cyprid permanent cement. In ecological terms, it is important that once the cyprid has committed itself to permanent attachment, the process of irreversible permanent adhesion occurs rapidly. This prevents dislodgement of the cyprid from its chosen settlement location by adverse physical environmental conditions and allows metamorphosis into an adult to occur rapidly after tidal exposure; preventing desiccation.

This larval stage, which is an obvious point of attack for novel antifouling strategies, has, thus far, been neglected in deference to studies of the adult barnacle adhesion systems.[28] Although Sun *et al.*[28] provided useful data, comprehensively describing the processes involved in the adhesion and removal of adult barnacles to commercial silicone coatings, these results are not directly transferable to the adhesion of barnacle larvae and separate study is clearly required. This applies not only to adhesion studies, but also to removal studies where conventionally applied crack propagation theory[8] is unlikely to apply to the micro-scale of planktonic larvae. It seems to the authors that the prevention of settlement/easy release of larvae is equally as important, if not more so, than the removal of adult foulers, and that better knowledge of the adhesives used by the propagules of fouling organisms (larvae and spores) will aid the development of coatings intended to prevent the initial colonisation of surfaces by fouling communities.

These data clearly suggest that there is a significant and distinct change in the material properties of the cement over time, with a significant decrease in pull off length (Figure 8.2C) over the course of the 45 min study. This is, theoretically, what would be expected if the system operates as proposed by Walker.[20] As crosslinking within the adhesive commenced, the proteins will have recoiled, becoming constrained within a network resulting in shorter pull-off lengths (Figure 8.2C). This will also have resulted in fewer free chains available at the surface, and, therefore, presenting the trend in Figure 8.1 where fewer pull-off events are observed over time. Clear bimodality of force/separation curves would have

supported the accepted hypothesis of a two-phase system, however, discreet differences in behaviour between proteins were not identifiable during this study. These minor differences in behaviour between the two component proteins were most probably masked by progressive conformational changes occurring inconsistently throughout the material, manifest in the high variability in Figure 8.2B.

As well as demonstrating time dependent 'curing' in *B. amphitrite* cyprid cement, interpretation of the present data also suggests some fundamental properties of the adhesive. Cyprid cement is known to be proteinaceous in nature, being easily stained with laboratory protein reagents[20] and Figure 8.2E is a force curve representative of those believed to show modular protein unfolding under tension. Although similar trends are provided by protein complexes undergoing reversible crosslinking, this is highly unlikely to be the case for a progressively hardening, quinnone tanned protein complex. Unfolding behaviour is highlighted in the inset Figure 8.2E and shows a regular saw-tooth characteristic, strikingly similar to that detected from glycoproteinaceouos diatom adhesive.[31] Although firm conclusions are difficult to draw from preliminary data of this type, it is suggested that the initial stretch length of up to 400 nm in Figure 8.2E is probably representative of the semi-cured protein's tertiary structure unfolding under a force of up to 4 nN. In addition, the unfolding behaviour as the proteins are stretched further could represent the breaking of quinone cross-links between phenolic amino acids. Extraction of individual proteins from the cement glands of *B. amphitrite* followed by AFM investigation would assist in this area, however, this presents a daunting challenge to the experimenter. Indeed, such work was attempted during the present study by microdissection of cement glands from *B. amphitrite*, however, variability in the results rendered them inconclusive.

The study of systems on this microscale presents significant difficulties and, unfortunately, the information provided by AFM was insufficient to exactly determine the permanent cement curing mechanism on this occasion; it is believed that this capability will be developed in the future. However, variability in force and separation suggest the presence of multiple components in this adhesive, supporting the hypothesis that the cyprid permanent cement is a dual component adhesive that cures over time. Interference with this curing process by the incorporation of commercial enzymes in coatings,[32] for example, may be one effective method of disrupting the attachment process in cyprids, however, not all target species will be affected by this method of attack in a similar way. The extracellular adhesives of diatoms, *U. linza* spores and, indeed, the 'footprint' secretion of barnacle cyprids are glycoproteinaceous in nature and have been shown to be susceptible to enzymatic

attack by serine proteases,[32] whereas the byssal adhesive of *M. edulis* is not.[33] This is but one example, suggesting why the study of bioadhesive composition and mode of action in many different fouling species is of crucial importance to coatings development in the anti-biofouling sector.

8.3 Conclusions

The present data allowed rough estimation of an ecologically relevant total curing time for the cement, similar to the one to three hours inferred from pull-off measurements for *Semibalanus balanoides*.[17] Rapid curing of this permanent cement is essential for intertidal barnacles since it is only with a secure attachment to the settlement surface that successful metamorphosis can occur, prior to potential desiccation on the ebb tide. On the basis of this research, we strongly believe that development of the AFM technique can provide a fundamental understanding of the nanomechanical properties of these materials that, in turn, will be invaluable to the development/evaluation of sustainable, non-biocidal, fouling resistant marine coatings,[6] as well as the furtherance of ecological understanding with regard to these organisms.

8.4 Experimental

Cyprid Culture. Barnacle cyprids were batch cultured in the laboratory at Newcastle University. Nauplii were released by adult *B. amphitrite* and raised on *Skeletonema costatum* according to Hellio *et al.*;[34] metamorphosis into cyprids occurred within 5 days. Cyprids were aged at 6 ^{o}C and used for experiments 5 days after metamorphosis.

Cyprid settlement. For experiments, cyprids were settled in a 1 cm^3 bead of artificial sea water (ASW [Tropic Marine]) onto acetone washed glass microscopy cover slips; 20 cyprids per bead. Typically, they would begin to settle in numbers after ~ 8 h at 25 ^{o}C. Permanent settlement behaviour in cyprids generally involves dorso-ventral arrangement of the body flat to the settlement surface. All thoracic flicking ceases and the cyprids adopt a state of apparent quiescence. This behaviour is accompanied by the expression of permanent cement over the course of a few minutes.

Immediately after permanent settlement behaviour was observed in an individual, the cyprid's antennules were incised using fine tungsten needles and the cement was transferred to the AFM (Figure 8.3). This process involved delicate lifting of the cyprid's 500 μm body at the anterior end using one needle, whilst simultaneously incising the antennules close to the body with a second needle. Rough handling at this stage can easily remove the cyprid and adhesive from the surface entirely, or else damage the adhesive plaque and render results equivocal. Time spent removing the cyprid, arranging cement within the AFM and successfully contacting the surface, meant that readings usually began ~ 45 min after cement expression. The AFM cantilever was positioned and engaged over the permanent cement and force-distance curves were taken continuously over a 45 min period. After this time, it was noted that evaporation of seawater within the wet cell began to diminish the laser signal due to refractive index changes. This suggested that salinity would also be increasing and

could possibly begin to affect the cement/measurements, however, it is not believed that this effect was significant before warming/evaporation began at ~ 45 min.

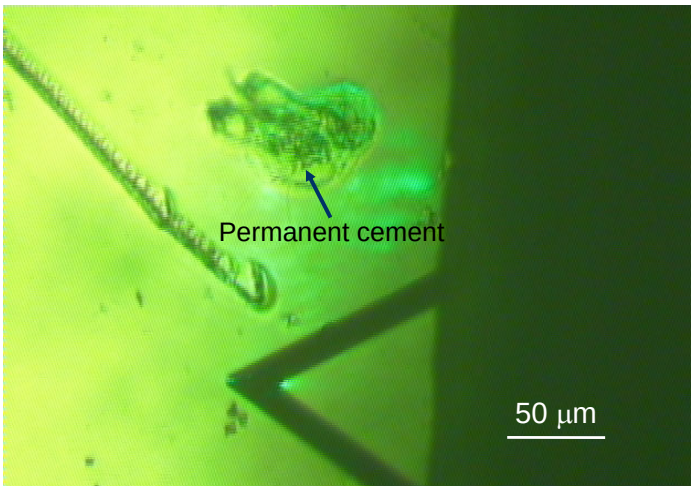

Figure 8.3. An AFM cantilever approaching the glass surface. Cyprid permanent cement plaque with embedded antennules is clearly visible.

Atomic force microscopy. AFM measurements were carried out using a NanoScope IIIa multimode AFM with J-scanner in 33 parts per thousand ASW. 'Wet' measurements were made using a liquid cell and triangular shaped silicon nitride cantilevers (Veeco/Digital Instruments (DI), Santa Barbara, CA). Cantilever spring constants were calibrated using the thermal noise method (Hutter and Bechhoefer, 1993) and the cantilever used for acquisition of the present results had a spring constant of 0.096 ± 0.013 Nm^{-1}. Both loading and unloading rates were fixed to 1.90 × 10^2 pNs^{-1}. Raw data was transformed and expressed as force-separation curves according to Janshoff *et al.*.[35]

8.5 Acknowledgements

Dr. Nikodem Tomczak is thanked for providing software for force-curve analysis and Dr. Nick Aldred for providing cyprid larva.

8.6 References

1. Crisp, D. J.; Walker, G.; Young, G. A.; Yule, A. B. *J. Colloids Interface Sci.* **1985,** *104*, 40-50.
2. Waite, J. H. *Int. J. Biol. Macromol.* **1990,** *12*, 139-144.
3. Relini, G.; Monranari, M. In *Macrofouling role of mussels in Italian seas: a short review.*, Proceedings 10th International Congress on Marine Corrosion and Fouling, Melbourne, 1999; Aeronautical and Maritime Research Laboratory: Melbourne, 1999; pp 17-33.
4. Callow, M. E.; Callow, J. A. *Biologist* **2002,** *49*, 10-14.
5. Brady, R. F. *Prog. Org. Coat.* **2001,** *43*, 188-192.
6. Swain, G. W.; Schultz, M. P. *Biofouling* **1996,** *10*, 187-197.
7. Yebra, D. M.; Kiil, S.; Dam-Johansen, K. *Prog. Org. Coat.* **2004,** *50*, 75-104.
8. Brady, R. F.; Singer, I. L. *Biofouling* **2000,** *15*, 73-81.
9. Christie, A. O.; Dalley, R., Barnacle fouling and its prevention. In *Barnacle biology*, Southward, A. J., Ed. AA Balkema: Rotterdam, 1987; Vol. Curstacean Issues, 5, pp 419-433.
10. Crisp, D. J.; Meadows, P. S. *Proc. R. Soc. London, Ser. B* **1962,** *156*, 500-&.
11. Walker, G.; Yule, A. B. *J. Mar. Biol. Ass. U. K.* **1984,** *64*, 679-686.

12. Clare, A. S.; Matsumura, K. *Biofouling* **2000,** *15*, 57-71.
13. Yule, A. B.; Walker, G. *J. Mar. Biol. Ass. U. K.* **1985,** *65*, 707-712.
14. Clare, A. S.; Freet, R. K.; McClary, M. *J. Mar. Biol. Ass. U. K.* **1994,** *74*, 243-250.
15. Kamino, K. *Biochem. J.* **2001,** *356*, 503-507.
16. Kamino, K.; Inoue, K.; Maruyama, T.; Takamatsu, N.; Harayama, S.; Shizuri, Y. *J. Biol. Chem.* **2000,** *275*, 27360-27365.
17. Yule, A.; Walker, G., Adhesion in Barnacles. In *Barnacle biology*, Southward, A. J., Ed. AA Balkema: Rotterdam, 1987; Vol. Curstacean Issues, 5, pp 389-423.
18. Okano, K.; Shimizu, K.; Satuito, C. G.; Fusetani, N. *J. Exp. Biol.* **1996,** *199*, 2131-2137.
19. Odling, K.; Albertsson, C.; Russell, J. T.; Martensson, L. G. E. *J. Exp. Biol.* **2006,** *209*, 956-964.
20. Walker, G. *Mar. Biol.* **1971,** *9*, 205-&.
21. Nott, J. A.; Foster, B. A. *Philos. Trans. R. Soc. London, Ser. B* **1969,** *256*, 115-134.
22. Oberhauser, A. F.; Marszalek, P. E.; Erickson, H. P.; Fernandez, J. M. *Nature* **1998,** *393*, 181-185.
23. Horber, J. K. H.; Miles, M. J. *Science* **2003,** *302*, 1002-1005.
24. Pelling, A. E.; Sehati, S.; Gralla, E. B.; Valentine, J. S.; Gimzewski, J. K. *Science* **2004,** *305*, 1147-1150.
25. Zou, S.; Schonherr, H.; Vancso, G. J. *J. Am. Chem. Soc.* **2005,** *127*, 11230-11231.
26. Smith, B. L.; Schaffer, T. E.; Viani, M.; Thompson, J. B.; Frederick, N. A.; Kindt, J.; Belcher, A.; Stucky, G. D.; Morse, D. E.; Hansma, P. K. *Nature* **1999,** *399*, 761-763.
27. Becker, N.; Oroudjev, E.; Mutz, S.; Cleveland, J. P.; Hansma, P. K.; Hayashi, C. Y.; Makarov, D. E.; Hansma, H. G. *Nat. Mater.* **2003,** *2*, 278-283.
28. Sun, Y. J.; Guo, S. L.; Walker, G. C.; Kavanagh, C. J.; Swain, G. W. *Biofouling* **2004,** *20*, 279-289.
29. Huber, G.; Mantz, H.; Spolenak, R.; Mecke, K.; Jacobs, K.; Gorb, S. N.; Arzt, E. *Proc. Natl. Acad. Sci. U. S. A.* **2005,** *102*, 16293-16296.
30. Callow, J. A.; Crawford, S. A.; Higgins, M. J.; Mulvaney, P.; Wetherbee, R. *Planta* **2000,** *211*, 641-647.
31. Dugdale, T. M.; Dagastine, R.; Chiovitti, A.; Mulvaney, P.; Wetherbee, R. *Biophys. J.* **2005,** *89*, 4252-4260.
32. Pettitt, M. E.; Henry, S. L.; Callow, M. E.; Callow, J. A.; Clare, A. S. *Biofouling* **2004,** *20*, 299-311.
33. Phang, I. Y.; Aldred, N.; Clare, A. S.; Vancso, G. J. *Nano**S*** **2007,** *01*, 35-39.
34. Hellio, C.; Marechal, J. P.; Veron, B.; Bremer, G.; Clare, A. S.; Le Gal, Y. *Mar. Biotechnol.* **2004,** *6*, 67-82.
35. Janshoff, A.; Neitzert, M.; Oberdorfer, Y.; Fuchs, H. *Angew. Chem. Int. Ed.* **2000,** *39*, 3213-3237.

Summary

The understanding of biointerfaces in contact with seawater is crucially important in tackling the problems of marine biofouling. Such biointerfaces involve the bioadhesives used by marine organisms to attach temporary or permanently to the surfaces immersed in water. The aim of this Thesis is to address a particular problem, i.e. barnacle adhesion, to the biointerface and the corresponding fouling process. We try to understand the first steps of the fouling process of this species, and help to set up design criteria for surfaces to suppress, or prevent, corresponding biofouling. The focus in this Thesis is on AFM-based nanoscale characterization of marine bio-interfaces created by barnacle cyprid larva during surface exploration. The application of AFM has the advantages of first visualizing the fouling interface (also in situ), and to measure its nano-scale properties featuring bioadhesives and adhesives in native environments. The morphology and nanomechanical properties of the cyprid temporary adhesive - “footprints” deposited on the surfaces were extensively studied. In addition, bio-interfaces created on surfaces with different wettabilities were used to investigate the settlement behavior of cyprid larvae in laboratory settlement assays and marine field tests. In-depth investigations of barnacle adhesive properties were performed by *in situ* monitoring of the enzymatic proteolysis degradation of footprint and the *in situ* curing process of cyprid permanent cement.

Chapter 1 provides a general introduction to this Thesis. Chapter 2 is a general introduction to marine biofouling and anti-fouling systems. The first part of Chapter 2 focuses on the fouling organisms, particularly barnacles and its life cycle. In addition, the adhesion process and the temporary adhesives used by cyprid larvae are discussed. The second part of Chapter 2 presents the essential elements of the “chain of knowledge” relevant for fouling, from the currently available antifouling systems to the assessment methods of antifouling coating, including nanoscale characterization technique (AFM), laboratory settlement assays, and marine environment field tests to study settlement behavior.

Chapter 3 reveals the first microscopic morphology of native footprints deposited by cyprid larva of *Semibalanus balanoide* on hydrophobic and hydrophilic surface. The footprint adhesives consisted of nanofibrils and microfibers, and the size of footprints on the micrometer scale corresponded well to the surface texture of the antennular disc of the settling larvae. Footprints showed a greater spreading on hydrophobic surfaces, with three

times less volume of material deposited as compared to hydrophilic (-NH_2 terminated) glass. Calculations suggested that for the cyprid to prevent detachment during exploration, both "footprint" and "nanohair" (i.e. dry adhesion via van der Waals forces) adhesion mechanisms were required to achieve maximal tenacity of the attachment by the cyprids.

In Chapter 4, the nanomechanical properties of footprints deposited by cyprid larva of *Balanus amphitrite* are tested by AFM-based force spectroscopy. Characteristic saw-tooth force extension curves and entropy-elastic stretch behavior were observed, depending on the degree of extension and deformation history. Hysteresis behavior was observed in repeated elongation-relaxation cycles. The sacrificial bond model (as introduced by P. Hansma) was proposed to explain the intra/intermolecular loading and unloading process. Delay/recovery time prior to testing of individual fibrils was found to be important. The effective time needed to reform sacrificial bonds was typically between 2 to 5 s, as estimated from stretching experiments with controlled delay. The force-extension curves were simulated by the classical worm-like chain polymer model to estimate the effective persistence and contour lengths. The change in persistence length with repeated testing indicated the breaking of sacrificial bonds between proteinaceous segments connected either in a parallel or in a serial fashion in the protein nanofibrils.

Chapter 5 exploits the interfacial properties of footprint and chemically-functionalized surfaces by AFM-based chemical force microscopy using chemically modified AFM tips. Force extension curves obtained from the footprints deposited on NH_2-functionalized glass by commercial untreated Si_3N_4 tip and CH_3-functionalized tips were investigated. All pull-off force histograms showed forces in the range of 0 - 2 nN, with a maximum at ca. 0.9 nN, which was attributed to breaking of sacrificial intermolecular bonds. Functionalized tips with CH_3-terminal chemistry gave an additional higher adhesion force as compared to untreated Si_3N_4 tips. This high force was attributed to changes in water distribution in the local environment of the protein, in contact by hydrophobic surfaces promoting hydrophobic interactions, which consequently affected the footprint protein conformation. The chemical force allowed mimicking and *in situ* monitoring of the deposition and interactions between footprints and surfaces at the molecular level.

Chapter 6 combined molecular information obtained from morphology and nanomechanical studies with the settlement behavior of cyprid larvae observed in laboratory and marine field tests. The footprint morphology appeared different, and the size of the oval shaped footprints obtained from CH_3-glass was five times larger and more porous than those found on NH_2-glass. The differences in footprint morphology on surfaces with different

wettabilities might indicate a difference in concentration of chemical cues near the different surfaces, “used” by the cyprids during surface exploration. The clearly distinguishable settlement behavior from the laboratory settlement assay and panel immersion test showed that the barnacle cyprids preferred to settle on the CH_3-glass rather than on NH_2-glass or borosilicate glass surfaces. By combining the observations from all the experiments at different length scales, it is believed that higher concentrations of settlement inducing cues, i.e. settlement inducing protein complex (SIPC), present on the NH_2-surface contribute to the preferred settlement of barnacle on amine-terminated surfaces.

Chapter 7 describes a study of the effect of an enzyme-serine protease, Alcalase®, on the adhesives of barnacle cyprids. The settlement assay results indicate cyprid preferred settled on surface treated with footprint. However, once these surfaces were treated with Alcalase®, the settlement of cyprid reduced. AFM results provided direct evidence of enzymatic proteolysis of cyprid footprints. After introduction of Alcalase®, the footprints were removed over the course of 30 mins. Force spectroscopy was used to monitor the *in situ* enzymatic proteolysis process. After a 16 mins exposure to Alcalase®, only a trace of the footprint remained on the substratum with fewer pull-off events from 2000 s onwards. Alcalase® showed no effect on the cured permanent cement. In contrast, uncured permanent cement was thinning over the course of 5 hours, which is highly susceptible to Alcalase®.

Chapter 8 indicates the first experimental step towards better understanding of the nanomechanical properties of barnacle cyprid permanent cement by AFM. Force extension curves were collected over the time of the permanent cement curing. The results showed a narrowing of the pull-off force distribution with time, as well as a reduction in molecular stretch length over time. It was clear that the properties of the proteinaceous permanent cement change significantly with time. In addition, there was a strong correlation between maximum pull-off force and molecular stretch length for the cement, suggesting ‘curing’ of the adhesive. This study provides the first direct experimental evidence in support of a putative ‘tanning’ mechanism in barnacle cyprid cement.

This Thesis demonstrates the versatility of AFM in the study of nano-mechanical properties of bioadhesives, which otherwise is inaccessible by other conventional characterization techniques. It also covers a broad range of assessment methods and measurements that would benefit the understanding of barnacle cyprid larva adhesion process. Morphological studies and nanomechanical property measurements uncover the “secrets” of the barnacle cyprid temporary and reversible attachment. We expect that the

knowledge acquired in this work will benefit an overall understanding of the fouling biology, the “interface” between materials science and biology, as well as materials science and coatings industry, and will eventually help in the design of a better antifouling surface.

Samenvatting

Een gedetailleerd inzicht in het gedrag en de eigenschappen van biogrensvlakken die in contact staan met zeewater is van cruciaal belang voor het oplossen van het probleem van ongewenste biologische aangroei op zee. Deze biogrensvlakken bevatten biokleefstoffen die gebruikt worden door zeeorganismen om zich tijdelijk of permanent te hechten aan onderwateroppervlakken. Het doel van dit Proefschrift is om een specifiek probleem, namelijk barnacle aanhechting aan biogrensvlakken en het bijbehorende aangroeiproces, te bestuderen. We proberen om de eerste stappen in het aanhechtingsproces van dit dier te begrijpen en willen ontwerpcriteria voor oppervlakken vaststellen om dit aanhechtingsproces te onderdrukken of om aanhechting te voorkomen. De nadruk ligt in dit Proefschrift op AFM-gebaseerde nanometerschaal karakterisering van biogrensvlakken zoals die op zee worden gecreëerd door barnacle cyprid larvae tijdens hun oppervlakteverkenning. Het toepassen van AFM heeft als voordeel dat het aangroeigrensvlak kan worden gevisualiseerd (ook *in situ*) en dat de nanoschaal eigenschappen van het oppervlak met biokleefstoffen in de oorspronkelijke omgeving kunnen worden bestudeerd. De morfologie en nanomechanische eigenschappen van de tijdelijke kleefstof-"voetafdrukken" die door de cyprids op de oppervlakken werden achtergelaten werden uitvoerig bestudeerd. Bovendien werden biogrensvlakken, gecreëerd op oppervlakken met verschillende oppervlakteenergie, gebruikt om het aanhechtingsgedrag van cyprid larvae in laboratorium aangroeitests en in dergelijke tests op zee te bestuderen. De eigenschappen van barnacle kleefstof werden diepgaand bestudeerd door het *in situ* volgen van de enzymatische proteolyse degradatie van voetafdrukken en het *in situ* uithardingsproces van permanent cyprid cement.

Hoofdstuk 1 geeft een algemene inleiding van het Proefschrift. Hoofdstuk 2 is een algemene inleiding over biologische aangroei op zee en over aangroeiwerende systemen. Het eerste deel van Hoofdtsuk 2 is gericht op de aangroeiende organismen, met name de barnacles, en hun levenscyclus. Bovendien worden het adhesieproces en de tijdelijke kleefstoffen, gebruikt door de cyprid larvae, besproken. Het tweede deel van Hoofdstuk 2 presenteert de essentiële elementen van de "chain of knowledge" relevant voor ongewenste bioaangroei, van de huidige beschikbare antiaangroeisystemen tot beoordelingsmethoden van

aangroeiwerende coatings, inclusief nanoschaal karakteriseringstechnieken (AFM), laboratorium aangroeistudies, en veldtesten op zee om aangroeigedrag te bestuderen.

Hoofdstuk 3 onthult de eerste microscopische morfologie van oorspronkelijke voetafdrukken, afgezet door *Semibalanus balanoide* cyprid larvae op hydrofobe en hydrofiele oppervlakken. De kleefstoffen uit de voetafdruk bestonden uit nanofibrillen en microvezels, en de grootte van de voetadrukken op micrometerschaal kwam goed overeen met de oppervlaktetextuur van de antennular disk van de zich vasthechtende larvae. Voetafdrukken vertoonden een grotere spreiding op hydrofobe oppervlakken, met een drie maal kleiner volume aan afgezet materiaal ten opzichte van hydrofiel (-NH_2 getermineerd) glas. Berekeningen suggereerden dat ter voorkoming van loslaten tijdens verkenning, zowel “voetafdruk”- en “nanohaar”- (droge adhesie door van der Waalskrachten) adhesiemechanismen noodzakelijk waren om een maximale hechtkracht van de cyprids te bereiken.

In Hoofdstuk 4 worden de nanomechanische eigenschappen van de voetafdrukken, achtergelaten door *Balanus amphitrite* cyprid larvae, onderzocht door middel van AFM-gebaseerde force spectroscopy. Karakteristieke zaagtand kracht-extensie curves en entropie-elastisch verstrekkingsgedrag werden waargenomen, afhankelijk van de mate van verstrekking en van de vervormingsgeschiedenis. Hysteresegedrag werd waargenomen in herhaalde verlenging-relaxatie cycli. Het sacrificial bond model (geïntroduceerd door P. Hansma) werd voorgesteld om het intra/intermoleculaire beladings- en ontladingsproces te beschrijven. De wachttijd voorafgaand aan het testen van individuele fibrillen bleek van belang te zijn. De effectieve tijd benodigd om sacrificial bonds weer opnieuw te vormen was typisch tussen 2 en 5 s, zoals werd geschat uit verstrekkingsexperimenten met een bepaalde wachttijd. De kracht-extensiecurves werden gesimuleerd met het klassieke worm-achtige polymeerketenmodel om de effectieve persistentie- en contourlengtes te schatten. De verandering in persistentielengte bij herhaald testen duidde op het breken van sacrificial bonds tussen of parallel of in serie verbonden eiwit segmenten in de eiwit nanofibrillen.

Hoofdstuk 5 onderzoekt de grensvlakeigenschappen van voetafdrukken en chemisch gefunctionaliseerde oppervlakken door AFM-gebaseerde chemical force microscopy waarbij chemisch gemodificeerde AFM tips worden gebruikt. Kracht-extensiecurves, verkregen van voetafdrukken die waren geplaatst op NH_2-gefunctionaliseerd glas, en gemeten met behulp van commerciële onbehandelde Si_3N_4 tips en met CH_3-gefunctionaliseerde tips, werden onderzocht. Alle pull-off kracht histogrammen lieten krachten in het gebied van 0 - 2 nN zien met een maximum bij ca. 0.9 nN, welke werd toegeschreven aan het breken van sacrificial

intermoleculaire bindingen. Gefunctionaliseerde tips met CH_3 eindgroepen gaven een hogere adhesiekracht in vergelijking tot onbehandelde Si_3N_4 tips. Deze hoge kracht werd toegeschreven aan veranderingen in de waterverdeling in de locale omgeving van het eiwit, dat in contact met hydrofobe oppervlakken hydrofobe interacties daarmee aanging, welke vervolgens de eiwitconformatie van de voetafdruk beïnvloedde. De chemical force microscopy maakte het mogelijk om de afzetting en interacties tussen voetafdrukken en oppervlakken op moleculair niveau na te bootsen en *in situ* te observeren.

Hoofdstuk 6 combineert moleculaire informatie verkregen uit morfologie- en nanomechanische studies met het aanhechtingsgedrag van cyprid larvae zoals waargenomen in laboratoriumtests en in veldtests op zee. De voetafdrukmorfologie leek anders en de afmeting van de ovaalvormige voetafdrukken gemeten op CH_3-gefunctionaliseerd glas was vijf maal groter en meer poreus dan die gevonden op NH_2-gefunctionaliseerd glas. Het verschil in voetafdrukmorfologie op oppervlakken met verschillende bevochtigbaarheid kan duiden op een verschil in concentratie van chemische signalen voor de diverse oppervlakken die de cyprids gebruiken tijdens hun oppervlakteverkenning. Bij combineren van de waarnemingen van alle experimenten op verschillende lengteschaal lijkt het dat hogere concentraties van aanhechting inducerende chemische signalen, ofwel settlement inducing protein complex (SIPC), aanwezig op het NH_2 oppervlak, bijdragen aan de voorkeur voor aanhechting van barnacle op amine-getermineerde oppervlakken.

Hoofdstuk 7 beschrijft een studie naar de invloed van een enzym-serine protease, Alcalase®, op de kleefstof van barnacle cyprids. De aanhechtingstestresultaten laten zien dat de cyprids zich bij voorkeur hechten aan met voetafdruk behandelde oppervlakken. Echter, bij behandeling van deze oppervlakken met Alcalase® nam de aanhechting van cyprids af. AFM resultaten gaven direct bewijs van enzymatische proteolyse van cyprid voetafdrukken. Na toevoegen van Alcalase® waren de voetafdrukken in 30 min verwijderd. Force spectroscopy werd gebruikt om het enzymatische proteolyseproces *in situ* te volgen. Na een 16 min durende blootstelling aan Alcalase® bleef slechts een zeer klein deel van de voetafdruk achter op het substraat met minder pull-off events vanaf 2000 s. Alcalase® had geen invloed op het uitgeharde permanente cement. In tegenstelling hiermee werd niet uitgehard permanent cement, wat heel gevoelig is voor Alcalase®, dunner in een tijdsbestek van 5 h.

Hoofdstuk 8 beschrijft de eerste experimentele stap richting een beter begrip van de nanomechanische eigenschappen van barnacle cyprid permanent cement door AFM. Kracht-

extensiecurves werden verzameld gedurende de uitharding van het permanente cement. De resultaten lieten een versmalling van de pull-off force verdeling in de tijd zien, en een afname in moleculaire verstrekkingslengte in de tijd. Het was duidelijk dat de eigenschappen van het eiwit-bevattende permanente cement aanzienlijk veranderen in de tijd. Bovendien was er een sterke correlatie tussen de maximale pull-off force en de moleculaire verstrekkingslengte van het cement, wat “uitharden” van de kleefstof suggereert. Deze studie verschaft het eerste directe experimentele bewijs voor een verondersteld “tanning” mechanisme in barnacle cyprid cement.

Dit Proefschrift demonstreert de veelzijdigheid van AFM in het bestuderen van nanomechanische eigenschappen van biokleefstoffen. Met conventionele karakteriseringstechnieken zijn dergelijke studies moeilijk uitvoerbaar. AFM verschaft ons een breed scala aan testmethoden en metingen die het begrip van het barnacle cyprid larvae adhesieproces verdiepen. Morfologische studies en metingen aan nanomechanische eigenschappen onthullen de “geheimen” van de tijdelijke en reversibele aanhechting van barnacle cyprids. We verwachten dat de kennis die is opgebouwd in deze studie zal bijdragen aan een algemeen inzicht in de biologie van ongewenste bioaangroei, het “grensvlak” tussen materiaalkunde en biologie, materiaalkunde en de coatingsindustrie, en uiteindelijk zal bijdragen aan het ontwerpen van betere aangroeiafstotende oppervlakken.

Acknowledgements

After reading so many acknowledgements in the past, it is my time to sit down and rewind the good and bad moments that had happened in the past few years. It is also the time to write down my gratitudes to those who had shared these moments with me. These four years would be one of the most unforgettable periods in my life. From the very beginning, my concept about Europe and the Netherlands was quite ambiguous. We (together with Xing Yi) were like the penguin trying to take a metro in Tokyo, i.e. completely clueless about Enschede. Worse still, the description about Enschede in the big travel guide publisher (L.P.) is not helpful at all. My friends were absolutely surprised by my decision to study in Enschede. Needless to say, it took me some time to explain to them the exact location of Enschede. Hence, one can imagine, starting from the very beginning, my experience in this lovely small town would be very interesting.

First of all, I would like to thank my promoter, Prof. Julius Vancso for giving me the opportunity to work under his supervision. I still remembered the day we had the interview on Valentine's day (!) in Raffles Plaza Hotel, Singapore, about four and half years ago. It is difficult to express my appreciation for your support in research and my career development. I thank you for giving me the total freedom in my research direction. I especially enjoy the friendly international environment that you have fostered in MTP, and your generous support in group social events, including Christmas dinner at your place, MBT meeting in Zurich and in Lunteren that brought the group members together.

I am also indebted to my collaborators at Newcastle University, Dr. Nick Aldred and Prof. Tony Clare for their supports and helpful discussions over the past few years. I especially thank Nick, who introduced me into the world of barnacle cyprid larva and footprints. Dear Nick, the outcome of this thesis also belongs to you. I admire your wordsmith ability and your courage to bear the risk of having brain hemorrhage while correcting our manuscripts, which I can only compensate with couple of pints during the promotion party.

I am also grateful to my mentor, Prof. Liu Tianxi, who is currently based in Fudan University, China. Dear Tianxi, thank you for introducing me into the world of research. I thank you for your guidance and patience when I was struggling with my master project (back then in Singapore). You were always there when I needed your help, no matter how busy you were. Without your encouragement, I would not have pursued my dream in the field of research. We appreciate your invaluable opinions while we were in difficulty or in uncertain situations.

I also owe a substantial debt to Prof. Holger Schönherr for the general AFM issues and discussions. I am sorry if I have annoyed you with so many "one minute disruption" and many other requests. I admired your rigorous mind and achievement in science. Other than that, I also enjoyed the yearly summer barbeque at your place, especially your guitar performance and your impressive beer opening skill.

This thesis would not be possible without the continuous supports from the "pillar of MTP"-Clemens. Lately I realized that Clemens is not only a computer genius, instrumental expert, but also a recreational beer consumer (in large quantity), semi-professional weight-lifter (during the MTP moving), professional poker player and house builder. In your presence, the group has so much fun! Thank you! I am also grateful to Marina for the continuous discussions and mutual complains on the AFM issues. I thank Mark for translating my Summary into Samenvatting. Mark, I always regard you as the "walking chemistry encyclopedia". I would like to thank Gen and Cindy for helping me to handling paper works and administrative works over the past four years.

My appreciations are also extended to Dr. Georg Bar, Dr. Greg Meyers, Dr. Joey Storer, Prof. Jens Høeg for their contributions to the initial phase of my PhD project. In particular, I thank Jens for spending a great deal of time "looking after" me during my visit in Copenhagen. I am also indebted to the people working in the biofouling project in Singapore, especially Sue, Dr. Ryan Chaw, Ryan Kang and Dr. William Birch (from IMRE, Singapore), who took care of the logistic and paper works while I was immersed in the AFM experiments. I also thank Chim Seng, Rozali and Dr. Serena Teo from TMSI, Singapore, who took care of my transportation and the samples at the RSYC raft. Dr. Sun Wan Xing is also acknowledged for allowing me to use their AFM machines in Veeco (Asia).

During my PhD, I had the opportunity to attend both ICMCF conferences in Rio de Janeiro and Kobe. I met a lot of nice and friendly people working in the same field and enjoyed conversations and discussions with them. In addition, I also thank them for showing me the local cultures. It was fun to dance Samba together and got drunk with different caipirinha. I enjoyed the scientific trip to mangrove forest although it ended up in Cachaça brewery (never mind!), and the pool side with more caipirinha. A special thanks goes to Prof. Shibata who brought us to different parts of Kobe to enjoy the authentic Japanese food culture.

Besides that, I would also like to thank those who spent their precious time reading and answering my "peculiar" emails over the past few years. I was a complete stranger to them but they provided me with their invaluable discussions and advices about general science, paper reprints, PhD theses via mail or even free samples for my experiments. I especially thank Dr. Wim van Egmond, who provided the optical micrograph of barnacle nauplius larva (shown in Figure 2.4).

I would also like to thank MTPers who gave me supports over the past four years. These people include Melba, Janet, Eddy, Johannes, Monique, Thomas ("SAXS" measurement???), Nikodem, Emilia, Joost, Nuria, Mathijs, Oya, Hong Jing, Cynthia, Marina, Denis, Chuan Liang (role model), Attila (ATD super hero), Sasha (nocturnal experimentalist – "bat man"), Igor, Ramon, Sandra (can you speak 200 words per second???), Joris (thanks for the microwave), Szczepan , Nina, Monique, Ewa, Jing, Yujie and Qi, Weiqing, Eugenia, Carlos (crystal lovers), Gen and Cindy.

The social events like borrels or group trips in MTP are the most memorable ones. No body will deny the fun on the way to Zurich, especially on the City Night Line, when Denis brought out bottles of Vodka from his backpack and we started drinking together (even with some strangers in the same cabin). Of course, we also enjoyed the sort of "Amazing Race 2005" to Bath that took us two days to arrive – including 16 hours train ride and several transfers, all thanks to Ryan air who cancelled our the flight!!! The best part was we (Eddy, Monique, Nikodem and I) met Simon "the Great" who sold us a "goody bag" of alcohol to tame our thirst. Mainz trip was as excited as usual. I am not sure who came up the idea to stand on the remains of a 16-inch tree trunk with as many of us as possible. Lunteren was always the best event of the year. The highlight always happened in the dungeon, like MTP best ping pong player Stijn lost to "Eindhoven girl team" even though we had an insider – Julius as the judge of the match. Eddy and Nikodem tried to sell some drawings to everyone during the after hours drinking session of Lunteren and etc. Wadlopen, is one of the activity that I will never forget in my life. Monique was the strong driving force behind the Wadlopen. For me, Wadlopen is sort of "semi suicide" mission. I always hesitated at the starting line, with a strong sense of regret after the first few steps. Yet, when we made it to the finishing line, it was such a relief! After doing it twice (thanks Richard for organizing the other one), it is definitely more than enough for me in my life time. ☺

The best part in the past four years was to get to know a lot of new (and now good) friends. They gave me invaluable supports and advices. They came and left. It would be great if everyone could stay a bit longer and spend more time together. They are Fernando and Lourdes, Michel and Marina, Soco and Rob, Alessio and Olga, Mirko and Itxcharo, Henk and Marloes, Hao and Lanti, Janet, Eddy and Denis (the JED). We spent most of the time having fun together, like the regular Tuesday dinner in Lipperkerkstraat (anti-girls night?), dinner at Hoogstraat, party at Javastraat. I have become more "borracho" after inheriting most of Fernando's alcohol collection. For Soco, Rob,

Mirko and Itxaro, although we spent one night at the not-so-Malaysia-truly-Asia "Nun hotel", I hope you enjoyed the Malaysia trip. We also enjoyed skiing in Winterberg, although Xing Yi's famous quote "I did not enjoy it!", which sometimes reverberated in my dream. At one time, on the way to Aarhus, we (Rob, XY, and me) got summoned by the immigration officials, Rob got a warning but most importantly, I realized that I will soon get a Dutch citizenship (at least according to the computer system). However, I must complain that, till today, I haven't received it yet! Together with Fernando, we were nearly killed by the ETA bomb in Madrid T4. In the same morning, Lourdes went to the wrong airport and missed the flight to Santiago. That was a shear mess, how bad can things get? Finally with lot of blessings, we arrived safely in Santiago, but without our luggage. ☺ That New Year, Fernando and I bought the same underwear for New Year Eve in Carballo Rastro. Thanks to Soco, we enjoyed Galicia so much and at each time, we ended up eating and drinking a lot (Spanish standard!). Of course, we always have a lot of fiesta and siesta. I am also amazed that Xing Yi has been to Galicia more often than to Amsterdam. After all these years, our cooking skills on tortilla, empanada, paella, patatas bravas and etc have no doubt very "typical" (authentic) Spanish! Salamanca is one of my favorite places I have visited, I always wonder whether it is because of Michel or because of the free tapas that come together with beer. The more you drink, and the more tapas you eat -what a good idea to get drunk and full at the same time. Or the other way round? Of course, the fancy colorful shots in El bolero are also one of the most memorable moments! I am sorry that we couldn't attend your wedding in Argentina, we will definitely visit you there someday. I also promise to run a full marathon together one day. Marina, hurray up for a Miguelito!!!

Another memorable trips was to Roses/Sabadell and to Alessio and Olga wedding. It was really nice, to have all the old friends spending most of the time sun bathing, cooking and eating together. Of course, the long anticipated "wedding of the century- Da Wedding". Alessio, *ciao bello*, thanks for the experience and the fun we had together. I especially admired Henk and Marloes who enjoy so much traveling, sun, sports and fun together. Istanbul is one of the largest cities I have ever been. I have never seen so many people loitering on the street at 2 am in the morning. With local guide (Janet), we have a wonderful time sightseeing around the city (with Chris and Nazir), trying different type of authentic food and bargaining furiously at the Bazaar. I also owed a substantial gratitude to the family of our friends, who had provided us with "free accommodations and dinners". These include Soco's family in Artes, Rob's family in Groningen, Alessio's family for the huge X'mas lunch and homemade pasta, Mirko's family (we almost missed the last train back to Verona), Fernando's family in Madrid, Michel's family in Salamanca and Janet's sisters and brother Katherine, Chris and Nazir in Istanbul. Big hugs and *besos* for your kind and warm hospitalities.

I would like to thank Hao and Lanti for the delicious dinners they had prepared and the wonderful time we spent together. Dear Hao, thank you for introducing me into the Sunday basketball and the Arriba heren team. I really envy the kind of "high-tech" lifestyle you have in Enschede. ☺ We also enjoyed a lot during the excursion to Greece (together with Jing) and to Berlin.

For JED, we have spent many hours in tasting Grolsch, Russian vodka, wines and any thing with alcohol. Especially with Eddy, whom I spent so many Friday afternoon, cooking and drinking together. Honestly, still, I do not understand why water has to be boiled for 20 min before you cook the pasta. For Janet and Eddy, thank you for being my paraninfen.

I would like to mention my "die hard gang", a gang of friends who grew up together with me. Lin How, Ji Yang, Alec, Yee Woon, Yong Kian and Ah Beh. Although we have seldom been together over the past few years, our friendship will still be the same.

Last, I owe my gratitude my family, especially to my parents Mr. Phang Choon Hean and Mrs. Fun Gang Eng. I have been away for so long and I regret for not spending enough time with you over the past ten years. Thank you for all the freedom you have given me to pursue my dream. You have given me the best part of your life and this thesis is dedicated to you. My dear brothers, every time I see you, it reminds me how fast time flies, you have grown from my little brothers to grown-ups! I wish both of you all the best in future. My gratitude also goes to my in-law family, for

providing endless supports to the sometimes naïve decisions that we have made, and also the time that we spent together in the past couple of years.

To Xing Yi, my dear, you are always there to support me no matter what happens. Without you, my life will be completely different from who I am now. You are my spiritual support who keep me going, and encourage me to follow my dream. Besides that, you are like the little bug in my stomach who instantly knows all the silly ideas in my mind. We have been through so many ups and downs in the past few years. Let's build our future and explore the world together. You are my best friend and my soul mate. I love you, ti amo.

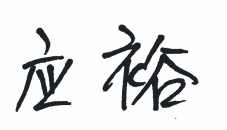

Fall 2008

List of publications

1 I. Y. Phang, K. C. Chaw, S. S. H. Choo, R. K. C. Kang, S. Lee, W. R. Birch, S. L. M. Teo, G. J. Vancso,
Marine Biofouling Field Tests, Settlement Assay and Footprint Micromorphology of cyprid larvae of *Amphibalanus amphitrite* on Model Surfaces.
Biofouling, accepted.

2 I. Y. Phang, N. Aldred, A. S. Clare, G. J. Vancso,
Towards a Nanomechanical Basis for Temporary Adhesion in Barnacle Cyprids (*Semibalanus balanoides*),
Journal of the Royal Society Interface, **2008**, *5*, 397-401.

3 N. Aldred, I. Y. Phang, S. L. Conlan, A. S. Clare, G. J. Vancso,
The effect of a serine protease, alcalase, on the adhesives of barnacle cyprids (Balanus amphitrite),
Biofouling, **2008**, *24*, 97-107.

4 X. Y. Ling, I. Y. Phang, D. N. Reinhoudt, G. J. Vancso, J. Huskens,
Supramolecular layer-by-layer assembly of 3D multicomponent nanostructure via multivalent recognition interactions,
International Journal of Molecular Science, **2008**, *9*, 486-497. (Invited article)

5 I. Y. Phang, T. X. Liu, W. D. Zhang, H. Schönherr, G. J. Vancso,
Probing the Buried Carbon Nanotubes within Polymer Matrix by Atomic Force Microscopy,
European Polymer Journal, **2007**, *43*, 4136-4142.

6 I. Y. Phang, N. Aldred, A. S. Clare, G. J. Vancso,
Development of Effective Marine Antifouling Coatings- Studying Barnacle Cyprid Adhesion with Atomic Force Microscopy,
NanoS, **2007**, 35-39. (Invited review)

7 I. Y. Phang, N. Aldred, A. S. Clare, J. A. Callow, G. J. Vancso,
An in situ study of the nanomechanical properties of barnacle (Balanus amphitrite) cyprid cement using Atomic Force Microscopy (AFM),
Biofouling, **2006**, *22*, 245-250.

8 X. F. He, J. Yang, L. C. Zhu, B. Wang, G. P. Sun, P. F. Lv, I. Y. Phang, T. X. Liu,
Morphology and Melt Rheology of Nylon 11/Clay Nanocomposites,
Journal of Applied Polymer Science, **2006**, *102*, 542-549.

9 W. D. Zhang, I. Y. Phang, T. X. Liu,
Growth of Carbon Nanotube on Clay: Unique Nanostructured Filler for High Performance Polymer Composites,
Advanced Materials, **2006**, *18*, 73-77.

10 L. Chen, I. Y. Phang, S. C. Wong, P. F. Lv, T. X. Liu,
Fracture behavior and mechanisms of nylon66/organoclay nanocomposites prepared by melt-compounding,
Materials and Manufacturing Processes, **2006**, *21*, 153-158.

11 L. Shen, I. Y. Phang, T. X. Liu,
Nanoindentation Studies on Polymorphism of Nylon 6,
Polymer Testing, **2006**, *25*, 249-253.

12 I. Y. Phang, J. H. Ma, L. Shen, T. X. Liu, W. D. Zhang,
Crystallization and melting behavior of multiwalled carbon nanotubes reinforced nylon-6 composites,
Polymer International, **2006**, *55*, 71-79.

13 S. F. Wong, L. Shen, Y. J. Tong, L. Chen, I. Y. Phang, P. Q. Lim, T. X. Liu,
Biopolymer Chitosan/Montmorillonite nanocomposites: Preparation and Characterization,
Polymer Degradation and Stability, **2005**, *90*, 123-131.

14 I. Y. Phang,
Malaysia can't thrive while it excludes minority talent,
Nature, **2005**, *437*, 518.

15 K.P. Pramoda, A. Mohamed, I. Y. Phang, T. X. Liu,
Crystal Transformation and Thermo-Mechanical Properties of Poly(vinylidene fluoride)/Clay Nanocomposites,
Polymer International, **2005**, *54*, 226-232.

16 L. Shen, I. Y. Phang, T. X. Liu, K. Y. Zeng,
Nanoindentation and morphological studies on nylon 66/organoclay nanocomposites. II. Effect of strain rate,
Polymer, **2004**, *45*, 8221-8229.

17 I. Y. Phang, T. X. Liu, A. Mohamed, K. P. Pramoda, C. B. He,
Morphology, Thermal and Mechanical Properties of Nylon 12/Organoclay Nanocomposites by Melt Compounding,
Polymer International, **2005**, *54*, 456.

18 Y. J. Tong, I. Y. Phang, J. C. Huang, L. Shen, T. X. Liu, C. B. He,
Melt-processing poly(etherimide/clay nanocomposites,
Materials Research Innovations, **2005**, *9*, 291-307.

19 W. D. Zhang, I. Y. Phang, L. Shen, S. Y. Chow, T. X. Liu,
Polymer Nanocomposites Using Urchin-Shaped Carbon Nanotubes-Silica Hybrid as Reinforcing Fillers,
Macromolecular Rapid Communication, **2004**, *25*, 1860-1864.

20 T. X. Liu, I. Y. Phang, L. Shen, S. Y. Chow, W. D. Zhang,
Morphology and Mechanical Properties of Multiwalled Carbon Nanotubs Reinforced Nylon-6 Composites,
Macromolecules, **2004**, *37*, 7214-7222.

21 L. Shen, I. Y. Phang, L. Chen, T. X. Liu, K. Y. Zeng,
Nanoindentation and morphological studies on nylon 66 nanocomposites. I. Effect of clay loading,
Polymer, **2004**, *45*, 3341-3349.

22 I. Y. Phang, L. Chen, W. W. C. Tjiu, S. Pisharath, T. X. Liu,
Nylon66/organoclay nanocomposites: I. Preparation, morphology, thermal and mechanical properties,
Materials Research Innovations, **2004**, *8*, 159.

23 I. Y. Phang, K. P. Pramoda, T. X. Liu, C. B. He,
Crystallization and melting behavior of polyester/clay nanocomposites,
Polymer International, **2004**, *53*, 1282-1289.

24 W. D. Zhang, L. Shen, I. Y. Phang, T. X. Liu,
Carbon Nanotube Reinforced Nylon 6 Composites Prepared by Simple Melt Compounding,
Macromolecules, **2004**, *37*, 256-259.

Submitted Manuscripts:

1 I. Y. Phang, N. Aldred, X. Y. Ling, J. Huskens, A. S. Clare, G. J. Vancso,
Glycoprotein "footprints" of barnacle cypris larva: Morphology and mechanical behavior at the nanoscale assessed by Atomic Force Microscopy,
Submitted for publication.

2 X. Y. Ling, I. Y. Phang, D. N. Reinhoudt, G. Julius Vancso, J. Huskens,
Freely suspended 3D supramolecular hollow ribbons
Submitted for publication.

Curriculum Vitae

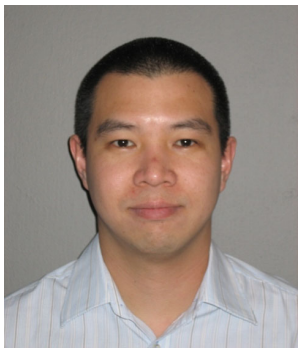

In Yee Phang was born on September 1, 1976 in Ipoh, Malaysia. He received his bachelor degree in Mechanical Engineering (2nd Class Upper, Honors) at the University of Adelaide, Australia in 1999. After that, he worked as project engineer in Malaysia and process engineer in Singapore, respectively. In year 2001, he continued his Master degree at Department of Mechanical Engineering of the National University of Singapore (NUS) and Institute of Materials Research and Engineering (IMRE). He received his Master degree in Engineering from NUS in January, 2004. In September 2004, he continued his PhD at the department of Materials Science and Technology of Polymer at University of Twente, the Netherlands under the supervision of Prof. G. Julius Vancso. His PhD research project focused on the investigation of morphology and nanomechanics of barnacle cyprid adhesion proteins by AFM based force spectroscopy. The results of his research are described in this Thesis.